Blending Nature and Technology: Optimizing Tinosporaside, a Natural Lead, for Advanced COVID-19 Therapy

GRIFFITH COLLEGE DUBLIN

This dissertation has been prepared as part of the requirements for the
MSc in Pharmaceutical Business and Technology
InnoPharma Labs and Faculty of Science
Griffith College Dublin

Dissertation Supervisor: Dr. Victor David Vendrell

Christy Saji
Feb 2024- May 2025

GRIFFITH COLLEGE DUBLIN

Assignment Cover Sheet

Learner name(s) : **Christy Saji**
Learner number(s):
Assignment Type : **Individual: YES**
Course : **MSc. Pharmaceutical Business & Technology** Stage/year:**3rd SEM**
Module: **Dissertation Module**
Study Mode: Full time Yes Part-time
Lecturer Name: **Dr. Prosper Anaedu** and **Dr. Regina Regan**
Assignment Title: **Blending Nature and Technology: Optimizing Tinosporaside, a Natural Lead, for Advanced COVID-19 Therapy**
No. of pages:
Uploaded to Moodle: **Yes** √
Additional Info:
Date due: **12/05/2025**
Date submitted: **09/05/2025**

Plagiarism disclaimer*:*
I understand that plagiarism is a serious offence and have read and understood the college policy on plagiarism. I also understand that I may receive a mark of zero if I have not identified and properly attributed sources which have been used, referred to, or have in any way influenced the preparation of this assignment, or if I have knowingly plagiarised my work or allowed others to plagiarise my work.
I hereby certify that this assignment is my own original work, based on my personal study and/or research, it is all written in my own words and I have acknowledged all references and sources used in its preparation. I also certify that the assignment has not previously been submitted for assessment and that I have not copied in part or whole or otherwise plagiarised the work of anyone else, including other students.
I have also not used any third parties, AI tools or websites to generate any parts of my assignment.

Signed & dated:  & 09/05/20

Please note: *Students **MUST** retain a hard / soft copy of **ALL** assignments as well as a receipt issued as proof of submission.*

GRIFFITH COLLEGE DUBLIN

DECLARATION

I confirm that the dissertation titled "***Blending Nature and Technology: Optimizing Tinosporaside, a Natural Lead, for Advanced COVID-19 Therapy"*** represents my own original work, completed as part of the requirements for the **Master of Science in Pharmaceutical Business and Technology** at **Griffith College**.

This research was carried out under the supervision of **Dr. Victor David Vendrell**, and I take full responsibility for the content presented. I further affirm that this work has not been previously submitted, either in whole or in part, for any academic award or qualification at Griffith College or any other institution.

Any ideas, texts, data, images, or other materials that are not my own have been identified and fully acknowledged by academic standards for referencing and citation.

Place: Dublin

Date: 09/05/2025

Candidate Name: Christy Saji

Signature: 

Supervisor: Dr. Victor David Vendrell

Signature: 

ACKNOWLEDGEMENTS

*First and foremost, I would like to express my profound gratitude to **God Almighty** for His abundant blessings, wisdom, and unwavering guidance, which have enabled me to successfully complete this dissertation.*

*I am deeply grateful to my supervisor, **Dr. Victor David Vendrell**, for his consistent support, insightful feedback, and invaluable encouragement throughout this research journey. I would also like to sincerely thank **Dr. Yolanda Alvarez** for her valuable feedback during the mini-viva, which greatly contributed to the refinement of my work. Their mentorship has played a pivotal role in shaping the direction and quality of this dissertation.*

*My sincere thanks also go to **Griffith College and Innopharma**, its faculty, and academic staff for providing the necessary resources, knowledge, and a supportive environment. I would especially like to thank **Dr. Prosper Anaedu** and **Dr. Regina Regan** for their guidance in academic writing, research methodology, and for coordinating the coursework that formed the foundation of this dissertation. Their contributions have been instrumental in helping me stay focused and organized throughout the process.*

*I am also grateful to **Dr. Prasanth Francis**, **Dr. Jessy Jacob**, **Dr. Bobby S. Prasad**, and **Dr. Saranya**, who taught me during my undergraduate studies, for their exceptional instruction and mentorship in **computational drug design**. Their expertise and encouragement helped build the foundation upon which this project was developed.*

*Above all, I owe my deepest love and thanks to my **beloved parents** for their selfless sacrifices, endless support, and unconditional love. I am equally thankful to my family members for their prayers, encouragement, and constant moral support.*

*Lastly, I would like to express heartfelt appreciation to all my **friends and well-wishers** who have contributed directly or indirectly to the successful completion of this dissertation. Your kindness and encouragement have made a meaningful difference in this journey.*

Christy Saji

Table of Contents

List of Tables

List of Figures

List of Abbreviations

Abbreviation	Full forms
2D	Two Dimensional
$3CL^{pro}$	3 Chymotrypsin-like Protease
3D	Three Dimensional
AA	Amino Acid
ACE2	Angiotensin - Converting Enzyme 2
ADME	Absorption, Distribution, Metabolism and Excretion
ADMET	Absorption, Distribution, Metabolism, Excretion And Toxicity
ADT	Autodock Tools
BBB	Blood-Brain Barrier
CAAD	Computer-Aided Drug Design
COVID 19	Coronavirus Disease 2019
ER	Endoplasmic Reticulum
FDA	Food And Drug Administration
GI	Gastrointestinal
GRAVY	Grand Average of Hydropathicity
iMOD	Internal Mode Analysis
II	Instability Index
pI	Isoelectric Point
IUPAC	International Union Of Pure And Applied Chemistry
IV	Intravenous
MD	Molecular Dynamics
M^{pro}	Main Protease
NMA	Normal Mode Analysis
NMR	Nuclear Magnetic Resonance
NSPS	Non Structural Proteins
ORF	Open Reading Frames
PAINS	Pan-Assay Interference Compounds
PDBQT	Protein Data Bank, Charges and Atom Type
PKCSM	Pharmacokinetics Computational Simulation Model
PL^{pro}	Papain- Like Protease
QSAR	Quantitative Structure Activity Relationship
RO5	Rule of Five
RTC	Replication-Transcription Complex

SARS-COV-2	Severe Acute Respiratory Syndrome Coronavirus 2
SBDD	Structure Based Drug Design
SDF	Structure-Data File
SMILES	Simplified Molecular Input Line Entry System
SOPMA	Self- Optimized Prediction Method with Alignment
S	Spike
TMPRSS	Transmembrane Serine Protease
WHO	World Health Organization

ABSTRACT

Blending Nature and Technology: Optimizing Tinosporaside, a Natural Lead, for Advanced COVID-19 Therapy

By Christy Saji

This study explored the antiviral potential of Tinosporaside, a natural compound found in *Tinospora cordifolia*, and its chemically modified versions, to identify a new treatment strategy against COVID-19. The research focused on two important viral enzymes-M^{pro} and PL^{pro}, that are essential for the virus to replicate and weaken the immune response. This research employed a quantitative, computational methodology rather than a survey-based approach. Techniques such as molecular docking and molecular dynamics simulations were used to design and evaluate 56 Tinosporaside analogs.

One particular derivative, T46, stood out for its strong and stable binding to both enzymes. It exhibited better performance than the original compound and possessed favorable drug-like properties, including high absorption, low toxicity, and chemical stability. Small structural modifications to the compound, such as the addition of a pyrrole ring, carboxylic acid, and a bromine atom, played a crucial role in enhancing its effectiveness. Further computer simulations confirmed that T46 could interact effectively with both viral targets, potentially disrupting the virus's ability to function.

These findings suggest that T46 has strong potential as a lead compound for future antiviral drug development. While the results are based on computer simulations, they provide a solid starting point for laboratory experiments and, eventually, real-world applications. This work also highlights how natural compounds can be refined and repurposed using modern tools to fight emerging diseases like COVID-19.

Keywords: Tinosporaside, *Tinospora cordifolia*, COVID-19, SARS-CoV-2, antiviral compound, molecular docking, dual inhibitor, in-silico study, natural product, drug discovery

CHAPTER 1

INTRODUCTION

1.1 Background of the Study

Natural remedies have long been a cornerstone in the development of modern medicine. From ancient times, plants and herbs have been used to treat various ailments, and many current treatments, such as antimalarial drugs and smallpox vaccines, have roots in these traditional practices. Over 70% of Food and Drug Administration (FDA)-approved synthetic drugs are derived from natural sources, underscoring the enduring value of traditional remedies. Natural products, in particular, play a crucial role in the development of antiviral treatments, with many current antiviral medications tracing their origins to compounds found in nature. As viruses continue to pose a global health threat, researchers are increasingly focused on isolating and refining these natural compounds to create more effective antiviral drugs, offering promising solutions to combat viral infections(El Sayed, 2000; WHO, 2023).

Tinospora species, especially those native to India, are widely recognized for their healing properties. These plants are known for their ability to support health in many ways, such as protecting the liver, reducing inflammation, fighting infections, fighting viruses, and helping with conditions like diabetes and ulcers. For centuries, they've been an important part of traditional medicines, and modern research continues to uncover their powerful benefits(Singh *et al.*, 2021). One of the key compounds, Tinosporaside, found in *Tinospora cordifolia*, is celebrated for its antioxidant and antimicrobial effects. This study aims to explore its potential in combating coronavirus disease 2019 (COVID-19), showcasing the continued importance of Tinospora in today's medical world(Khan *et al.*, 1989).

The need for new antiviral treatments, especially for COVID-19, has become more urgent due to the limited effectiveness of current options, particularly for immunocompromised individuals. Existing therapies are struggling with challenges like the virus evading the immune system, making it clear that we need fresh, innovative solutions. Targeting dual enzymes could improve how well treatments work, offering better ways to stop the virus

from spreading, especially when combined with other therapies or new delivery methods, to better fight COVID-19 and future viral outbreaks(Focosi *et al.*, 2025).

1.2 Investigating Tinosporaside: Purpose and Research Context

This study takes a closer look at Tinosporaside, a natural compound found in *Tinospora* plants, to see if it could be a possible treatment for COVID-19. The research specifically focuses on how Tinosporaside and its modified structures interact with viral proteases, like the main protease (M^{pro}), with Protein Data Bank (PDB) ID 7ALH, and papain-like protease (PL^{pro}) with PDB ID 6WX4, which are key to the virus's ability to replicate. By understanding how the molecules affect these proteins, we might uncover new ways to stop the virus from spreading. The study uses advanced computational tools, such as molecular docking and simulation software, to explore how Tinosporaside and its modified structures bind to these viral proteins. It will also look into how stable these interactions are and whether these molecules have the right properties to be a drug. Additionally, the study will examine whether the modified structures could enhance or diminish the viral activity.

This approach is particularly exciting because computational methods offer a faster, more cost-effective way to test compounds compared to traditional drug development. This efficiency allows for quicker refinement of compounds before they even enter clinical trials, potentially reducing the time it takes to find effective treatments for COVID-19. Beyond COVID-19, the research emphasizes the growing potential of plant-based compounds and the crucial role of modern technology in drug discovery. By combining nature with cutting-edge science, this study could not only help combat COVID-19 but also address future global health challenges. It’s thrilling to think that blending traditional plant-based remedies with modern technology could open up new pathways for treating viral infections like COVID-19, offering hope for faster, more effective treatments.

1.3 Significance and Justification for the Study

Exploring the plant-derived compound Tinosporaside as an antiviral agent directly addresses the urgent need for innovative solutions to combat COVID-19, especially with the emergence of new variants since 2019. Previous studies have highlighted Tinosporaside’s activity against the severe acute respiratory syndrome coronavirus 2 (SARS-CoV-2) M^{pro} (PDB ID-

6LU7), prompting further investigation into its effects on other crystal structures of viral proteases (PDB ID's: 7ALH & 6WX4) involved in viral replication and host cell metabolization. By evaluating its efficacy against different protease structures and exploring structural modifications, this research aims to make a significant contribution to antiviral drug discovery.

Moreover, the study aligns with the growing emphasis on sustainable drug development through Computer-Aided Drug Design (CADD). This method accelerates drug discovery while reducing the environmental impact by minimizing chemical waste and resource consumption and adhering to green chemistry principles. CADD has already proven successful in optimizing antiviral therapies such as Remdesivir. By integrating the precision of CADD with the untapped potential of plant-based compounds, this research strives to offer sustainable and effective therapeutic options for addressing COVID-19 and other viral health crises.

1.4 Research Question and Hypothesis

1.4.1 Research Question/ Objective

1. Can Tinosporaside effectively bind and inhibit SARS-CoV-2 proteases (Main protease and Papain-Like protease), and how do its binding affinities vary in structurally modified derivatives?
2. Can Tinosporaside function as a dual inhibitor by targeting both viral proteases simultaneously, and can its modified ligands enhance this dual inhibitory effect to improve antiviral potential against SARS-CoV-2?
3. How do structural modifications of Tinosporaside affect its selectivity, and interactions with SARS-CoV-2 proteases, and which molecular features are critical for optimal inhibition?
4. Can novel Tinosporaside-based analogs be designed to improve protease inhibition, drug-likeness, and pharmacokinetic properties using in silico methods such as molecular docking, pharmacophore modeling, and ADMET (Absorption, Distribution, Metabolism, Excretion, and Toxicity) analysis?

5. Can the findings from this research support the advancement of Tinosporaside and its analogs towards preclinical and clinical development as antiviral agents?

1.4.2 Hypothesis

This study is grounded in the hypothesis that by modifying its chemical structure, **Tinosporaside** can more effectively bind to SARS-CoV-2 proteases, thereby enhancing its ability to inhibit the virus. Furthermore, optimizing its drug-like properties will increase its potential as a safe and efficacious antiviral treatment.

The aim is to demonstrate that with the right structural modifications, **Tinosporaside** could serve as a powerful tool in combating SARS-CoV-2 viral infections. Leveraging advanced computational analysis, this research seeks to offer a faster approach to drug discovery, paving the way for real-world applications in the fight against future viral threats.

1.5 Roadmap and Future Prospects

Looking ahead, this research paves the way for future studies that could unlock the full potential of Tinosporaside in tackling viral diseases. The main goal is to explore how Tinosporaside interacts with SARS-CoV-2 proteases and see if altering its structure can improve its effectiveness. By using computational tools like AutoDock Vina, iMod, and pkCSM, it will examine how modifying structures might improve things like stability, bioavailability, and safety, with a focus on boosting its ability to target both proteases for greater therapeutic impact.

The literature review will provide a solid background on the current state of antiviral drug development, particularly about SARS-CoV-2 and the crucial role of proteases in viral replication. The findings from this review will help shape the design of our experiments and guide the direction of the research. The results section will present findings from molecular docking, dynamics simulations, and ADMET predictions. Comparisons will be made between the unmodified and modified versions of Tinosporaside in terms of binding affinity, stability, and drug-like properties. Any structural modifications implemented to enhance efficacy will be analyzed, with a particular focus on their impact on the compound's potential as an antiviral agent.

In conclusion, this research aims to contribute to global health efforts by addressing the urgent need for treatments for COVID-19 viral diseases. By investigating plant-based compounds like Tinosporaside, this study seeks to highlight new avenues for antiviral drug discovery while promoting a more sustainable approach to addressing viral health crises. Ultimately, the findings could play a significant role in the development of scalable, plant-based therapeutic solutions, strengthening the global health system's ability to respond to future pandemics.

CHAPTER 2

LITERATURE REVIEW

2.1 SARS- COV-2

In late 2019, reports of a mysterious pneumonia outbreak in Wuhan, China, began to surface. At first, it was thought to have come from a seafood market, but as cases quickly spread, it became clear that the virus was passing from person to person. Scientists have debated its origins ever since, with recent studies suggesting it most likely came from infected animals rather than a lab(Plummer, 2024). The virus, later named SARS-CoV-2, led to COVID-19, a disease that reshaped the world in ways no one could have predicted. From mild flu-like symptoms to severe respiratory failure, COVID-19 affected millions, with the most vulnerable suffering the worst(WHO, 2020; Carvajal *et al.*, 2024).

Fig 1:Corona Virus (Credits: Marcin Wojciechowski, Mohammed Haneefa Nizamudeen, Kirstypargeter, NiseriN (iStock, 2020))

Five years later, in 2024, the World Health Organization (WHO) called on China to share more data about the virus's origins, stressing that transparency is key to preventing future pandemics. Reflecting on the global response, the WHO acknowledged the sacrifices made by healthcare workers and the massive impact COVID-19 had on daily life. While the immediate crisis has passed, experts continue to warn that the world must stay prepared because another pandemic could be just around the corner(Plummer, 2024).

As of February 28, 2025, health experts are keeping a close watch on SARS-CoV-2 variants to understand their potential impact. These variants are categorized based on their risk level, from those under monitoring to those considered more concerning. Among the latest COVID-19 variants being tracked- Eris, Fornax, and Arcturus. Eris and Fornax share a mutation that allows them to spread more rapidly than other variants(Ada, 2025).

Right now, no variants are classified as highly dangerous, but Omicron BA.2.86 and KP.3 are being closely observed, with KP.3 being the most common in some areas. Other variants, like Omicron XEC and LP.8.1, are also on scientists' radars, though they haven't shown any major changes in how the virus spreads or how severe infections become. Meanwhile, older variants like Alpha, Beta, Gamma, Lambda, and Mu have faded away and no longer pose a threat. Researchers continue to track new variants through genetic sequencing and global collaboration to stay ahead of any potential risks(ECDC, 2025).

2.2 Protease Enzymes

Protease enzymes are essential for coronavirus replication, making them valuable targets for antiviral drugs. Two key enzymes, M^{pro} (or it is called as $3CL^{pro}$ -3-Chymotrypsin-like protease) and PL^{pro} , help break down large viral proteins (poly proteins (1a & 1ab)) into smaller, functional components necessary for the virus to reproduce(Grum-Tokars *et al.*, 2008; Báez-Santos, St. John, *et al.*, 2015). These enzymes belong to a group known as non-structural proteins (Nsps), meaning they play a vital role in the virus's life cycle without forming part of its outer shell. A significant advantage of targeting these proteases is their consistency across different variants, reducing the likelihood of drug resistance. Additionally, because they have no close human equivalent, treatments designed to inhibit them are less likely to cause harmful side effects(Mukherjee and Dikic, 2023).

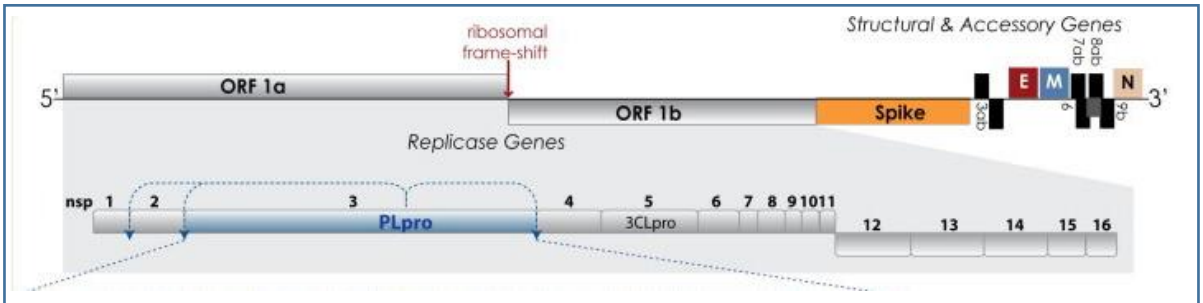

Fig 2: The organization of the SARS-CoV-2 Nsp (1-16) domain includes both structural and accessory genes. The replicase gene is encoded by two open reading frames (ORFs), which, upon viral infection, undergo ribosomal frameshifting to translate into polyproteins. These polyproteins are then processed into 16 non-structural protein (Nsp) domains essential for viral replication and transcription(Báez-Santos, St. John, *et al.*, 2015).

2.2.1 Viral Lifecycle and Drug Targets

The infection begins when the virus's spike (S) protein binds to human cell receptors - ACE2 (Angiotensin-Converting Enzyme 2**)**, with a host enzyme (TMPRSS-Transmembrane Serine Protease) aiding viral entry. Once inside, the virus releases its genetic material and hijacks the cell's machinery to produce large polyproteins(Cascella *et al.*, 2025). The proteases M^{pro} and PL^{pro} break these into smaller units, forming the replication-transcription complex (RTC), which generates viral genome copies and proteins for new virus assembly. Structural proteins facilitate the formation of new viral particles within the ER (Endoplasmic Reticulum) and the Golgi apparatus. Once fully assembled, the virus exits the host cell via exocytosis, spreading the infection. Since M^{pro} and PL^{pro} remain stable across variants, they are key targets for antiviral drugs to disrupt replication and transmission(V'kovski *et al.*, 2021).

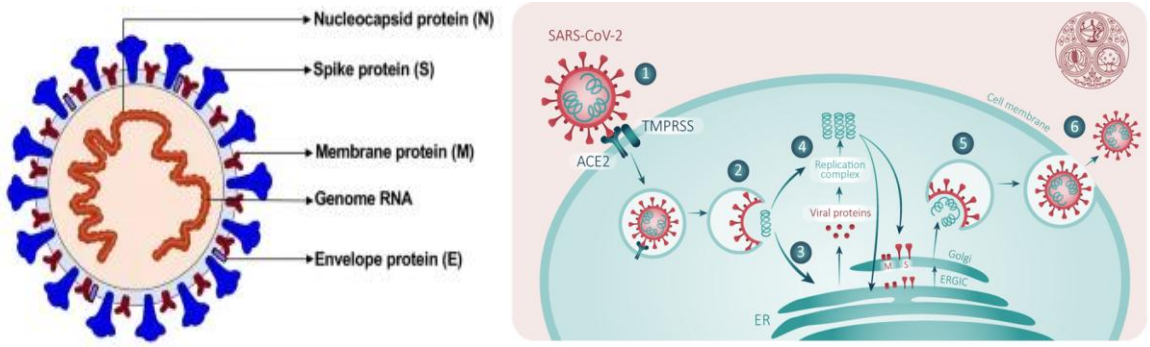

(a) (b)

Fig 3: (a) Schematic diagram of four structural proteins (S, N, M, E) (Zhang *et al.,* 2021). (b) Viral Lifecycle in humans*(*Ward *et al.,* 2020*)*.

2.2.2 Main Protease (M^{pro}/$3CL^{pro}$)

The M^{pro}, Nsp5, is a cysteine hydrolase found in beta-coronaviruses(Hu *et al.*, 2022). Due to its ability to crystallize under various conditions, numerous crystal structures have been recorded in the PDB. Among them, 7ALH is a well-documented structure determined by X-ray diffraction, featuring a high resolution of 1.65 Å, strong validation data, and no mutations. Water molecules present in PDB structures are usually removed to optimize the model. Unlike some other entries, 7ALH does not contain additional ligands. It consists of a single chain (Chain A) with 306 amino acids. Based on ProtParam analysis, it is considered a stable protein, with an instability index (II) of 27.65(PDB, 2020b; Costanzi *et al.*, 2021).

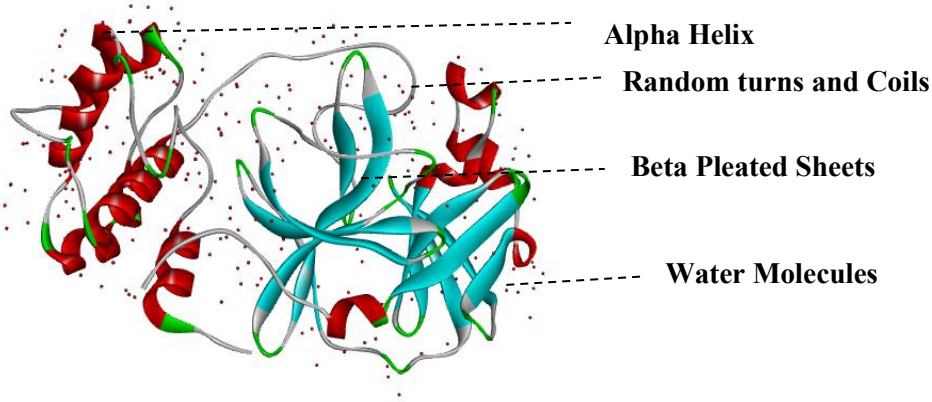

Fig 4: 3D Structure of 7ALH with water molecules (red dots) generated using Discovery Studio

M^{pro} of coronaviruses, plays a vital role in viral replication by acting as a molecular scissor, breaking down large viral proteins into smaller fragments essential for the virus's survival and replication. By inhibiting Mpro, certain antiviral treatments can disrupt the virus's ability to replicate, ultimately preventing its spread within human cells (Yevsieieva *et al.*, 2023). Its activity depends on key amino acids, where His41 and Cys145 play a catalytic role, while Met49, His164, Glu143, Glu166, Leu167, Ser144, His163, Met165, Asp187, Arg188, Gln189, Thr190, Ala191, and Gln192 help maintain structural integrity and support enzyme function(Liu *et al.*, 2020). Given its crucial role, inhibiting Mpro presents a promising strategy for halting viral replication and preventing the spread of infection.

2.2.3 Papain-like Protease (PL^{pro})

The PL^{pro}, Nsp3, is a key enzyme in SARS-CoV-2, working alongside M^{pro}. It plays a crucial role in processing viral polyproteins, which are necessary for the virus to replicate and that can also effect the immune system of the host organism(Osipiuk *et al.*, 2021). That is, it helps the virus evade the immune system by removing certain protein markers that alert the body to an infection. By weakening the immune response, the virus gains a better chance to spread. Because of its dual role in replication and immune suppression, PLpro has become an important target for antiviral drug research(Osipiuk *et al.*, 2021).

One well-studied version of PLpro is the 6WX4 crystal structure in PDB, determined by X-ray diffraction, with a high resolution of 1.66 Å and strong validation data. This structure includes a single protein chain (Chain D) with 326 amino acids, along with an additional viral inhibitor (VIR251) and essential ligands like zinc and L-peptide(PDB, 2020a). Zinc ions play a key role in keeping PLpro stable, while specific amino acids, such as Cys111, His272, and Asp286, are essential for its function. Other residues, like Tyr268, Met208, and Gln269, help the enzyme recognize viral proteins, while certain cysteine residues assist in maintaining its overall structure(Osipiuk *et al.*, 2021).

Classified as a stable protein by ProtParam(Expasy, 2024), with an II of 34.99, it serves as a valuable model for experimental research. Understanding these structural details is critical for developing antiviral drugs that can block PL^{pro}'s activity, potentially slowing viral replication and preventing the virus from suppressing the immune system(Osipiuk *et al.*, 2021).

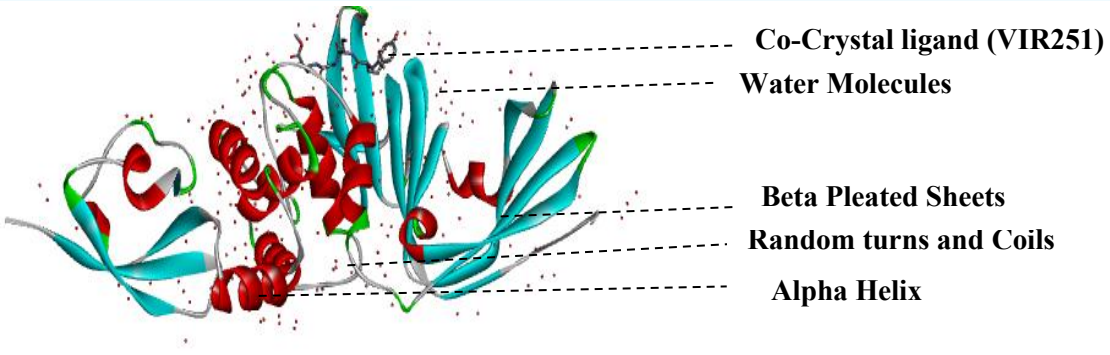

Fig 5: 3D structure of 6WX4 with water molecules (red dots) and the ligand (carbon chain) generated using Discovery Studio

2.2.4 Journey to 3D Protein Folds

The process starts with the primary structure, which is simply the sequence of amino acids. This sequence folds into secondary structures, such as alpha-helices and beta-sheets, stabilized by hydrogen bonds. As the protein continues to fold, it forms its tertiary structure, with side-chain interactions defining its unique 3D (Three Dimensional) shape. Some proteins also have a quaternary structure, where multiple chains come together to function, like hemoglobin. Even small changes in the amino acid sequence can drastically affect the protein's structure and function(Cheriyedath, 2017; khanacedamy, 2025).

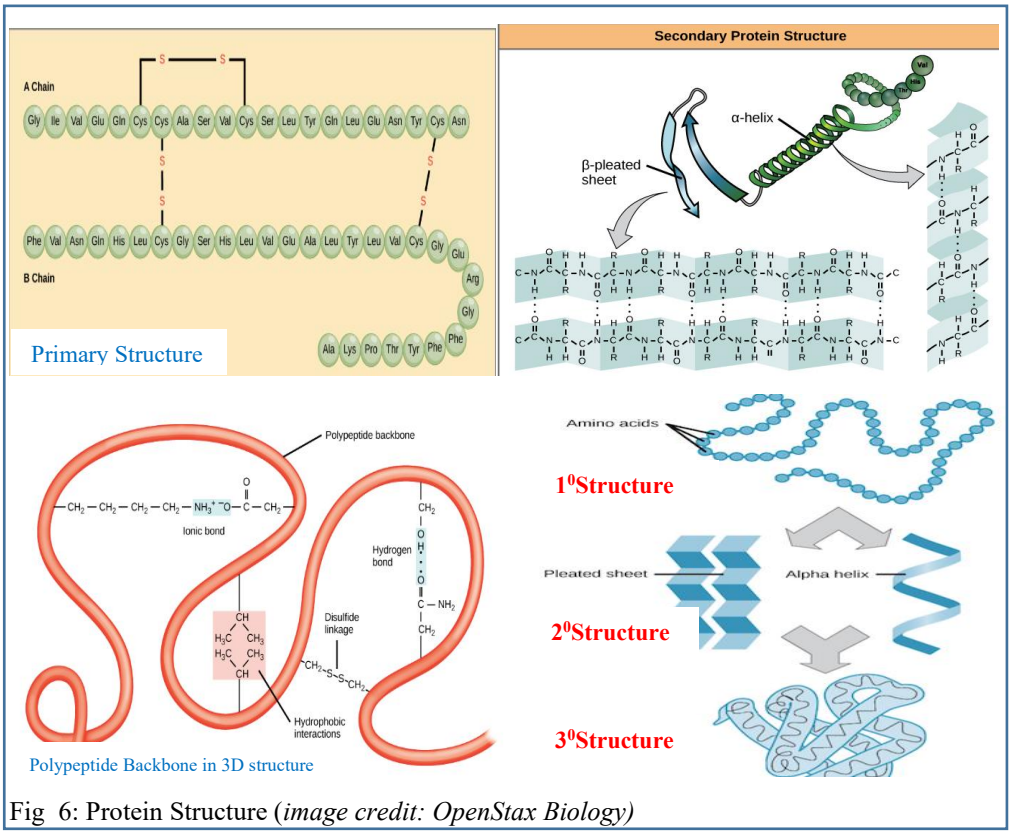

Fig 6: Protein Structure (*image credit: OpenStax Biology)*

2.3 Natural Compounds as Antiviral Agents

For centuries, natural compounds have been explored for their potential to fight viral infections, offering an alternative to synthetic drugs. Many plant-derived compounds have shown the ability to block viral replication, break down virus structures, or strengthen the immune system. Their natural availability and lower risk of resistance make them attractive candidates for antiviral treatments. However, challenges like inconsistent plant extracts,

limited knowledge of their molecular mechanisms, and potential safety concerns still need to be addressed(Atampugbire *et al.*, 2024).

Viral infections, including COVID-19, continue to challenge global health systems, with limited treatment options. This has sparked renewed interest in natural remedies, particularly medicinal plants, which have been valued for their healing properties for centuries(Adeosun and Loots, 2024). In several countries, herbal medicines are often preferred due to their affordability, accessibility, and reduced risk of side effects when compared to synthetic drugs.

Recently, researchers have been investigating the role of plant-based compounds in fighting SARS-CoV-2, the virus responsible for COVID-19. Bioactive compounds like flavonoids, alkaloids, terpenoids, and polyphenols have shown antiviral properties in lab studies. A well-known example is green tea (theanine, vitamins, flavonoids & phenols); its components may help by interfering with viral replication, blocking viral entry into cells, or regulating the immune response, which could potentially ease severe symptoms. However, despite these promising findings, no natural compound has been clinically proven to prevent or cure COVID-19(NCCIH, 2022).

2.3.1 Natural Leads

Natural leads are essential compounds found in nature that have the potential to become powerful medicines. These compounds come from various sources, such as plants, marine organisms, fungi, and bacteria. What makes them so valuable is that nature has “designed” these compounds to interact with biological systems, making them a great starting point for treating human diseases.

For example, **Plitidepsin**, a natural product from a marine organism called *Aplidium albicans*, has shown promise in the fight against COVID-19. It works by targeting a protein in human cells that the virus uses for replication. In certain studies, Plitidepsin even outperformed remdesivir, a drug that was widely used during the pandemic(Xu *et al.*, 2022).

But natural compounds don't stop at fighting viruses. They also hold promise in the battle against other diseases (Ying *et al.*, 2008). These examples emphasize how nature provides

us with bioactive molecules that have the potential to address most pressing health challenges. Although extracting and developing these compounds can be challenging, advances in science and technology are helping to streamline the process. As we face increasing health threats like drug resistance and chronic diseases, natural leads are becoming a more exciting and promising avenue for drug discovery(Xu *et al.*, 2022).

2.3.2 Tinosporaside: A Key Bioactive from Medicinal *Tinospora*

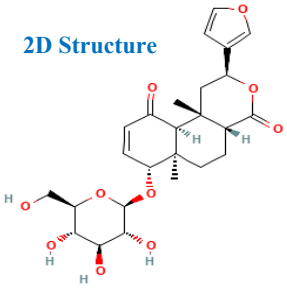

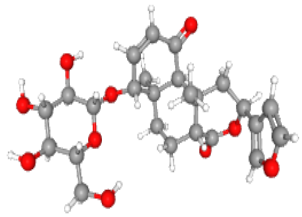

Fig 7*:* Tinospora Cordifolia(stem, leaves & roots)(Jain, 2020) and Chemical Structure of Tinosporaside (PubChem, 2007)

Tinosporaside, a diterpenoid + furanolactone ring extracted from the stem of an Indian Medicinal plant named *T. cordifolia,* (Mishra *et al.*, 2023), is gaining attention for its medicinal potential. *T.* species (decoctions, extracts, or powders from various plant parts) have long been valued in traditional medicine for their ability to combat infections, reduce inflammation, enhance immune function and healing properties. As the search for effective antiviral treatments continues, plant-derived compounds like Tinosporaside present a promising avenue for developing accessible and sustainable therapeutic options, particularly in areas with limited access to modern healthcare (Najmi *et al.*, 2020).

For centuries, *T.* species have been valued in traditional medicine for their therapeutic properties and minimal side effects. Among them, *T. cordifolia* i.e., Guduchi in Ayurveda, has been extensively used to support overall health and manage conditions such as diabetes, fever, jaundice, skin disorders, and viral infections. Its diverse array of natural compounds contributes to its significance in herbal medicine. Over the past three decades, scientific research has extensively examined the phytochemical and medicinal properties of Tinospora species, with *T. cordifolia* being the primary focus (Chaudhary *et al.*, 2024).

The rise of **COVID-19** has pushed scientists to look for new antiviral solutions, including plant-based remedies. Since viruses like SARS-CoV-2 rely on protease to multiply, this research has used advanced computational methods to see if the Tinosporaside and its analogs could block this enzyme(Chowdhury, 2020). It could offer a plant-based alternative for managing viral infections, reinforcing the wisdom of traditional medicine in modern healthcare.

2.4 Computational Drug Discovery Approaches

Computational tools have completely changed the game in drug discovery, making the process faster and more efficient, thanks to the power of AI, machine learning, and advanced computing. Now, researchers can accurately predict which drug candidates might work best, using methods like structure-based virtual screening to see how compounds interact with target proteins and narrow down the options before heading to the lab. These breakthroughs not only speed things up but also save money, taking some of the financial pressure off compared to the old-school ways of developing drugs(Sadybekov and Katritch, 2023).

Molecular docking, a go-to computational tool, helps researchers figure out how small molecules like drugs or natural compounds might interact with target proteins, shedding light on their potential to treat diseases. It's a big player in drug discovery, letting scientists test the health benefits of both natural and synthetic compounds through simulations. But since its accuracy depends on computational models that don't always match real-life scenarios, it's often teamed up with molecular simulations to get a better, more dynamic picture of how molecules behave over time. Even with its flaws, molecular docking is still a vital part of pushing medicine forward and creating new treatments(Agu *et al.*, 2023).

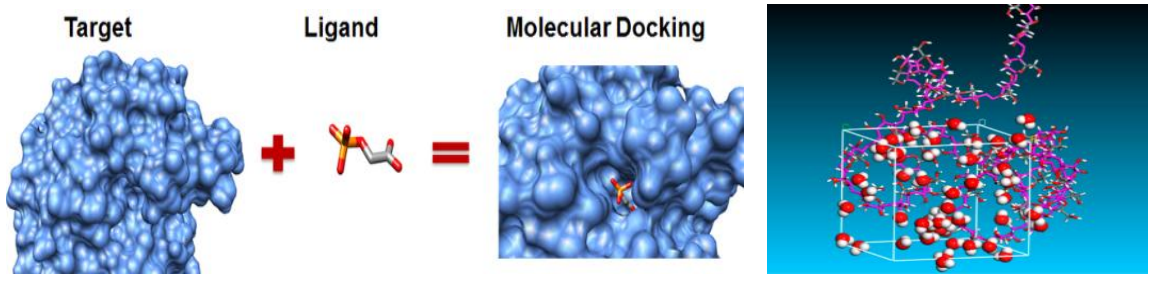

(a) (b)

Fig 8: (a) Molecular docking(Tenorio, 2013) & (b) Molecular dynamic simulation-method analysing physical movements of atoms & molecules - cellulose amorphous region-water molecule model(Jiang *et al.*, 2023).

This research focuses on **semi-flexible docking** and **structure-based drug design (SBDD)**, which play crucial roles in optimizing drug-target interactions. Semi-flexible docking considers the flexibility of ligands while keeping the protein rigid, offering a balance between accuracy and computational efficiency(Zhang *et al.*, 2022). This approach allows researchers to study how small structural modifications affect binding affinity and overall drug effectiveness. SBDD, on the other hand, relies on detailed knowledge of the target protein's 3D structure to develop potent inhibitors or agonists. By combining these methods, this study aims to refine drug candidates, improve binding efficiency, and contribute to the ongoing advancements in computational drug discovery(Anderson, 2003).

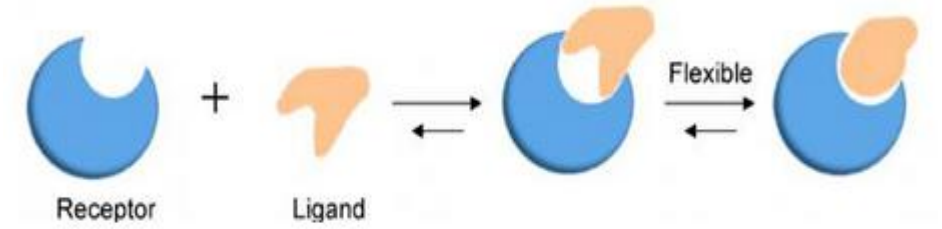

Fig 9: Semi-flexible docking & structure-based drug design, where ligand is flexible and receptor is rigid(Fan *et al.*, 2019).

2.4.1 Computational Software

Computational tools have become an essential part of modern scientific research, helping scientists understand how molecules interact, predict drug behavior, and analyze biological data. These tools play a major role in drug discovery, from designing molecular structures to assessing a drug's effectiveness and safety.

2.4.1a Molecular Docking and Visualization Software

AutoDock Vina, along with **AutoDock Tools (ADT)**, is widely used to simulate drug-protein interactions by estimating binding affinities and molecular conformations. **AutoDock Vina** simplifies and accelerates the study of how molecules interact with one another. It uses smart algorithms and a simplified scoring system to speed up the docking process, delivering reliable results without much hassle. While it simplifies some details, like **hydrogen bonds and electrostatics**, it still works well for most biological systems. Its quick performance and user-friendly design make it a practical and powerful tool for virtual screening in drug discovery(Trott and Olson, 2010; Forli *et al.*, 2016; Eberhardt *et al.*, 2021).

ADT complements AutoDock Vina by offering an easy-to-use interface for setting up and analyzing docking simulations. It simplifies the preparation of receptor and ligand files by adding hydrogens, assigning charges, and defining flexible bonds. ADT also helps define the docking area, set grid parameters, and create the files needed for simulations. With batch processing support, ADT is a great tool for drug discovery research.(Forli *et al.*, 2016).

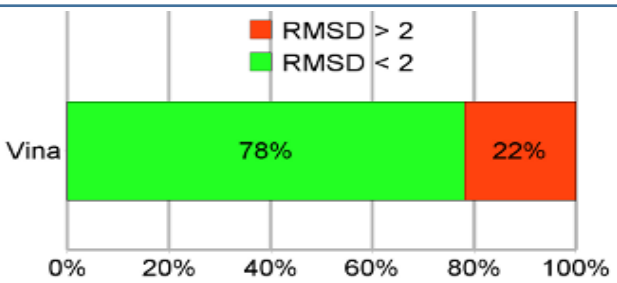

Fig 10: Prediction accuracy of binding modes on the test set for AutoDock Vina (symbol- black)(mgl-admin, 2018)

BIOVIA Discovery Studio 2021 further enhances drug discovery with molecular structure preparation, advanced three-dimensional(3D)/two-dimensional(2D) visualization, and simulations. Discovery Studio streamlines drug design by modeling molecular interactions, optimizing drug candidates, and supporting bio-therapeutic development. Its user-friendly interface allows researchers to analyze complex biological systems with ease. By integrating cutting-edge computational techniques, Discovery Studio helps bridge the gap between theoretical research and real-world drug development (Dassault Systèmes, 2025).

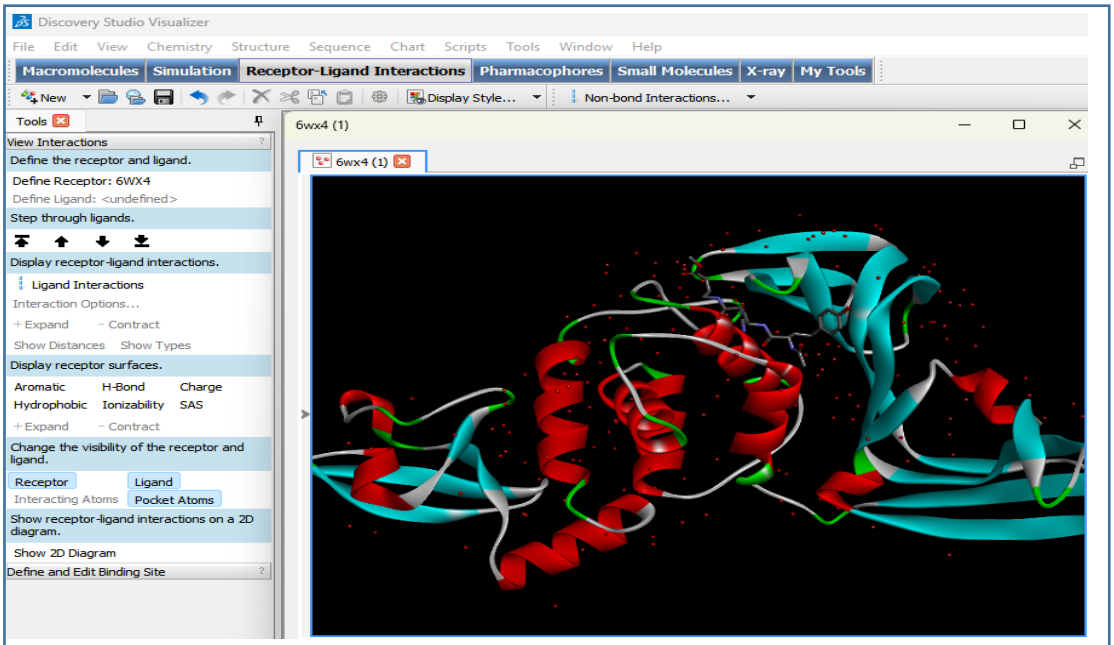

Fig 11: Discovery Studio Visualizer with 6WX4(Dassault Systèmes, 2025)

The **Protein-Ligand Interaction Profiler (PLIP)** is a free, user-friendly tool that helps analyze molecular interactions by identifying key binding forces such as hydrogen bonds, hydrophobic interactions, halogen bonds and salt bridges. Without requiring a complex setup, it detects crucial interactions from PDB files or docking results. PLIP generates clear, publication-ready images, customizable PyMOL session files, and detailed reports for further analysis(Salentin *et al.*, 2015; Adasme *et al.*, 2021).

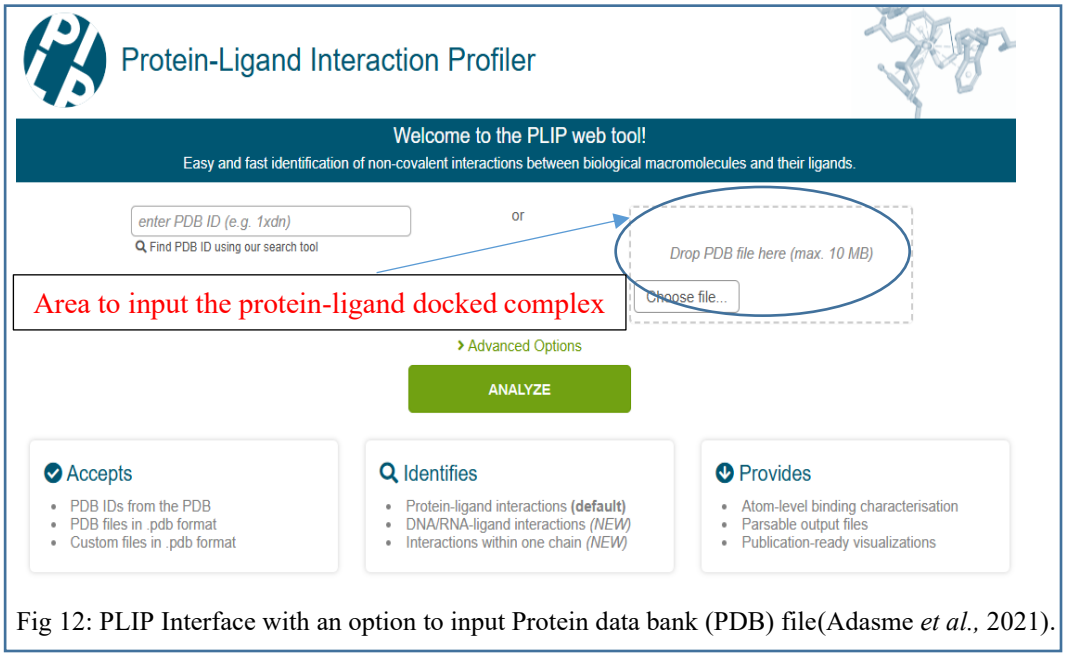

Fig 12: PLIP Interface with an option to input Protein data bank (PDB) file(Adasme *et al.,* 2021).

2.4.1b Chemical Structure and Format Conversion Software

Cheminformatics tools are vital for researchers to design, visualize, and alter chemical structures, ensuring precise results in computational studies. **ChemSketch** is a comprehensive software that allows users to generate molecular diagrams, view structures in 3D, generate structures using SMILES (simplified molecular input line entry system), and calculate important molecular properties such as molecular weight, formulas, density etc. It is widely used in both academic research and education to create detailed visuals and perform molecular analysis(ACD/Labs, 2024). **Syntelly,** AI driven open source online software to generate IUPAC (International union of pure and applied chemistry) names. It can predict 5 names from which most accurate one is selected(Syntelly, 2024).

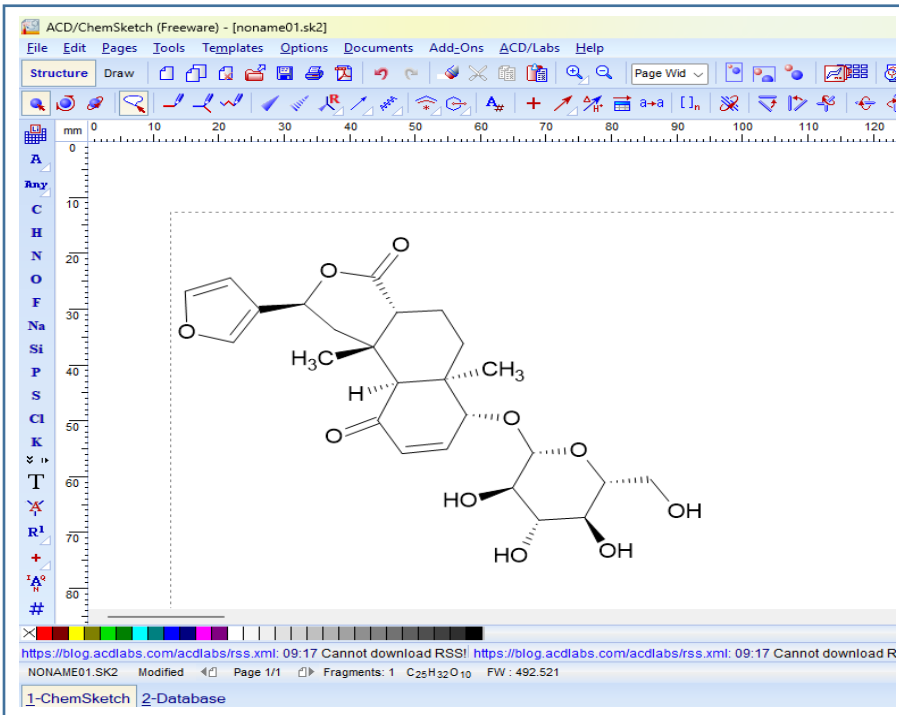

Fig 13: Structure of Tinosporaside generated using Smiles Notations from PubChem (ACD/Labs, 2024).

2.4.1c Molecular Databases and Bioinformatics Analysing Software

Comprehensive molecular databases are essential for retrieving information on chemical properties, biological activity, and protein structures. **PubChem** is an incredibly useful resource for scientists studying small molecules and their effects on biology. It provides a massive database with test results for over 700,000 compounds, making it a go-to platform for drug discovery and toxicology research(Wang *et al.*, 2009).

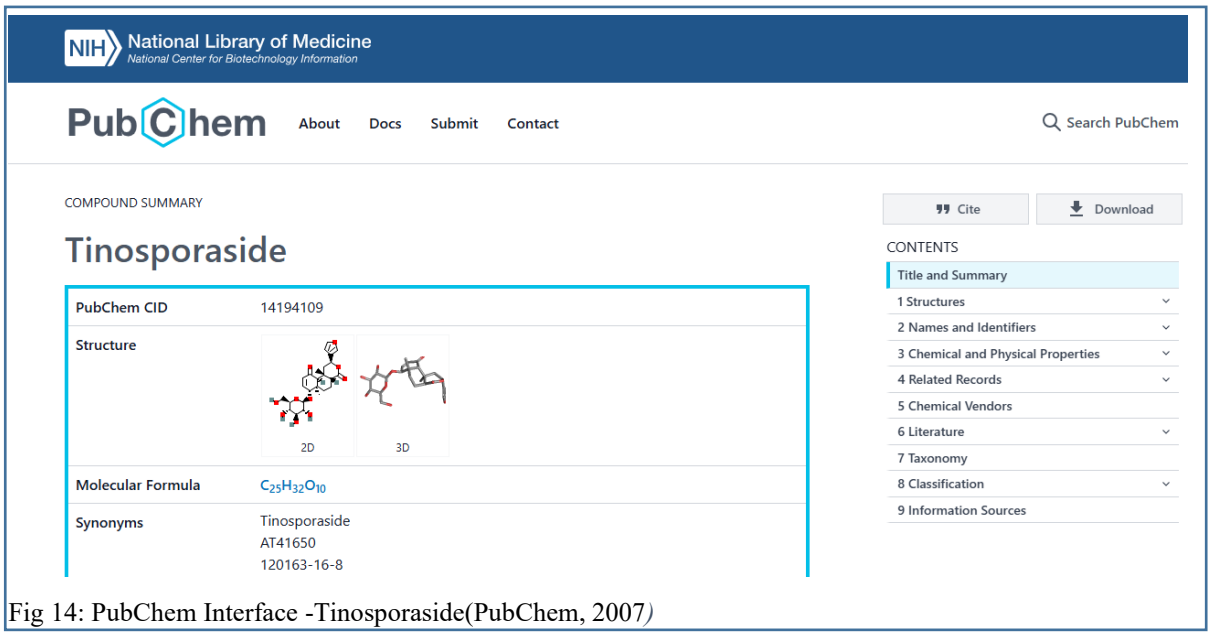

Fig 14: PubChem Interface -Tinosporaside(PubChem, 2007)

The **Protein Data Bank** serves as a global resource for 3D structures of biomolecules/targets, facilitating structural biology studies. The database is continually updated to ensure data accuracy and security. Scientists globally contribute molecular structures obtained through methods such as X-ray crystallography, nuclear magnetic resonance (NMR) spectroscopy, and electron microscopy. Accessible online at no cost, the PDB serves millions of researchers, educators, and students by offering valuable tools and learning resources to enhance the understanding of biomolecular structures. (Burley *et al.*, 2022).

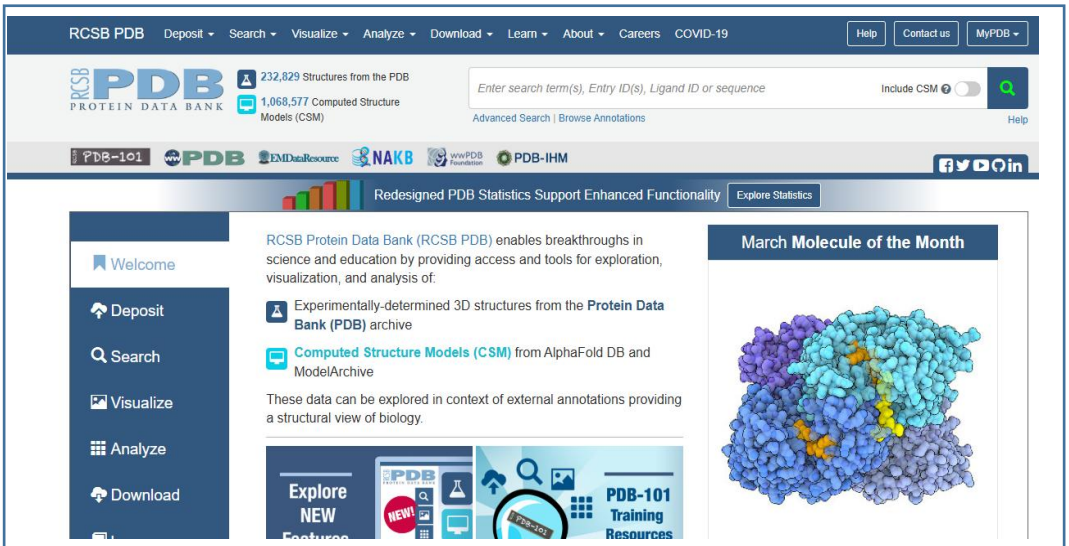

Fig 15: PDB interface(PDB, 2025)

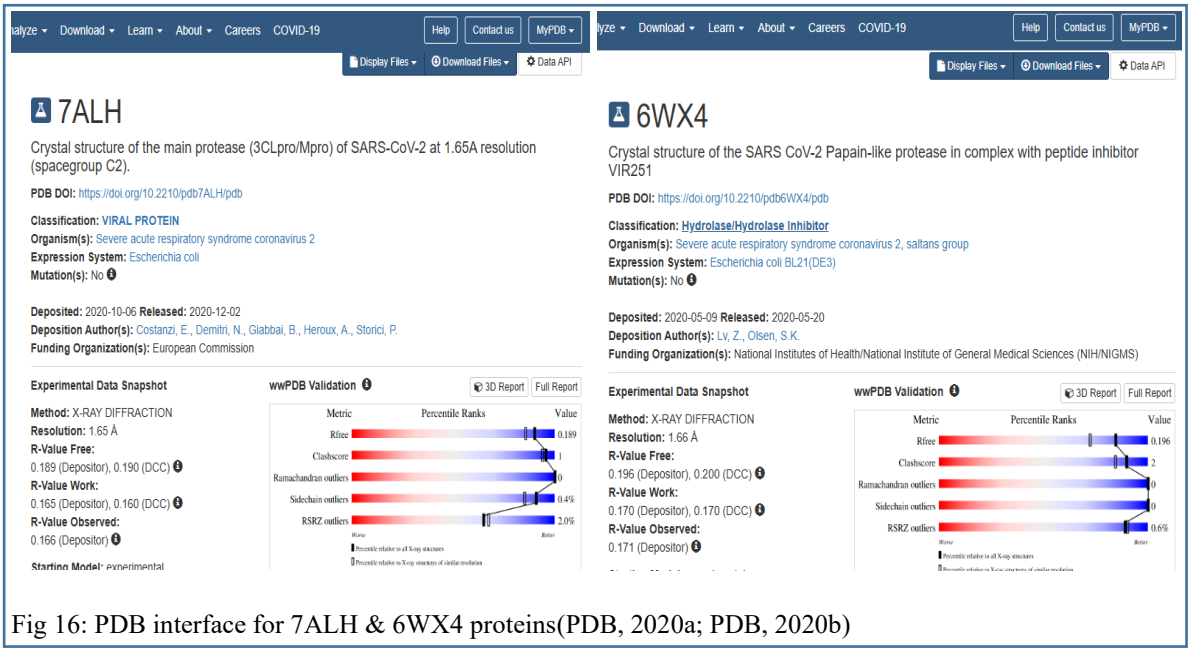

Fig 16: PDB interface for 7ALH & 6WX4 proteins(PDB, 2020a; PDB, 2020b)

PyMOL is a popular tool for visualizing molecular structures, widely used in fields like structural biology, computational chemistry, and drug discovery. It helps researchers create detailed 3D models of proteins, nucleic acids, and small molecules while also allowing molecular editing, ray tracing, and animation. With its powerful features for analyzing protein-ligand interactions and structural data, it's an essential tool for scientists and educators working in molecular research and drug design (yuan *et al.*, 2024).

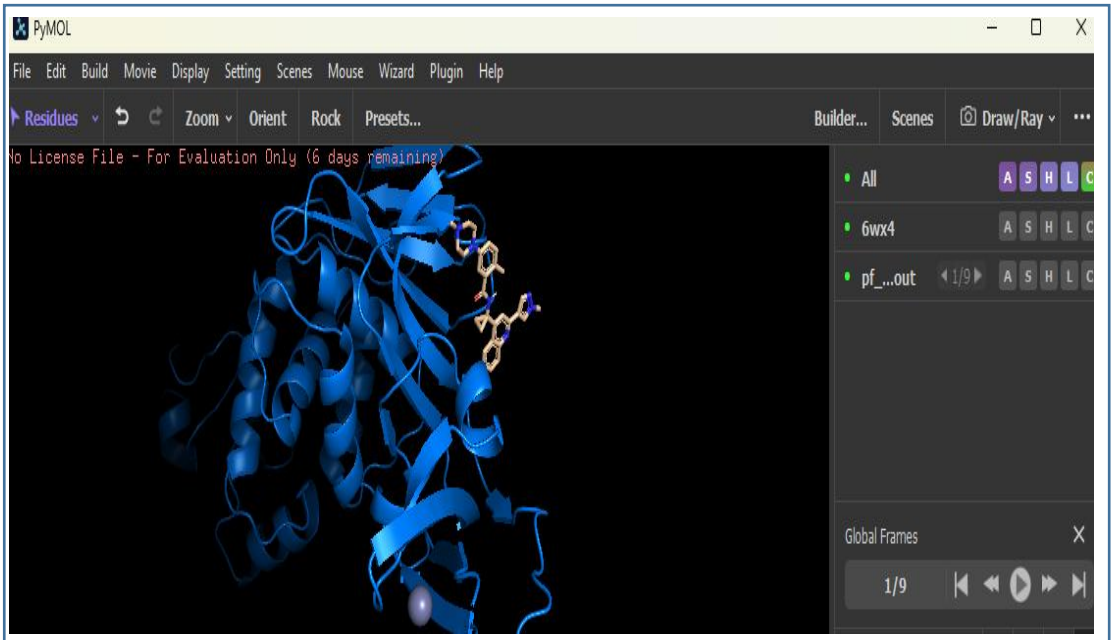

Fig 17: PyMOL with the 3d visualisation of 6WX4 and tinosporaside(After Docking)

2.4.1d Pharmacokinetics and Drug-Likeness Predicting Software

Predicting how a drug behaves in the human body is essential for assessing its safety and effectiveness. **SwissADME** evaluates drug-likeness- Absorption, distribution, metabolism, and excretion (ADME) properties, helping researchers determine whether a compound has favorable pharmacokinetic characteristics (Daina *et al.*, 2017). It also checks if a molecule adheres to **Lipinski's Rule of five (RO5)**, which predicts oral bioavailability based on criteria such as molecular weight under 500 Da, a maximum of 5 hydrogen bond donors, no more than 10 hydrogen bond acceptors, and a logP or octanol-water partition coefficient value of 5 or less(Lipinski *et al.*, 2001).

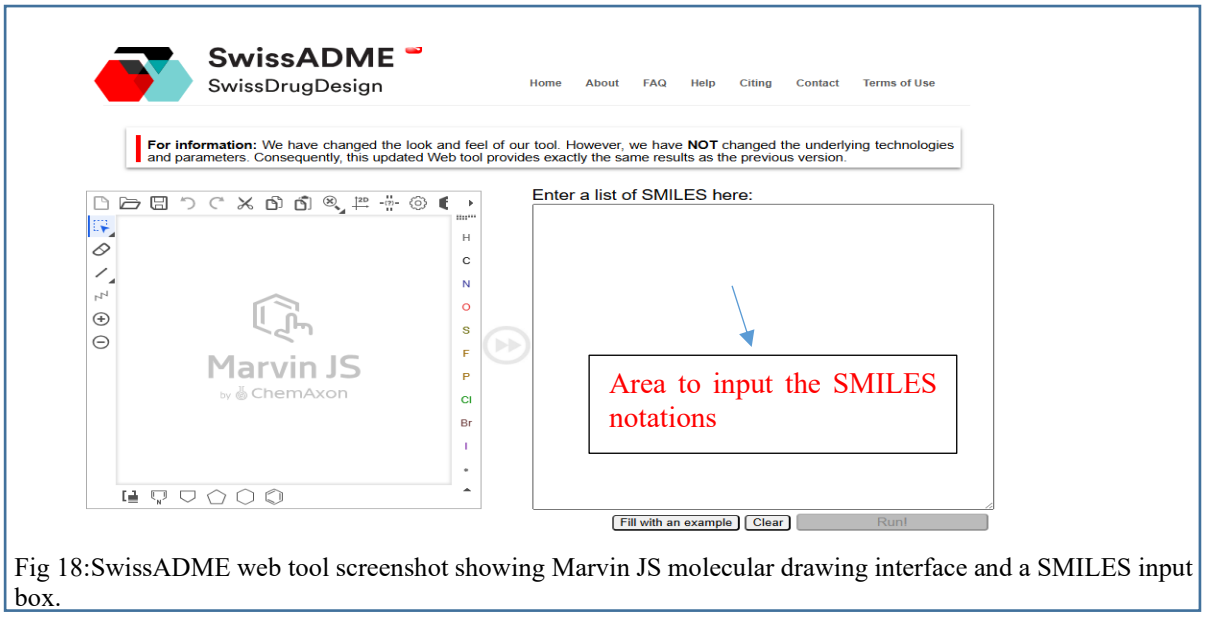

Fig 18:SwissADME web tool screenshot showing Marvin JS molecular drawing interface and a SMILES input box.

The **pkCSM (Pharmacokinetics Computational Simulation Model)** is a computational tool designed to predict how drug-like compounds interact within the body, with a focus on ADMET. It extends these predictions by assessing drug absorption, potential toxicity, and side effects, helping researchers identify issues early in drug development to improve success rates. As a free online software, it has demonstrated accuracy comparable to or better than existing approaches (Pires *et al.*, 2015).

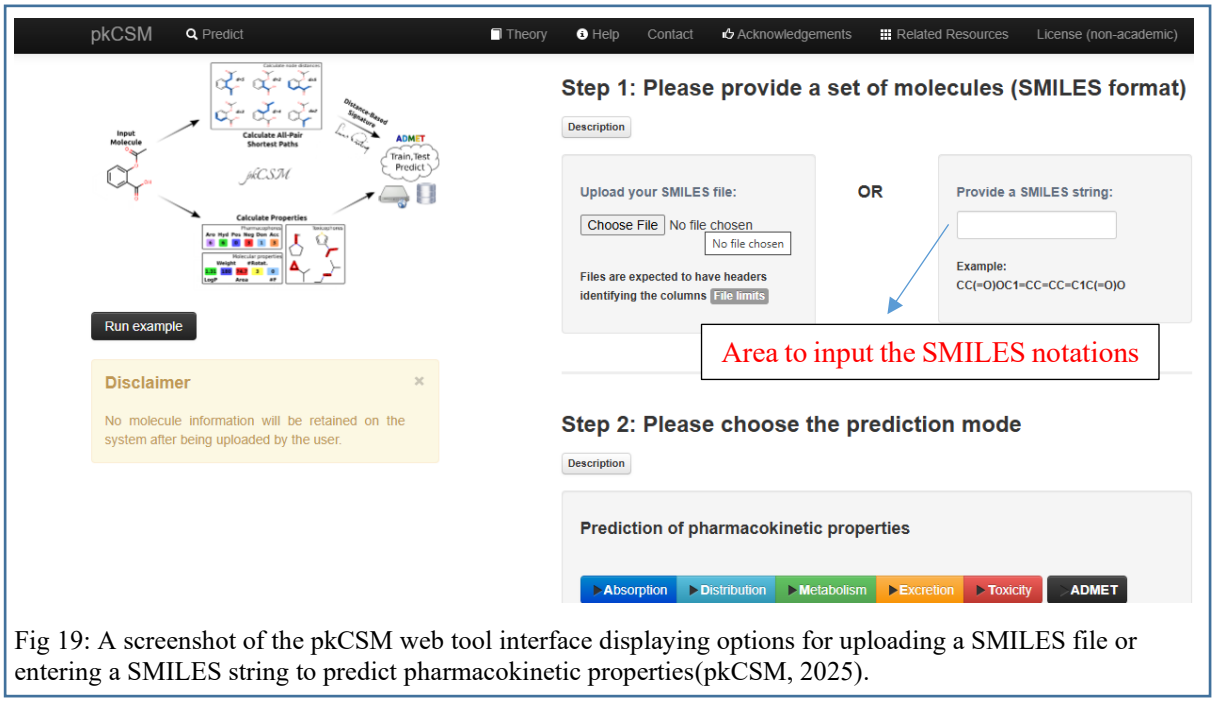

Fig 19: A screenshot of the pkCSM web tool interface displaying options for uploading a SMILES file or entering a SMILES string to predict pharmacokinetic properties(pkCSM, 2025).

ProTox 3.0 is a user-friendly online platform that predicts the potential toxicity of small molecules, an essential step in drug development. By utilizing machine learning, molecular features, and structural similarities, it offers quick and reliable insights without the necessity of animal testing(Banerjee *et al.*, 2024). It also classifies compounds based on their predicted toxicity levels, using LD_{50} (Lethal Dose/ Median Lethal Dose) values (the dose at which 50% of test subjects might be affected)(Snapse, 2025)following the **globally harmonized system.** The dose is typically measured in mg/kg(Pillai, Parvathy, 2024):

- **Class I:** Fatal if swallowed ($LD_{50} \leq 5$ mg/kg)
- **Class II:** Fatal (5–50 mg/kg)
- **Class III:** Toxic (50–300 mg/kg)
- **Class IV:** Harmful (300–2000 mg/kg)
- **Class V:** May be harmful (2000–5000 mg/kg)
- **Class VI:** Non-toxic ($LD_{50} > 5000$ mg/kg)

ProTox 3.0 facilitates early safety assessments, saving time and assisting in making better drug design decisions.

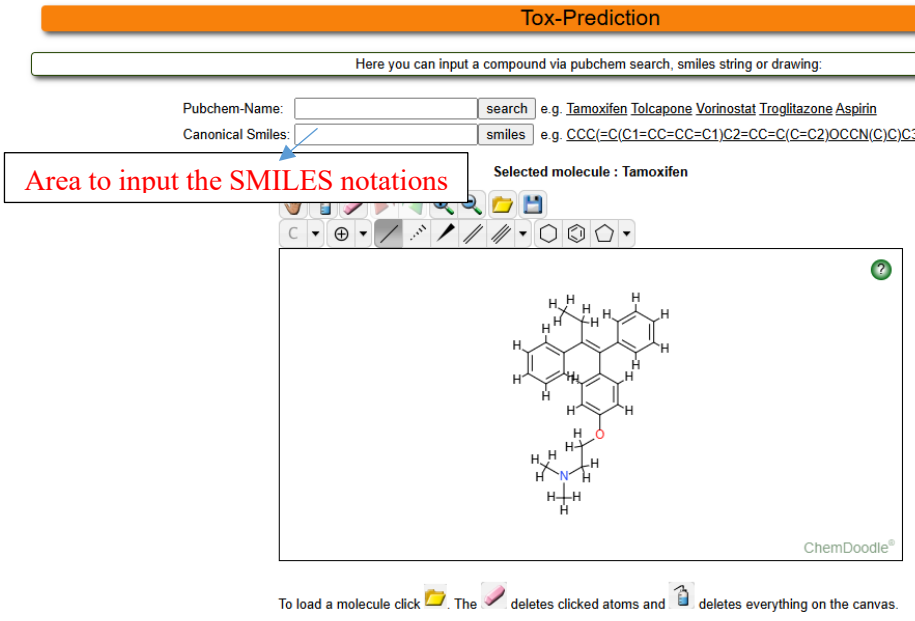

Fig 19:Tox-Prediction screenshot displaying a molecular structure in ChemDoodle, with PubChem and SMILES input options.

2.4.1e Protein Structure Analysis and Molecular Simulation Software

Understanding protein stability and flexibility is crucial in drug development. **ProtParam (**part of the ExPASy database) is a useful tool for studying proteins, allowing researchers to analyze their physical and chemical properties. Whether working with protein sequences from the UniProtKB database or custom sequences, users can calculate important characteristics such as isoelectric point (pI), molecular weight, amino acid (A.A) composition, and stability indicators like the instability index, etc. By offering a detailed look at protein behavior under different conditions, ProtParam is a valuable resource for scientists studying protein function, stability, and interactions (Expasy, 2024).

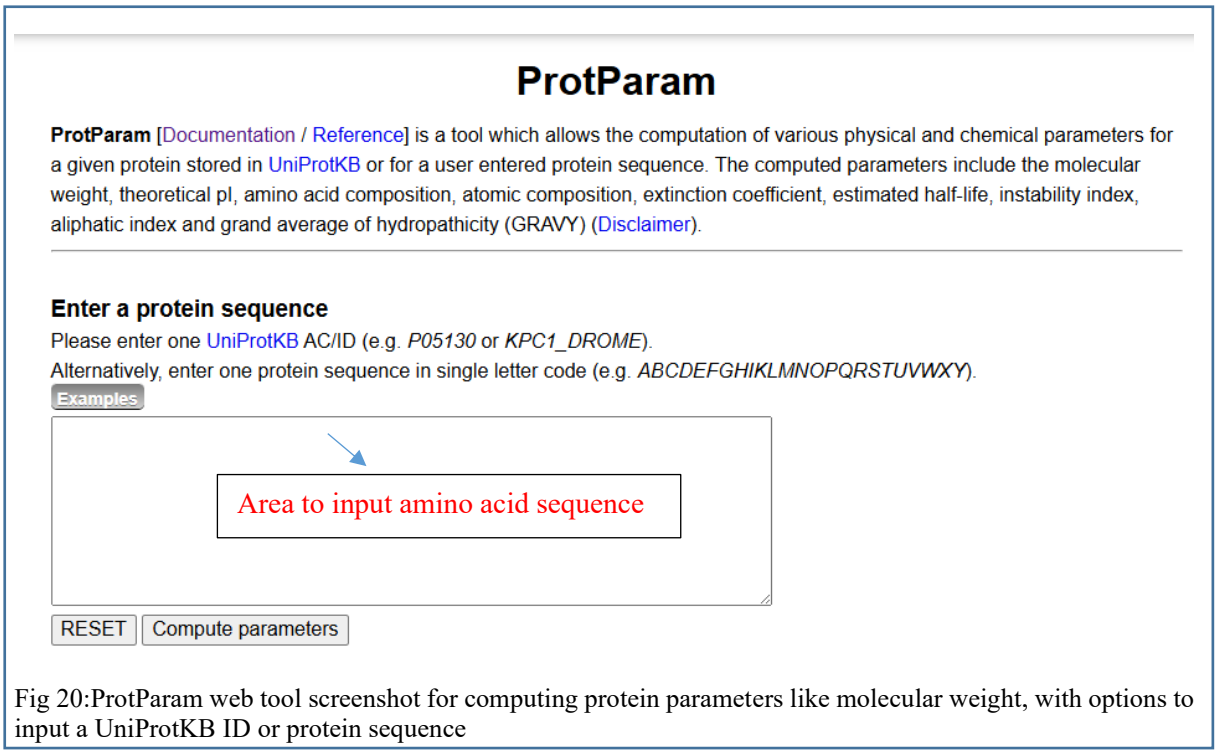

Fig 20:ProtParam web tool screenshot for computing protein parameters like molecular weight, with options to input a UniProtKB ID or protein sequence

Understanding the secondary structure of proteins like alpha-helices, beta-sheets, and coils is essential to figuring out how they work. To help with this, an upgraded version known as the **Self-Optimized Prediction Method with Alignment (SOPMA)** was used. This method works better by looking at families of related proteins and comparing their aligned sequences. Thanks to this improvement, SOPMA could correctly predict the folding pattern of about

69.5% of amino acids in a large set of diverse proteins(Geourjon and Deléage, 1995; Combet *et al.*, 2000).

DeepSite is a freely- available online software that makes it easy for you to find ligand binding pockets in your protein of interest using a user-friendly, neural network predictor(Jiménez *et al.*, 2017).

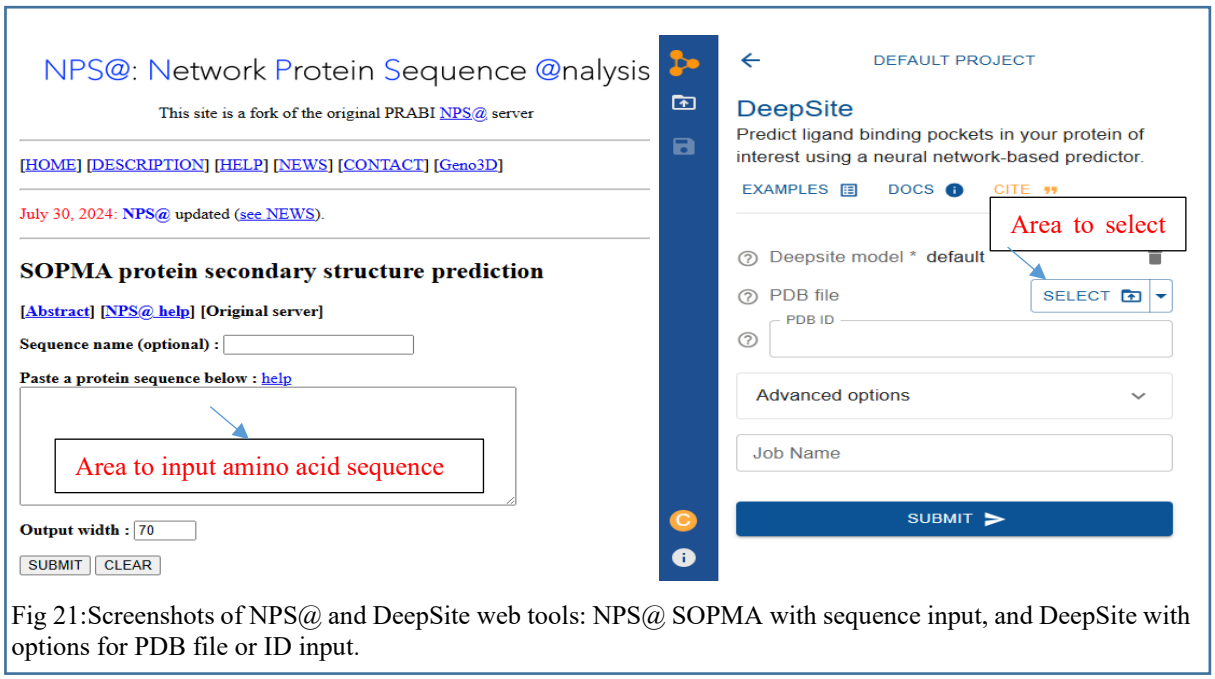

Fig 21:Screenshots of NPS@ and DeepSite web tools: NPS@ SOPMA with sequence input, and DeepSite with options for PDB file or ID input.

iMOD (Internal Modes Analysis) is a computational tool used in molecular simulations to study protein flexibility and structural changes that may affect drug binding and function. It is an interactive web-based platform that utilizes normal mode analysis (NMA) to predict molecular flexibility and transition pathways while maintaining structural integrity. It offers features such as motion animations, vibrational analysis, and trajectory modeling, making it useful for exploring conformational changes in macromolecules. Designed for both beginners and experts, iMODS provides customizable modeling options and advanced visualizations of molecular dynamics (MD). As a freely available resource, it supports research in structural biology, molecular modeling, and drug discovery(Lopéz-Blanco *et al.*, 2011).

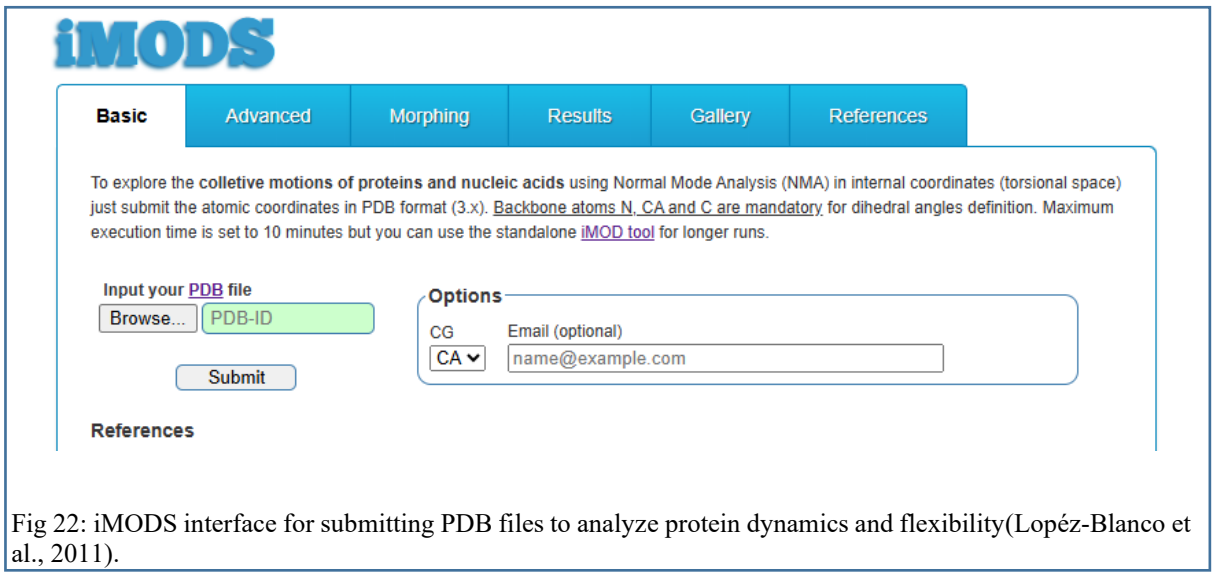

Fig 22: iMODS interface for submitting PDB files to analyze protein dynamics and flexibility(Lopéz-Blanco et al., 2011).

These powerful digital tools have reshaped the way we discover new drugs. By combining techniques like molecular docking, visualization, pharmacokinetics, and protein simulations, researchers can better understand how drugs interact with the body. This not only speeds up the discovery process but also helps create more effective and targeted treatments.

2.5 Molecular Modification in Drug Discovery

Developing new drugs is a long, expensive, and uncertain process, but molecular modification offers a smarter way to improve existing medications. By making small changes to a drug's molecular structure, scientists can enhance its effectiveness, improve its solubility, and increase its selectivity while reducing side effects. This approach makes treatments safer and more efficient and speeds up drug development by building on what already works rather than starting from scratch(Nadendla and Yemineni, 2024).

A great example is Cyclophosphamide, a chemotherapy drug modified to be more stable and less toxic while effectively targeting cancer cells. These changes made it a key treatment for conditions like lymphoma, leukemia, and even some autoimmune diseases(Ogino and Tadi, 2025). Molecular modification isn't just for cancer drugs- it plays a crucial role in improving antibiotics, antivirals, and pain medications, helping to overcome issues like poor absorption or unwanted side effects. As medicine advances, refining existing drugs through molecular modification will continue to be a game-changer.

This process involves two main strategies: **molecular disjunction**, which simplifies drug structures to create improved analogs (such as modifying estradiol to develop trans-diethylstilbestrol), and **molecular conjunction**, where different molecules are combined to enhance therapeutic effects. Techniques like **molecular addition** (introducing new functional groups to improve solubility) help refine drug properties. Additionally, specialized modifications like **ring closure and opening**, used in anticancer drugs like Taxol further enhance drug performance. These molecular modifications not only improve existing treatments but also provide a cost-effective way to develop safer and more targeted therapies(Nadendla and Yemineni, 2024).

Molecular modification and modeling are transforming drug development, but they come with challenges. Small chemical tweaks can unexpectedly change a drug's potency or absorption, requiring extensive testing to ensure safety and effectiveness. On the other hand, molecular modeling, which helps predict how drugs will behave, faces its hurdles. Simulating complex biochemical systems is still tricky- factors like protein motion, solvent interactions, and the limitations of machine learning models make accurate predictions difficult(Jogalekar, 2021).

Beyond technical issues, the human side of drug discovery presents another challenge. Modelers rely on chemists to test their predictions, but without direct control over which compounds get made, they often don't get the feedback needed to refine their models. However, advances in AI and computational chemistry are improving predictions, and better collaboration between scientists could help bridge these gaps. With the right approach, molecular modification and modeling can lead to faster, safer, and more effective treatments(Jogalekar, 2021; Nadendla and Yemineni, 2024).

2.5.1 Quantitative Structure-Activity Relationship

Quantitative Structure-Activity Relationship (QSAR) models help scientists predict how different chemical compounds will behave based on their molecular structure. However, their accuracy depends on careful data selection and validation- otherwise, they might capture random noise instead of real patterns(Davis, 2017).

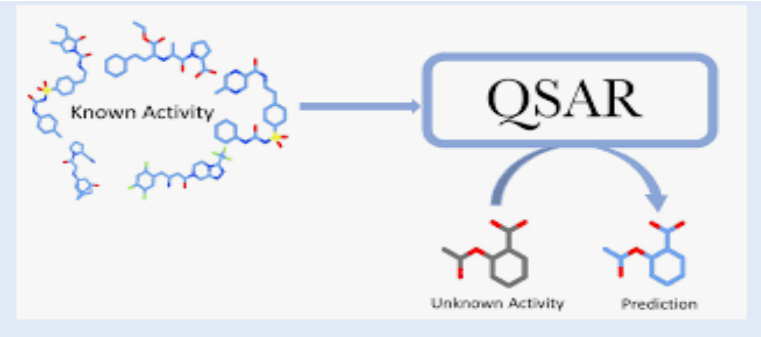

Fig 23: QSAR Depiction

The WHO declared COVID-19, caused by SARS-CoV-2, a global pandemic due to its rapid spread and severe social and economic impact. To accelerate the search for effective treatments, researchers explored existing inhibitors designed for other viruses as a starting point for developing anti-SARS-CoV-2 drugs. One powerful approach in this process was QSAR modeling, which helped identify and evaluate potential drug candidates. By enabling the screening of large molecular databases, QSAR played a key role in discovering new antiviral treatments(Bastikar *et al.*, 2022).

2.6 Key Insights and Path Forward

The search for effective COVID-19 treatments has shown just how important targeted antiviral drugs are- especially those that block key viral enzymes like M^{pro} and PL^{pro}. These enzymes help the virus replicate and spread, but because they stay largely unchanged across different coronavirus variants, they make excellent long-term drug targets (Tumskiy *et al.*, 2023). Stopping them in their tracks could significantly slow the virus, making this approach a promising way to develop broad-spectrum antiviral medications.

Advancements in AI, molecular modeling, and predictive analytics have made it easier to identify potential drug candidates. Scientists can now screen thousands of natural and synthetic compounds, predicting their effectiveness before even stepping into a lab. However, no matter how powerful computational tools are, real-world testing is essential. Lab experiments- like enzyme inhibition studies and cell culture tests- help confirm whether a compound truly works against the virus, ensuring that only the most promising candidates move forward.

Nature has always been a source of powerful medicines, and traditional medicinal plants are once again proving their value. **Tinospora** species, long used in Ayurvedic medicine, contain bioactive compounds with potential antiviral properties. One of these, **Tinosporaside**, shows promise but may need slight structural modifications to improve how it works in the body. Enhancing its stability, potency, and absorption through molecular modification could make it a stronger and more reliable treatment option.

By integrating advanced technology with traditional medicinal knowledge, researchers are driving the development of safer and more effective antiviral therapies. This strategy is not only crucial for combating COVID-19 but also essential for anticipating and addressing future viral threats, ensuring better preparedness and global health protection.

2.7 Conceptual framework

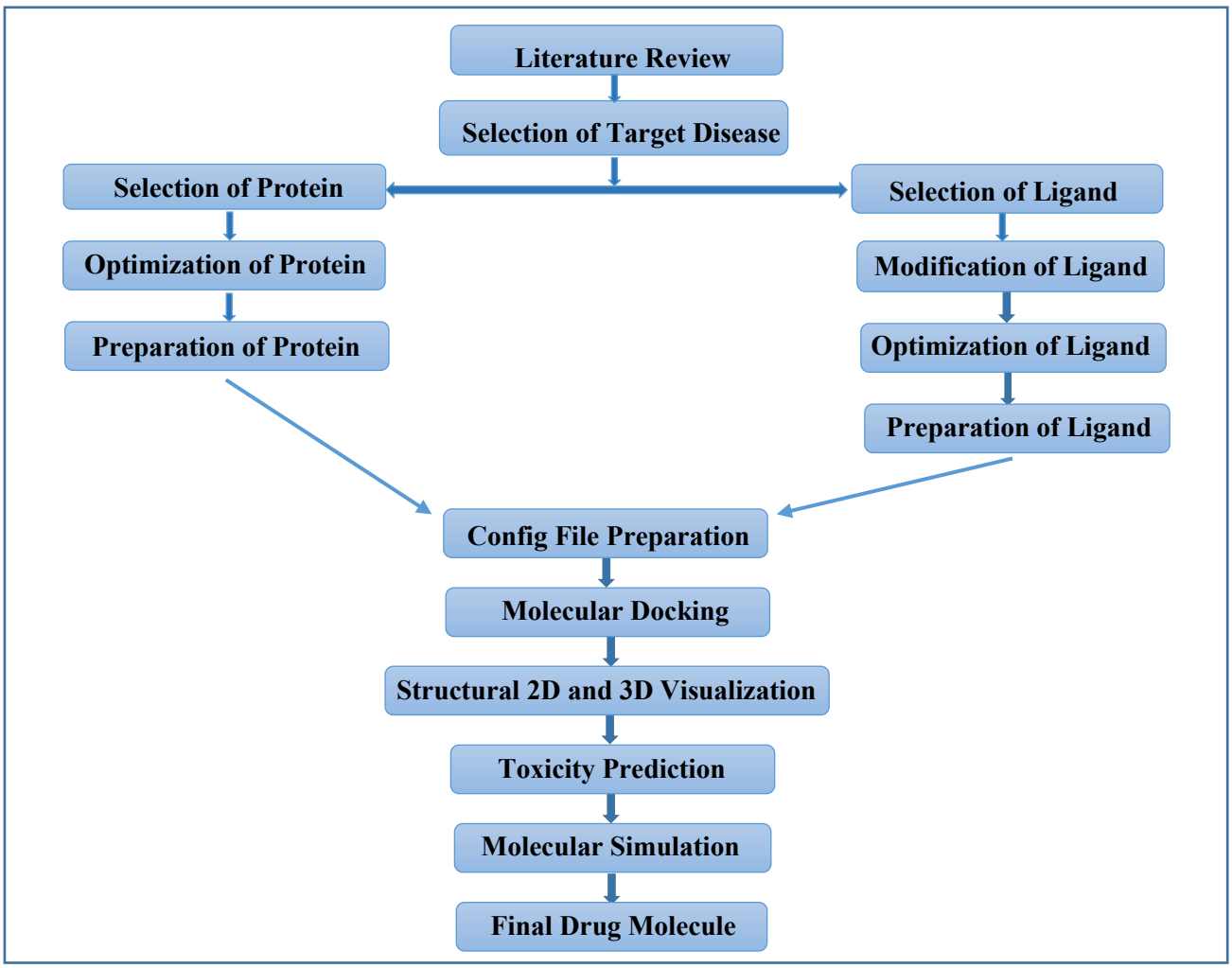

CHAPTER 3

RESEARCH METHODOLOGY

This section outlines the strategy and steps used to explore potential COVID-19 treatments through computational drug discovery. Instead of relying on traditional lab experiments or previously collected data, this study harnessed the power of in-silico techniques to simulate how modified compounds might interact with two crucial viral proteins. The approach adopted here is efficient, cost-effective, and timely, qualities that are essential in addressing rapidly evolving global challenges. What follows is an in-depth look into the rationale behind choosing this method, the structure of the workflow, how it was implemented, and the various digital tools and simulations that supported each phase.

3.1. Rationale for Method Selection

The methodology hinges on computational drug discovery- an approach that uses sophisticated software to predict how potential drug molecules might behave inside the human body. This strategy has gained popularity due to its ability to screen large numbers of compounds quickly, and without the high costs or time commitments typically associated with laboratory-based research. It accelerates discovery while adhering to **green chemistry principles** by minimizing chemical waste and resource use. Techniques such as molecular docking and MD simulations make it feasible to analyze interactions at the atomic level, providing meaningful predictions about binding affinities, stability, and safety.

This study focused on two target proteins from the SARS-CoV-2 virus: M^{pro} and PL^{pro}. These proteins are essential for the replication of the virus, making them excellent targets for antiviral drug development. Their structures have been resolved and are publicly accessible through PDB, offering high-quality data to base simulations on. To maintain consistency and scientific rigor, additional computational tools like BIOVIA Discovery Studio, ADT, AutoDock Vina, ChemSketch, SwissADME, pkCSM, ProTox-3.0, SOPMA, ProtParam, DeepSite, PyMOL, PLIP, and iMODS were used throughout the research.

Table 1: Databases and Software Links

Application Area	Databases and Software	Websites	Software Access (Offline & Online Versions)
Docking Software	BIOVIA Discovery Studio	https://discover.3ds.com/discovery-studio-visualizer-download	Offline
	AutoDock Tools	https://ccsb.scripps.edu/mgltools/downloads/	Offline
	AutoDock Vina	https://vina.scripps.edu/downloads/	Offline
Design software	ChemSketch	https://www.acdlabs.com/resources/free-chemistry-software-apps/chemsketch-freeware/	Offline
	Syntelly	https://app.syntelly.com/smiles2iupac	Online
ADMET and Toxicity Prediction Software	SwissADME	http://www.swissadme.ch/	Online
	pkCSM	https://biosig.lab.uq.edu.au/pkcsm/	Online
	ProTox-3.0	https://tox.charite.de/protox3/	Online
Protein Structure Analysis software	SOPMA	https://npsa.lyon.inserm.fr/cgi-bin/npsa_automat.pl?page=/NPSA/npsa_sopma.html	Online
	Protparam	https://web.expasy.org/protparam/	Online
Binding site Prediction	DeepSite	https://open.playmolecule.org/tools/deepsite	Online
Protein data Bank	PDB	https://www.rcsb.org/	Online
Ligand Database	PubChem	https://pubchem.ncbi.nlm.nih.gov/	Online
Visualization and Analyzation software	PyMOL	https://pymol.org/edu/	Offline
	PLIP	https://plip-tool.biotec.tu-dresden.de/plip-web/plip/result/b6cb1f94-09e7-466b-9873-27134b77ee3a	Online
	iMODS	https://imods.iqf.csic.es/	Online

3.2. Design of the Quantitative Methodology

The entire research process was structured like a sequential pipeline, where each step laid the foundation for the next. The major stages included protein selection and preparation, lead molecule selection, modification and preparation, docking studies, interaction analysis, toxicity and ADME assessments, and finally, stability simulations(mgl-admin, 2018; Joshi and Kaushik, 2021).

3.2.1 Onion Framework

The study adopted a positivist paradigm, using a deductive approach to test hypotheses through computational methods. It followed a quantitative, cross-sectional design, employing in-silico tools (Seuring *et al.*, 2024).

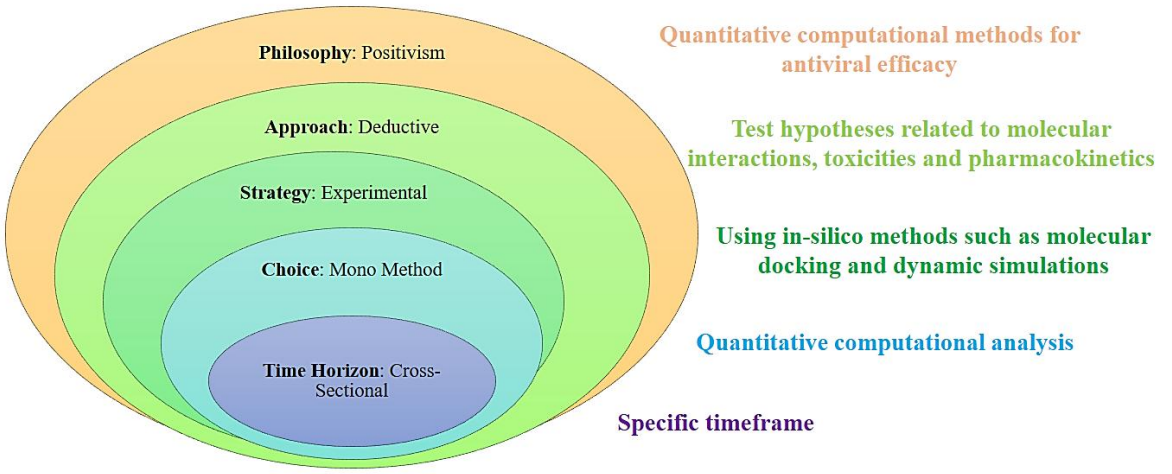

Fig 24: Research Onion

3.2.2 Protein Selection

Two standout proteins were selected for docking studies: 7ALH, M^{pro} with a sharp resolution of 1.65 Å, and 6WX4, PL^{pro} bound to the inhibitor VIR251, resolved at 1.66 Å. Both were obtained from PDB in PDB format, and labelled as Protein A (7ALH) and Protein B (6WX4) for this study.

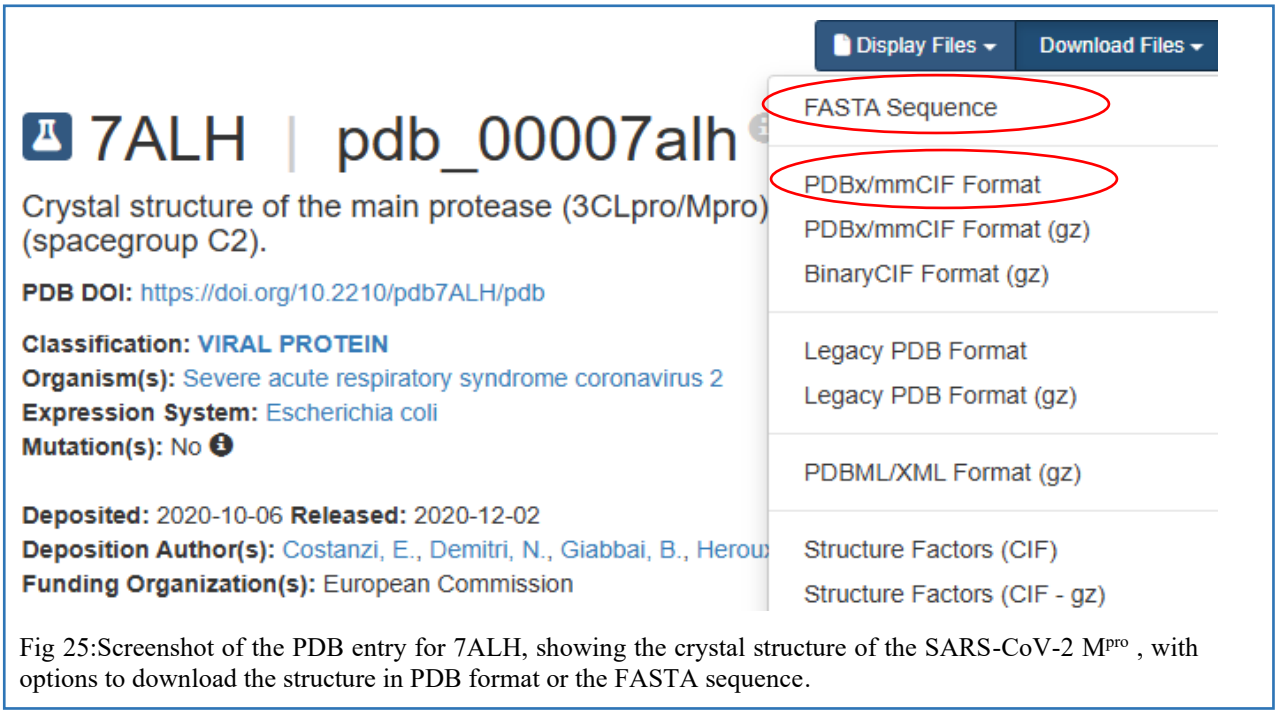

Fig 25:Screenshot of the PDB entry for 7ALH, showing the crystal structure of the SARS-CoV-2 M^{pro} , with options to download the structure in PDB format or the FASTA sequence.

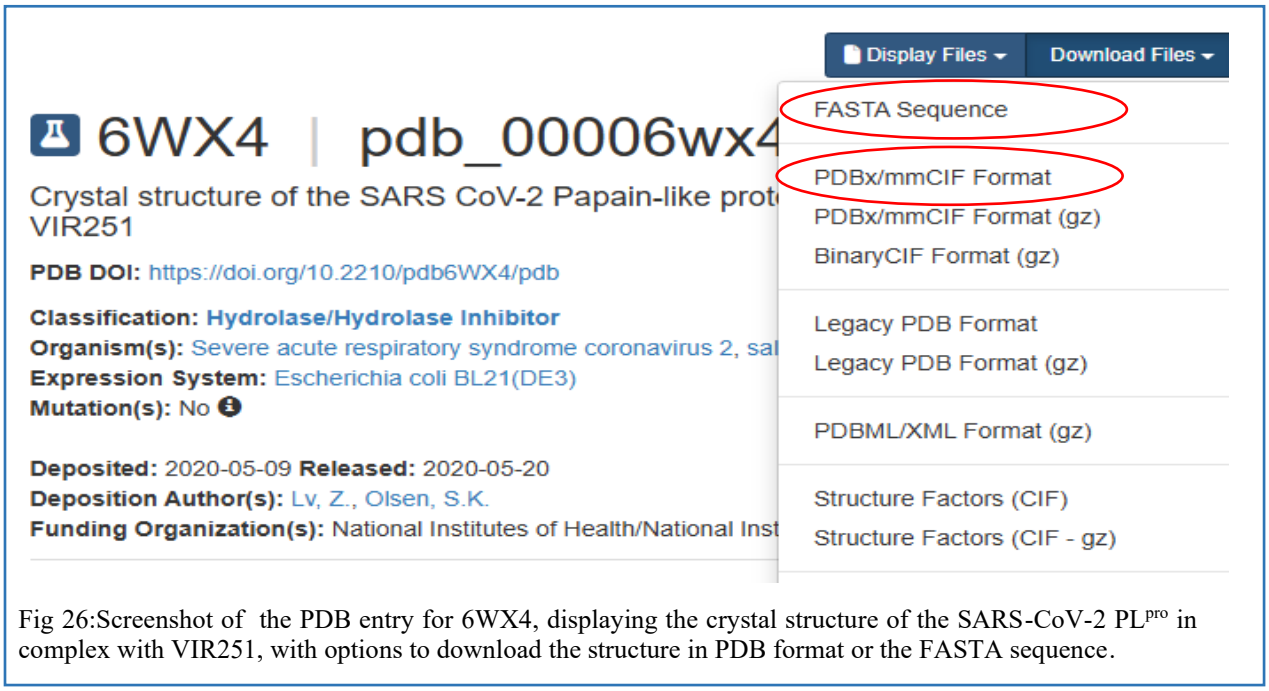

Fig 26:Screenshot of the PDB entry for 6WX4, displaying the crystal structure of the SARS-CoV-2 PL^{pro} in complex with VIR251, with options to download the structure in PDB format or the FASTA sequence.

Structural quality checks showed that **Chain A of 7ALH** is a well-modelled structure, exhibiting very high geometric quality, with 97% of its residues free from structural issues and showing an excellent fit to the electron density. Likewise, **Chain D of 6WX4** demonstrates high geometric quality**,** with 93% of residues having no issues and a good overall fit to the electron density**.** These metrics indicate that both chains are structurally reliable and well-suited for further analysis, including molecular docking studies.

Fig 27:Structural quality assessment of Chain A, a 306-residue protein, showing 97% of residues with ideal geometry (green) and 3% minor issues (yellow), with a minimal fraction exhibiting poor electron density fit (red), indicating a high-quality model for structural analysis.

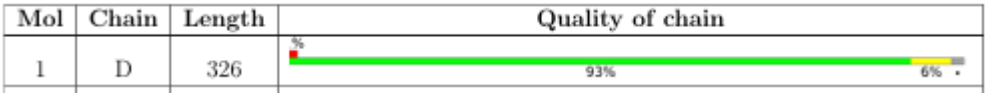

Fig 28: Quality assessment of Chain D (6WX4), a 326-residue protein, displaying 93% of residues with ideal geometry (green), 6% with minor geometric issues (yellow), and 1% un-modeled (grey), with a small fraction showing poor electron density fit (red), confirming its reliability for structural studies.

FASTA sequences (text based format) extracted from the PDB files were analysed using ProtParam to evaluate basic physicochemical properties and overall stability. For 7ALH, the

theoretical pI was found to be around 5.95, with a molecular weight of approximately 33.8 kDa and an instability index classifying it as stable. Similarly, 6WX4 had a theoretical pI of 7.94, a molecular weight of roughly 37.1 kDa, and was also predicted to be stable.

SOPMA was used to gain insights into secondary structure composition. The analysis for 7ALH showed 24.51% alpha helices, 27.78% extended strands, and 47.71% random coils, reflecting a balanced and flexible structural profile. For 6WX4, the predictions were 25.46% helices, 25.46% strands, and 49.08% coils, indicating a similarly well-distributed architecture. These structural and physicochemical features support the suitability of both proteins for molecular docking studies.

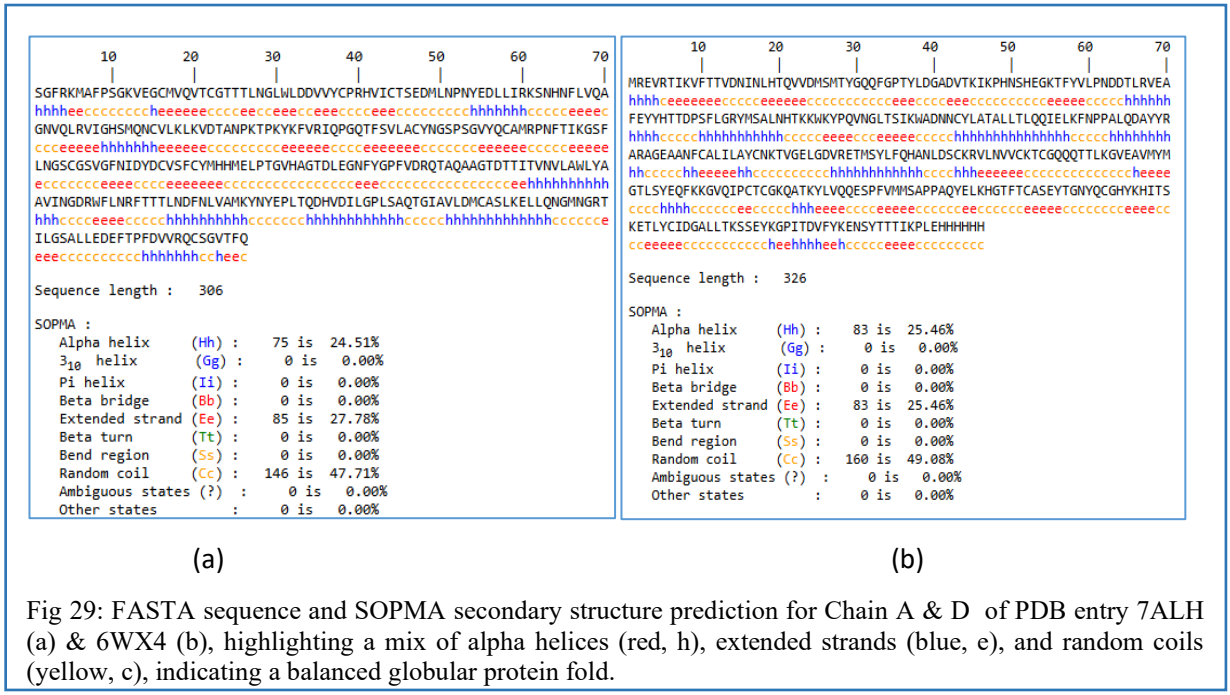

Fig 29: FASTA sequence and SOPMA secondary structure prediction for Chain A & D of PDB entry 7ALH (a) & 6WX4 (b), highlighting a mix of alpha helices (red, h), extended strands (blue, e), and random coils (yellow, c), indicating a balanced globular protein fold.

3.2.3 Molecule Selection and Modification

Tinosporaside, a bioactive compound from *T. cordifolia*, was chosen as the lead molecule. *T. cordifolia* is well-known properties, makes Tinosporaside a strong base for further modifications. A total of 56 derivatives (T1–T56) were designed using ChemSketch by modifying side chains and functional groups to enhance pharmacological activity. These modifications incorporated structural features known to contribute to antiviral efficacy.

Each derivative was screened using SwissADME to evaluate drug-likeness based on Lipinski's RO5. The compounds passing the criteria were advanced to the docking phase. This pre-screening ensured that only orally bioavailable candidates progressed further, optimizing both efficacy and safety.

3.3 Execution of the Quantitative Workflow via Computational Tools

The implementation involved multiple stages, each supported by specific tools and software.

3.3.1 Protein Preparation for Docking

Protein structures were opened in BIOVIA Discovery Studio to remove extraneous elements such as water molecules and additional ligands, particularly VIR251 in 6WX4 (Protein B). These extraneous molecules can distort the binding pocket and negatively affect docking accuracy.

Following the addition of hydrogens, the two proteins were individually saved as PDB files, labeled Protein A and Protein B, for use in subsequent docking studies. Adding hydrogen atoms to molecular docking structures is vital because they enable the accurate representation of biomolecular interactions, especially hydrogen bonds, which are essential for protein-ligand binding, DNA stability, and molecular functionality, thereby allowing docking software to effectively predict binding poses and interaction patterns.

The PDB files were opened in ADT, where a thorough inspection and correction of missing atoms took place, followed by the addition of Kollman charges to enhance the docking simulation's accuracy by better capturing the electrostatic interactions between the protein and ligand- essential for predicting binding affinity and mode- before being saved as a PDBQT (Protein Data Bank, Charges, and Atom Type) file with the same name for subsequent docking studies.

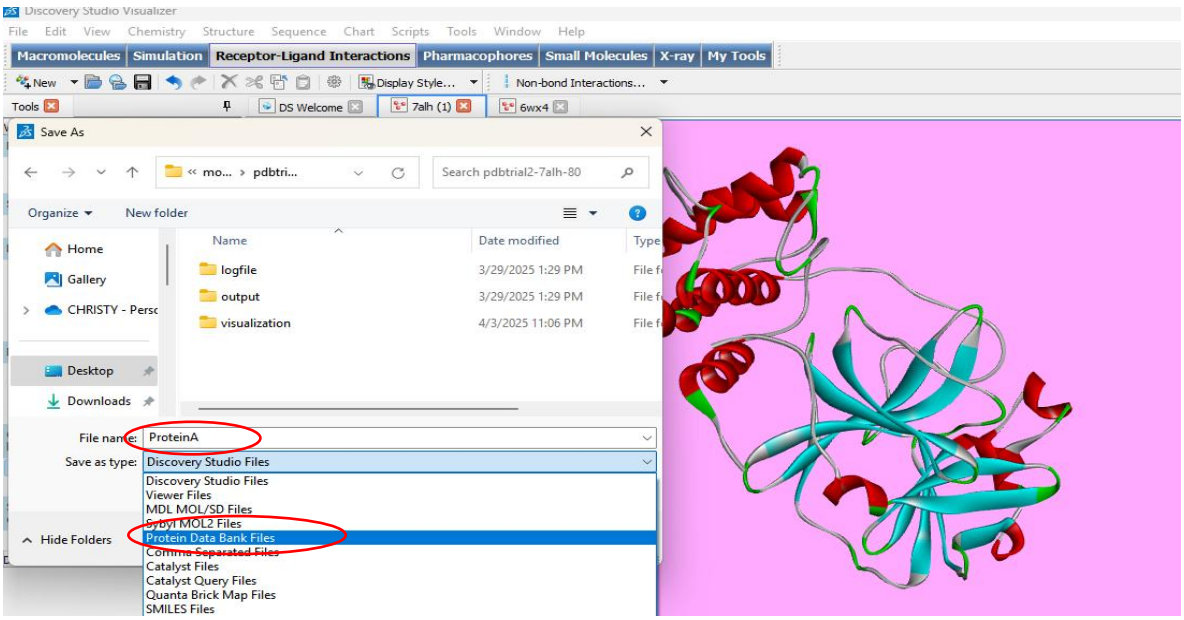

Fig 30: BIOVIA Discovery Studio interface displaying the cleaned structure of Protein A (derived from 7ALH) after hydrogen addition, with the protein saved as a PDB file. Similarly, Protein B (derived from 6WX4) is also saved as a PDB file.

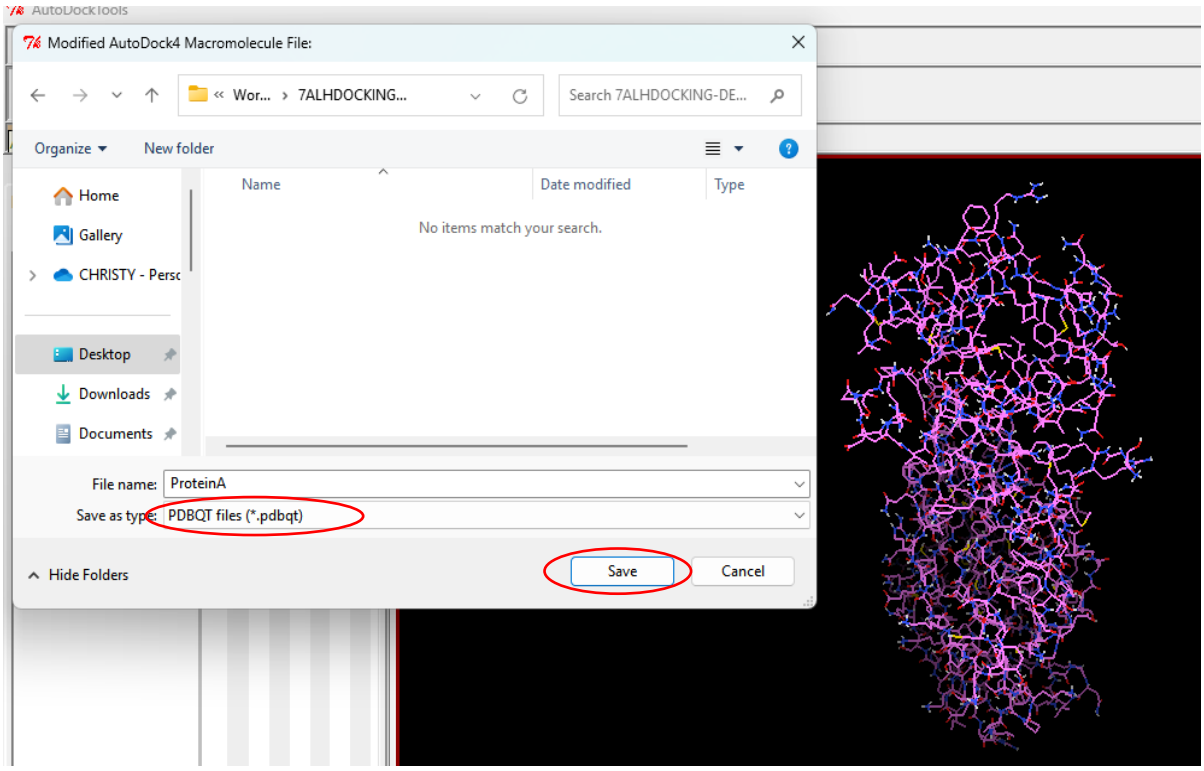

Fig 31: AutoDock Tools interface displaying ProteinA (from 7ALH) after atom correction and Kollman charge addition, saved as a PDBQT file for docking, with ProteinB (from 6WX4) prepared similarly.

3.3.2 Ligand Preparation

3.3.2.1 Lead Preparation

Tinosporaside (T0) was downloaded as a Structure-Data File (SDF) from PubChem, opened in BIOVIA Discovery Studio to add hydrogens, before adding hydrogens structure was optimised in Chemsketch, and saved as a PDB file. It was subsequently loaded into ADT to detect the root, select torsions- locking rotatable bonds to maintain structural integrity during docking- and then saved as a PDBQT file for the docking process.

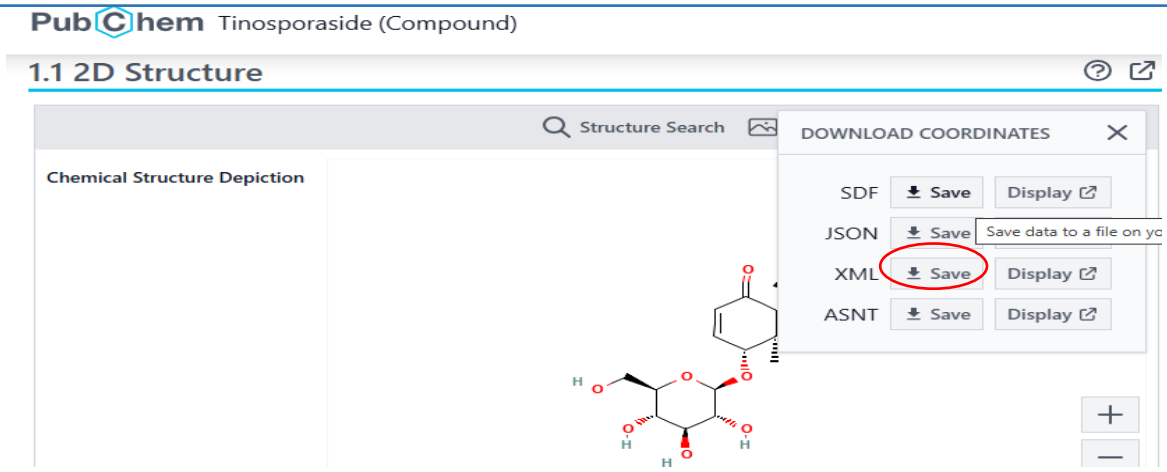

Fig 32: PubChem interface showing the 2D structure of T0, with options to download its coordinates as an SDF file for molecular docking preparation.

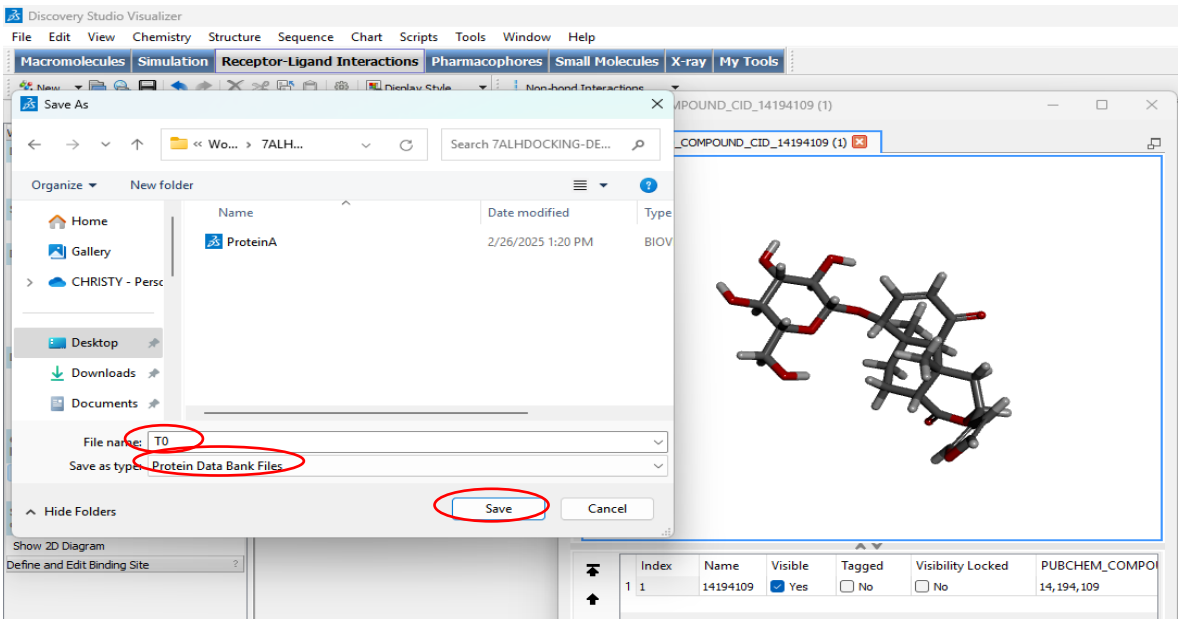

Fig 33: BIOVIA Discovery Studio interface displaying the structure of T0 and saved as a PDB file.

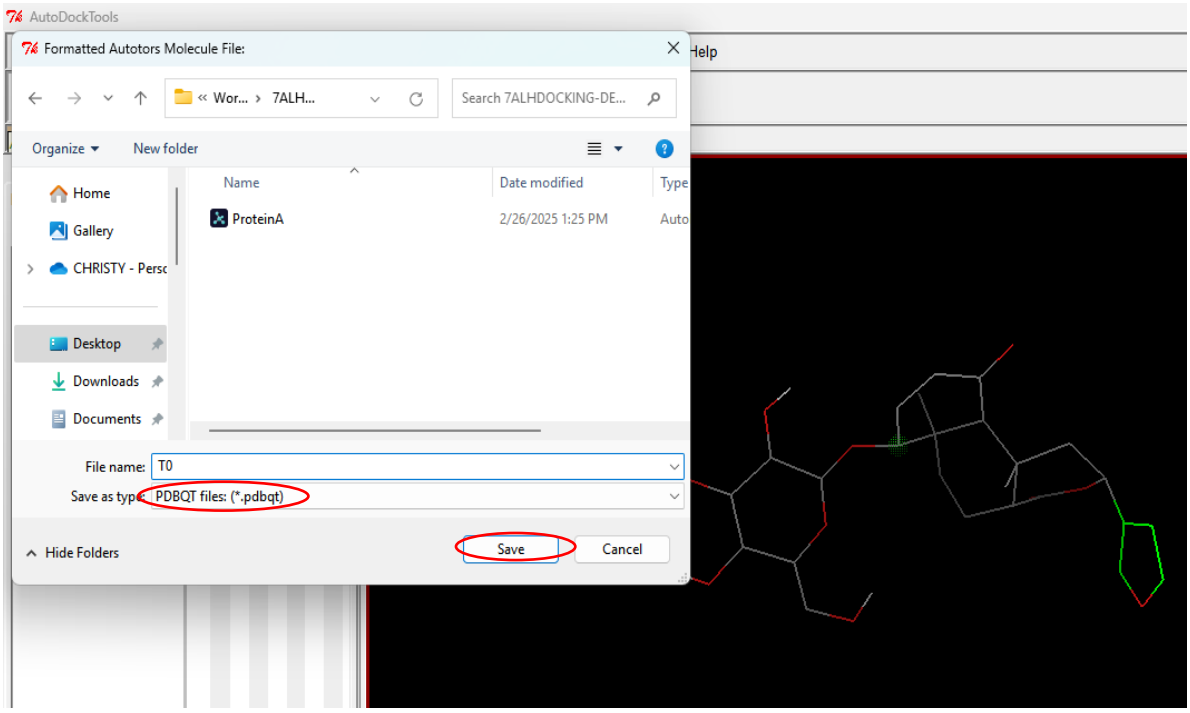

Fig 34:AutoDock Tools interface displaying T0, & saved as a PDBQT file for docking.

3.3.2.2 Modified Structure Preparation

The SMILES notation for Tinosporaside was obtained from PubChem and used to generate its 2D molecular structure in ChemSketch. Based on this initial structure, 56 modified derivatives (T1–T56) were designed by incorporating structural variations to explore potential enhancements in antiviral activity. The modified ligands were sketched in ChemSketch, and those that followed RO5 were saved in MOL format after removing explicit hydrogen atoms and optimizing the molecular geometry for stability. These MOL files were then imported into BIOVIA Discovery Studio, prepared for docking by adding necessary hydrogen atoms, saved to the PDB file, and subsequently saved in PDBQT format (in ADT) - ready for molecular docking similar to the reference ligand T0.

Table 2: PubChem ID and SMILES Notation for T0

Compound	**PubChem ID**	**SIMLES Notation**
Tinosporaside (T0)	14194109	O=C1O[C@@H](C[C@@]2(C)[C@@H]3C(=O)C=C[C@@H](O[C@@H]4O[C@H](CO)[C@@H](O)[C@H](O)[C@H]4O)[C@]3(C)CC[C@@H]12)c1ccoc1

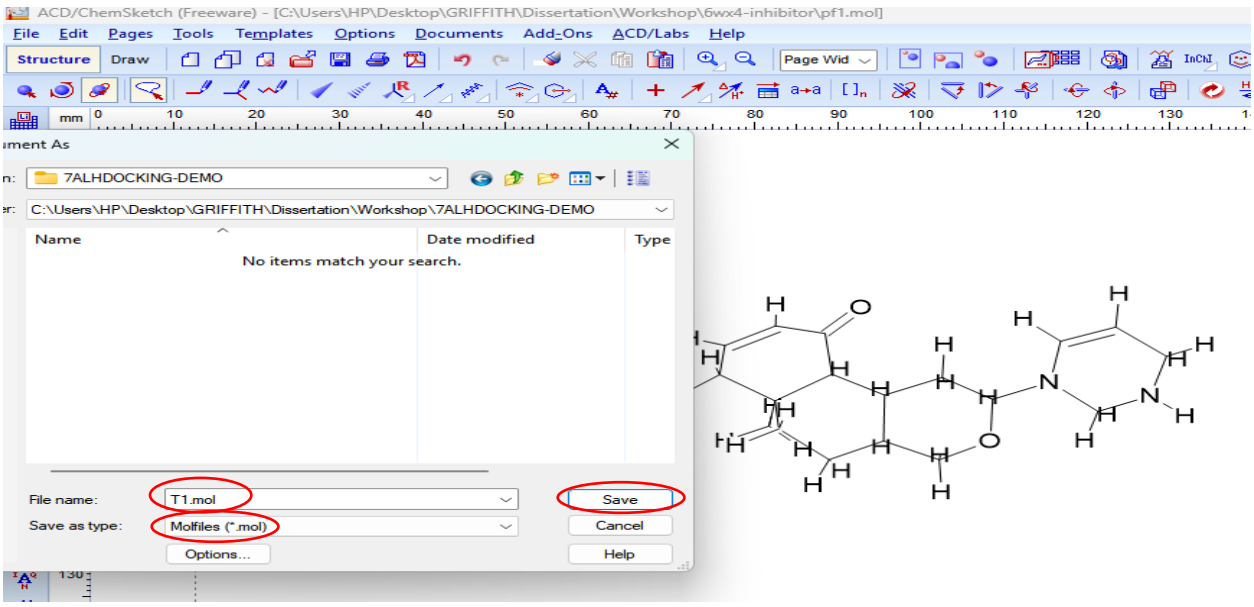

Fig 35: Structure Preparation and Saving of Modified Ligand (T1) in ChemSketch. Similarly, other 45 molecules that followed Lipinski RO5

3.3.3 Docking Configuration

A configuration file (config file) was created to define the parameters for AutoDock Vina. Binding site coordinates were identified using DeepSite:

- For 7ALH: x = -0.64, y = -15.561, z = -37.936
- For 6WX4: x = 1.82, y = -19.97, z = -45.86

A search box with dimensions of 80 Å in all directions ensured that the docking space was ample enough to accommodate ligand movement. The exhaustiveness parameter was set to 8 (default value), balancing thoroughness with computational efficiency.

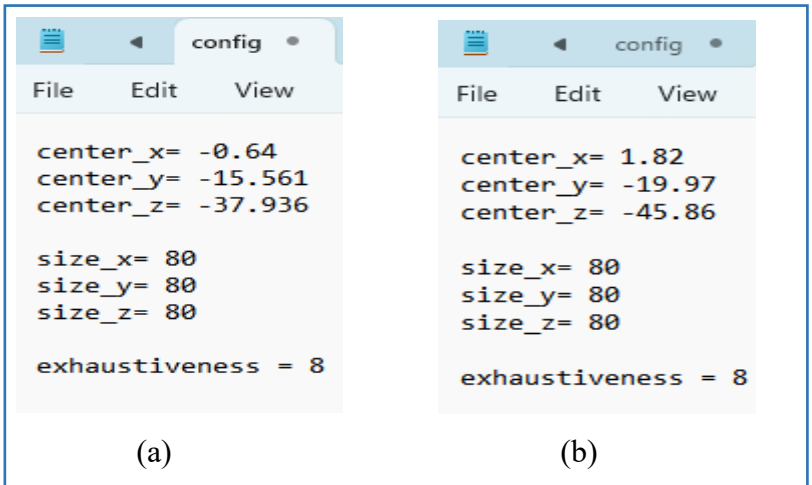

(a) (b)

Fig 36: Config file for Protein A (a) and Protein B (b)

3.3.4 Folder Management

Each protein was assigned its directory containing the PDBQT files for the protein and ligands (T1 –T46), the config file, the Vina program, and separate folders for storing docking results and log files. This structured organization facilitated smooth execution and easy tracking of outputs.

3.3.5 Preliminary Evaluation and Refinement with Tinosporaside

An initial assessment was performed to investigate the binding interactions of the lead molecule, T0, with the target proteins prior to full-scale docking simulations. Using binding site data from DeepSite, a config file was created, and Tinosporaside was docked with proteins A and B, followed by the analysis of docking scores and visualization in BIOVIA Discovery Studio to determine key interacting amino acids. Toxicity evaluations were also conducted to confirm the lead molecule's viability, laying a robust groundwork for further optimization in the design process.

3.3.6 Docking Process

3.3.6.1 Protein-Ligand Docking

A command-line script automated the docking of ligands (T1-T40) against each protein. AutoDock Vina systematically analyzed each ligand, determining binding affinity by identifying the pose with the lowest binding energy (kcal/mol). Each docking batch was completed within 10–15 minutes, showcasing the efficiency of in-silico techniques.

Fig 37: Command used to run the vina- batch docking (where molecule*- T1-T40)

3.3.6.2 Benchmarking

The known inhibitor Nirmatrelvir (Shawky *et al.*, 2024)(an antiviral drug developed by Pfizer against M^{pro}) and PF-07957472(Garnsey *et al.*, 2024) (PL^{pro} inhibitor) were docked with both proteins A and B as control benchmarks. Comparing their binding scores and amino acid interactions with those of the new ligands helped contextualize the results and validate the docking process.

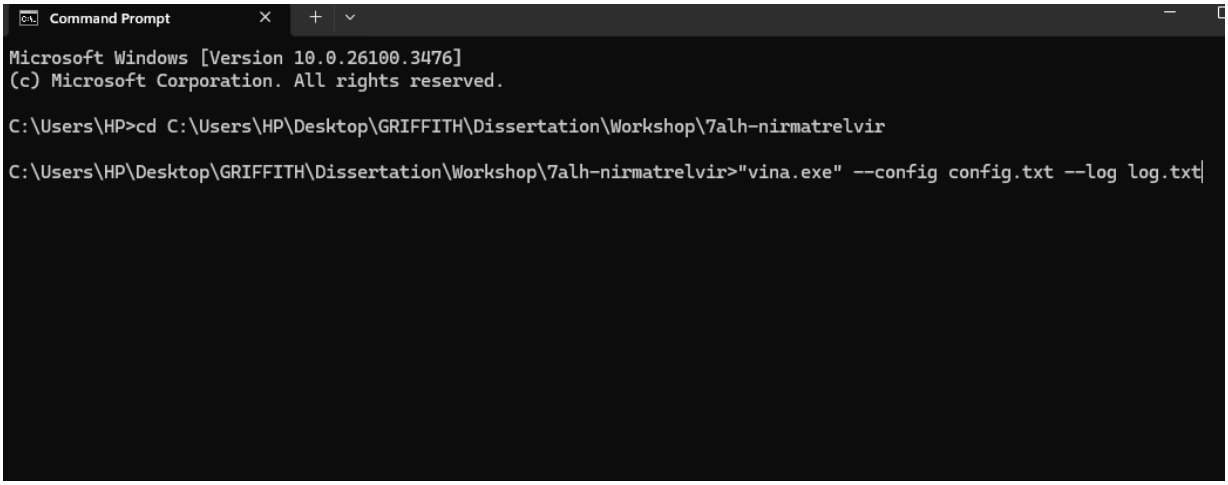

Fig 38: Command used for docking the individual ligand and protein (in case of benchmarking analysis and T0 docking)

3.3.7 Visualization and Interaction Analysis

3.3.7.1 Docking Output Analysis Using PyMOL and Discovery Studio

The docking output files (With Increased negative binding affinity) along with the corresponding protein PDB files were visualized using PyMOL to generate 3D representations of the docked complexes. The best docking poses were then exported as a PDB file and reloaded into BIOVIA Discovery Studio for further interaction analysis. Discovery Studio provided comprehensive 2D and 3D interaction maps, highlighting key amino acid interactions. These visualizations offered deeper insights into the binding mechanisms and stability of the ligand-protein complexes.

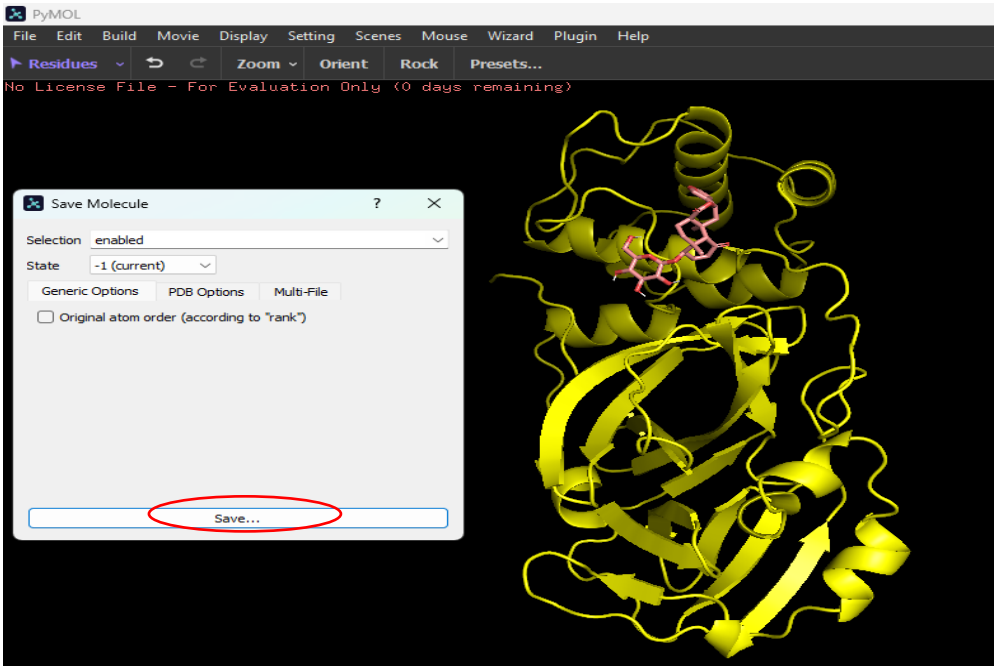

Fig 39: Pymol interface containing the protein A- pdb file (yellow) and ligand T0- outfile (pink). Saved as a PDB file & similarly, other selected ligands

3.3.7.2 Hydrogen and hydrophobic interactions

These interactions were noted for the selected ligands using PLIP. Hydrogen bonding and hydrophobic interactions are crucial in molecular docking because they significantly influence the binding affinity and specificity of ligand-protein complexes, driving the formation of stable and energetically favourable interactions. The PDB file of the docked protein-ligand was uploaded to PLIP to determine the interactions.

3.3.8 Toxicity and ADME Profiling

Only the most promising compounds underwent digital toxicity screening. Their SMILES notations were input into:

- **SwissADME**: to evaluate pharmacokinetics such as Gastrointestinal (GI) absorption and Blood-brain barrier (BBB) permeability.
- **pkCSM**: to predict ADME profiles, mainly focusing on systemic toxicity.
- **ProTox-3.0**: to assess potential toxicological effects and to predict the class of drug.

Compounds with relatively low toxicity and promising pharmacokinetic properties were selected for further consideration.

3.3.9 Stability Simulations

The final step involved assessing the structural stability of the docked complexes using simulation platforms:

- **iMODS**: conducted NMA to analyze deformability, B-factors (thermal stability), eigenvalues (energy required for movement), and variance. These metrics helped evaluate how well the complexes would perform under biological conditions.

3.4. Evaluation and Significance

The combination of tools and techniques used was not arbitrary but intentionally designed to maximize predictive accuracy while minimizing resource use. Each software component played a distinct role:

- **AutoDock Vina** efficiently predicted binding affinities.

- **PyMOL** and **Discovery Studio** aided in visualizing docking results and analyzing ligand-protein interactions.

- **PLIP** identified key hydrogen bonds and hydrophobic interactions important for binding.

- **SwissADME**, **pkCSM**, and **ProTox-3.0** assessed pharmacokinetics and toxicity to ensure safety and drug-likeness.

- **iMODS** validated complex stability under physiological conditions.

Together, these computational methods created a powerful and efficient workflow, one that could screen countless compounds, pinpoint the most promising ones, and assess their potential, all without the need for a physical lab. This approach proved to be not only robust and scalable but also incredibly valuable during times of urgency, such as the COVID-19 pandemic. In conclusion, this research highlights a modern, data-driven approach to drug discovery that brings together powerful computational tools and a well-structured workflow. It also shows how computational biology can play a broader role in responding to global health crises, now and in the future.

CHAPTER 4

FINDINGS AND ANALYSIS

This section presents the results and quantitative analyses from computational studies optimizing Tinosporaside as a potential COVID-19 therapeutic targeting SARS-CoV-2 proteases. Using various in-silico tools, we evaluated binding affinity, stability, and drug-likeness.

4.1 Analysis of SARS-CoV-2 Proteases as Drug Targets (Proteins)

The amino acid sequences of two key SARS-CoV-2 proteases were retrieved and analysed to evaluate their potential as drug targets for tinosporaside. As part of the study:

- The **Main Protease (M^{pro})**
  - **PDB ID**: 7ALH
  - **Chain**: A
  - **Designated as**: **Protein A**
- The **Papain-like Protease (PL^{pro})**
  - **PDB ID**: 6WX4
  - **Chain**: B
  - **Designated as**: **Protein B**

Both proteins were analyzed using **ProtParam** and **SOPMA** to evaluate their physicochemical properties and secondary structures. The **ProtParam** revealed **GRAVY (**Grand Average of Hydropathicity) **scores** of -0.019 for Mpro and -0.433 for PLpro**,** indicating slight hydrophilicity and good solubility in aqueous environments. Additionally, both proteins were predicted to be **stable**, supporting their suitability for computational analysis. **SOPMA** results further confirmed structural integrity, validating their use in **molecular docking and MD simulations**. These features highlight their potential to interact favourably with Tinosporaside as a therapeutic agent. The full amino acid sequences are provided in Annexure I.

4.2 Tinosporaside (Ligand) and Modified Compounds Analysis

4.2.1 Molecular Profiles

A library of fifty-six structurally modified derivatives of the parent ligand Tinosporaside (designated as T0) was successfully generated for docking studies. The modifications were designed to explore QSAR and improve binding affinity. The SMILES notations and molecular formulas of all compounds, including T0, were generated using **ChemSketch** and compiled in Annexure II**.**

4.2.2 Structural Modifications using ChemSketch

The chemical structures of T0 and its fifty-six modified compounds, along with their modifications and IUPAC names, are tabulated in Table 3. These modifications, including addition, deletion, substitutions, ring opening, and ring substitutions, were designed using ChemSketch based on substituents that enhance antiviral activity, lipophilicity, membrane permeability, binding affinity to viral proteins, hydrogen bonding, selectivity, and metabolic stability. Compounds forty-one to forty-six are additional molecules developed in later stages of the study, based on the structure of compound four, to improve the safety profile and reduce toxicity. The most accurate IUPAC names were generated using Syntelly.

Table 3:Chemical Structures, Structural Modifications, and IUPAC Names of Tinosporaside and Its Fifty-Six Designed Derivatives.

Compound No.	Structure	Modifications	IUPAC
T0	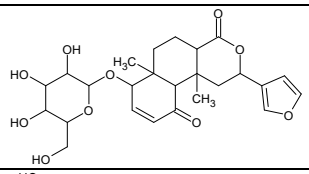	No Modifications	2-(furan-3-yl)-6a,10b-dimethyl-7-[3,4,5-trihydroxy-6-(hydroxymethyl)oxan-2-yl]oxy-2,4a,5,6,7,10a-hexahydro-1H-benzo[f]isochromene-4,10-dione
T1	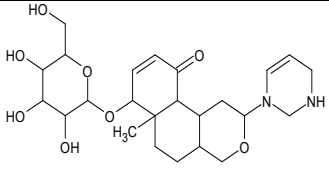	The furan ring was replaced with a six-membered ring. The ketone group was removed from the lactone ring. One of the methyl (CH_3) groups at the junction was removed.	2-(2,6-dihydro-1H-pyrimidin-3-yl)-6a-methyl-7-[3,4,5-trihydroxy-6-(hydroxymethyl)oxan-2-yl]oxy-2,4,4a,5,6,7,10a,10b-octahydro-1H-benzo[f]isochromen-10-one

T2	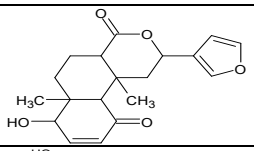	The attached glucose ring was removed.	2-(furan-3-yl)-7-hydroxy-6a,10b-dimethyl-2,4a,5,6,7,10a-hexahydro-1H-benzo[f]isochromene-4,10-dione
T3	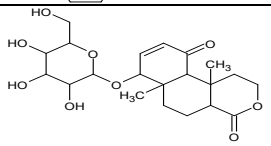	The attached furan ring was removed	6a,10b-dimethyl-7-[3,4,5-trihydroxy-6-(hydroxymethyl)oxan-2-yl]oxy-2,4a,5,6,7,10a-hexahydro-1H-benzo[f]isochromene-4,10-dione
T4	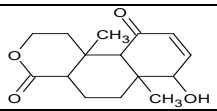	The attached furan ring and glucose ring were removed	7-hydroxy-6a,10b-dimethyl-2,4a,5,6,7,10a-hexahydro-1H-benzo[f]isochromene-4,10-dione
T5	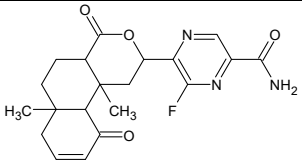	The attached glucose ring was removed. The furan ring was replaced with 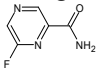 -part of favipiravir (Antiviral drug)	5-(6a,10b-dimethyl-4,10-dioxo-2,4a,5,6,7,10a-hexahydro-1H-benzo[f]isochromen-2-yl)-6-fluoropyrazine-2-carboxamide
T6	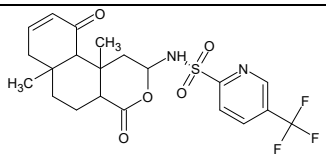	The attached glucose ring was removed. The furan ring was replaced with 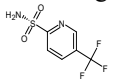 -part of Tipranavir (Antiviral drug)	N-(6a,10b-dimethyl-4,10-dioxo-2,4a,5,6,7,10a-hexahydro-1H-benzo[f]isochromen-2-yl)-5-(trifluoromethyl)pyridine-2-sulfonamide
T7	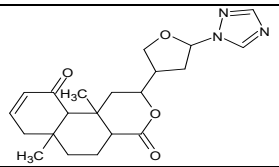	The attached glucose ring was removed. The triazole ring was attached to the furan ring	6a,10b-dimethyl-2-[5-(1,2,4-triazol-1-yl)oxolan-3-yl]-2,4a,5,6,7,10a-hexahydro-1H-benzo[f]isochromene-4,10-dione
T8	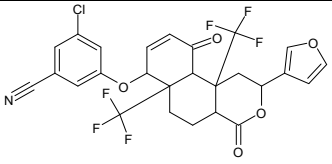	The attached glucose ring was substituted with 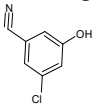 part of Doravirine (Antiviral Drug). Also Substituted two CH3 group at junctions with F3 (fluorine)	3-chloro-5-[[2-(furan-3-yl)-4,10-dioxo-6a,10b-bis(trifluoromethyl)-2,4a,5,6,7,10a-hexahydro-1H-benzo[f]isochromen-7-yl]oxy]benzonitrile
T9	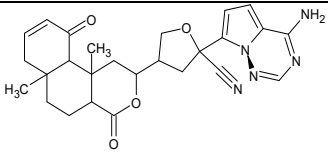	The attached glucose ring was removed. The furan ring was attached with 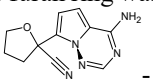 - part of remdesvir (antiviral drug)	4-(6a,10b-dimethyl-4,10-dioxo-2,4a,5,6,7,10a-hexahydro-1H-benzo[f]isochromen-2-yl)-2-(4-aminopyrrolo[2,1-f][1,2,4]triazin-7-yl)oxolane-2-carbonitrile
T10	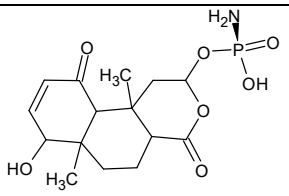	The attached glucose ring was removed. The furan ring was replaced with 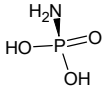 part of remdesvir (antiviral drug)	(7-hydroxy-6a,10b-dimethyl-4,10-dioxo-2,4a,5,6,7,10a-hexahydro-1H-benzo[f]isochromen-2-yl)oxyphosphonamidic acid

T11	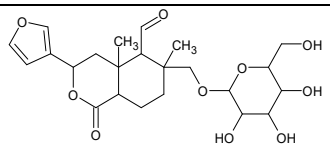	One of the rings of the diterpenoid structure was opened.	3-(furan-3-yl)-4a,6-dimethyl-1-oxo-6-[[3,4,5-trihydroxy-6-(hydroxymethyl)oxan-2-yl]oxymethyl]-3,4,5,7,8,8a-hexahydroisochromene-5-carbaldehyde
T12	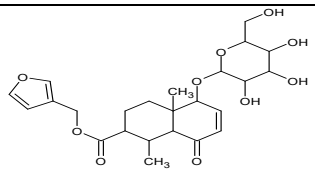	The lactone ring was opened.	furan-3-ylmethyl 1,4a-dimethyl-8-oxo-5-[3,4,5-trihydroxy-6-(hydroxymethyl)oxan-2-yl]oxy-1,2,3,4,5,8a-hexahydronaphthalene-2-carboxylate
T13	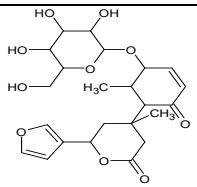	The middle ring was opened	6-(furan-3-yl)-4-methyl-4-[6-methyl-2-oxo-5-[3,4,5-trihydroxy-6-(hydroxymethyl)oxan-2-yl]oxycyclohex-3-en-1-yl]oxan-2-one
T14	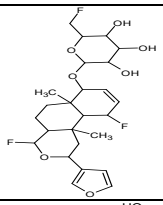	Ketone substitutions were replaced with halogen fluorine.	2-[[4,10-difluoro-2-(furan-3-yl)-6a,10b-dimethyl-2,4,4a,5,6,7,10,10a-octahydro-1H-benzo[f]isochromen-7-yl]oxy]-6-(fluoromethyl)oxane-3,4,5-triol
T15	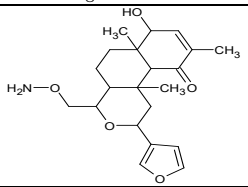	Substitution of ketone with CH30NH2 to the lactone ring. Glucose is replaced with CH3 group.	4-(aminooxymethyl)-2-(furan-3-yl)-7-hydroxy-6a,9,10b-trimethyl-1,2,4,4a,5,6,7,10a-octahydrobenzo[f]isochromen-10-one
T16	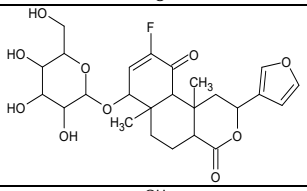	Substitution of Fluorine to the ring attached to glucose	9-fluoro-2-(furan-3-yl)-6a,10b-dimethyl-7-[3,4,5-trihydroxy-6-(hydroxymethyl)oxan-2-yl]oxy-2,4a,5,6,7,10a-hexahydro-1H-benzo[f]isochromene-4,10-dione
T17	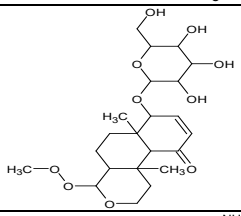	The furan ring was removed. Ketone of the lactone ring was replace to HOOCH3	4a,6a-dimethyl-4-methylperoxy-7-[3,4,5-trihydroxy-6-(hydroxymethyl)oxan-2-yl]oxy-2,4,5,6,7,10a-hexahydro-1H-benzo[f]isochromen-10-one
T18	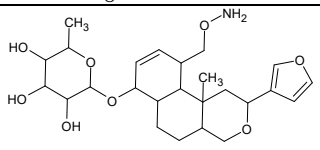	Removal of ketones. Addition of CH30NH2 to the ring near glucose	2-[[10-(aminooxymethyl)-2-(furan-3-yl)-10b-methyl-1,2,4,4a,5,6,6a,7,10,10a-decahydrobenzo[f]isochromen-7-yl]oxy]-6-methyloxane-3,4,5-triol
T19	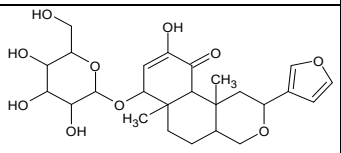	Removal of Ketone in the lactone ring. Addition of the OH group to the second Ketone ring.	2-(furan-3-yl)-9-hydroxy-6a,10b-dimethyl-7-[3,4,5-trihydroxy-6-(hydroxymethyl)oxan-2-yl]oxy-1,2,4,4a,5,6,7,10a-octahydrobenzo[f]isochromen-10-one

T20	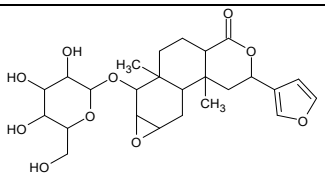	An epoxide group was added to the ring adjacent to glucose, and the ketone group, along with the double bond, was removed from the second ring.	4-(furan-3-yl)-2,10-dimethyl-11-[3,4,5-trihydroxy-6-(hydroxymethyl)oxan-2-yl]oxy-5,13-dioxatetracyclo[8.5.0.0^2,7.0^12,14]pentadecan-6-one
T21	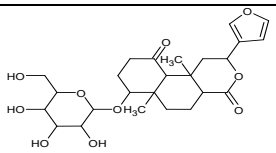	Removed the double bond in the 2nd ketone ring.	2-(furan-3-yl)-6a,10b-dimethyl-7-[3,4,5-trihydroxy-6-(hydroxymethyl)oxan-2-yl]oxy-2,4a,5,6,7,8,9,10a-octahydro-1H-benzo[f]isochromene-4,10-dione
T22	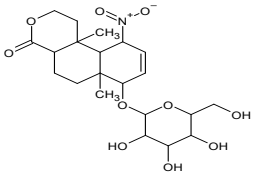	The Furan ring was removed. Added NO2 and removed the ketone in the ring near glucose	6a,10b-dimethyl-10-nitro-7-[3,4,5-trihydroxy-6-(hydroxymethyl)oxan-2-yl]oxy-1,2,4a,5,6,7,10,10a-octahydrobenzo[f]isochromen-4-one
T23	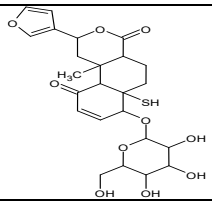	The replacement of one of the CH3 with SH	2-(furan-3-yl)-10b-methyl-6a-sulfanyl-7-[3,4,5-trihydroxy-6-(hydroxymethyl)oxan-2-yl]oxy-2,4a,5,6,7,10a-hexahydro-1H-benzo[f]isochromene-4,10-dione
T24	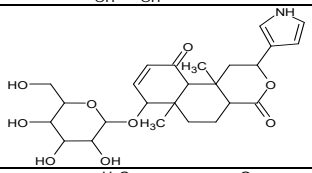	Furan ring replaced with pyrrole ring.	6a,10b-dimethyl-2-(1H-pyrrol-3-yl)-7-[3,4,5-trihydroxy-6-(hydroxymethyl)oxan-2-yl]oxy-2,4a,5,6,7,10a-hexahydro-1H-benzo[f]isochromene-4,10-dione
T25	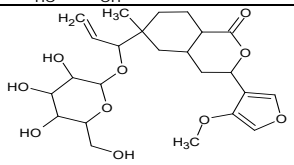	Ring opening near glucose and addition of the OCH3 group to the furan ring	3-(4-methoxyfuran-3-yl)-6-methyl-6-[1-[3,4,5-trihydroxy-6-(hydroxymethyl)oxan-2-yl]oxyprop-2-enyl]-4,4a,5,7,8,8a-hexahydro-3H-isochromen-1-one
T26	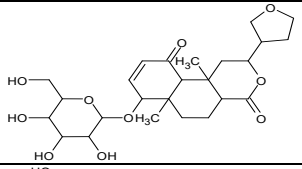	The furan ring was reduced to a tetrahydrofuran ring.	6a,10b-dimethyl-2-(oxolan-3-yl)-7-[3,4,5-trihydroxy-6-(hydroxymethyl)oxan-2-yl]oxy-2,4a,5,6,7,10a-hexahydro-1H-benzo[f]isochromene-4,10-dione
T27	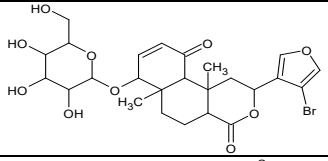	Halogen Bromine was added to the 3rd position of the furan ring.	2-(4-bromofuran-3-yl)-6a,10b-dimethyl-7-[3,4,5-trihydroxy-6-(hydroxymethyl)oxan-2-yl]oxy-2,4a,5,6,7,10a-hexahydro-1H-benzo[f]isochromene-4,10-dione
T28	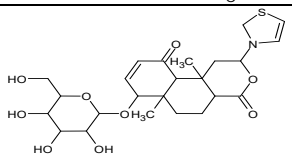	Replacement of the Furan ring with the thiazole ring.	6a,10b-dimethyl-2-(2H-1,3-thiazol-3-yl)-7-[3,4,5-trihydroxy-6-(hydroxymethyl)oxan-2-yl]oxy-2,4a,5,6,7,10a-hexahydro-1H-benzo[f]isochromene-4,10-dione

T29	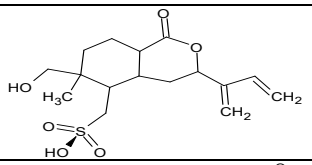	The glucose was removed. The furan ring and the 2nd ketone ring were opened, and the addition of the SO3OH group.	[3-buta-1,3-dien-2-yl-6-(hydroxymethyl)-6-methyl-1-oxo-4,4a,5,7,8,8a-hexahydro-3H-isochromen-5-yl]methanesulfonic acid
T30	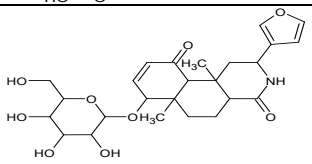	The oxygen atom in the lactone ring was replaced by an NH group.	2-(furan-3-yl)-6a,10b-dimethyl-7-[3,4,5-trihydroxy-6-(hydroxymethyl)oxan-2-yl]oxy-1,2,3,4a,5,6,7,10a-octahydrobenzo[f]isoquinoline-4,10-dione
T31	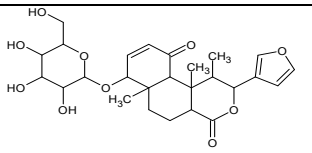	Addition of the CH3 group to the lactone ring	2-(furan-3-yl)-1,6a,10b-trimethyl-7-[3,4,5-trihydroxy-6-(hydroxymethyl)oxan-2-yl]oxy-2,4a,5,6,7,10a-hexahydro-1H-benzo[f]isochromene-4,10-dione
T32	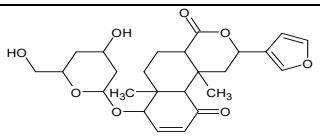	OH groups at the 2nd and 4th positions of the glucose were removed.	2-(furan-3-yl)-7-[4-hydroxy-6-(hydroxymethyl)oxan-2-yl]oxy-6a,10b-dimethyl-2,4a,5,6,7,10a-hexahydro-1H-benzo[f]isochromene-4,10-dione
T33	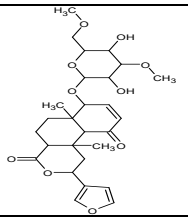	OCH3 groups were added to the 3rd and 6th positions of the glucose.	7-[3,5-dihydroxy-4-methoxy-6-(methoxymethyl)oxan-2-yl]oxy-2-(furan-3-yl)-6a,10b-dimethyl-2,4a,5,6,7,10a-hexahydro-1H-benzo[f]isochromene-4,10-dione
T34	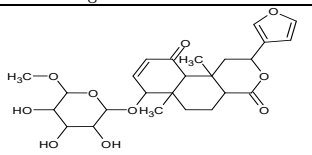	The OCH3 group was attached to the 6th position of glucose.	2-(furan-3-yl)-6a,10b-dimethyl-7-(3,4,5-trihydroxy-6-methoxyoxan-2-yl)oxy-2,4a,5,6,7,10a-hexahydro-1H-benzo[f]isochromene-4,10-dione
T35	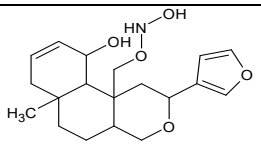	The glucose molecule was removed. The ketone ring was removed and replaced with an OH group. One of the CH3 groups at the junction was replaced with a CONHOH group.	2-(furan-3-yl)-10b-[(hydroxyamino)oxymethyl]-6a-methyl-2,4,4a,5,6,7,10,10a-octahydro-1H-benzo[f]isochromen-10-ol
T36	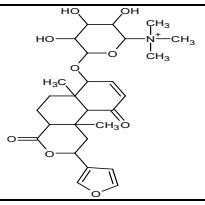	Replacement of the OH group with N (CH3)3 in the glucose molecule.	[6-[[2-(furan-3-yl)-6a,10b-dimethyl-4,10-dioxo-2,4a,5,6,7,10a-hexahydro-1H-benzo[f]isochromen-7-yl]oxy]-3,4,5-trihydroxyoxan-2-yl]-trimethylazanium
T37	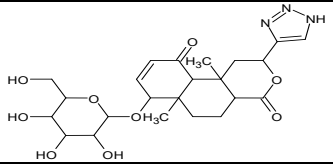	The furan ring was replaced with a triazole ring.	6a,10b-dimethyl-2-(1H-triazol-4-yl)-7-[3,4,5-trihydroxy-6-(hydroxymethyl)oxan-2-yl]oxy-2,4a,5,6,7,10a-hexahydro-1H-benzo[f]isochromene-4,10-dione

T38	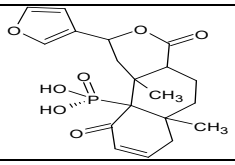	The glucose molecule was replaced with a Phosphate group.	[2-(furan-3-yl)-6a,10b-dimethyl-4,10-dioxo-2,4a,5,6,7,10b-hexahydro-1H-benzo[f]isochromen-10a-yl]phosphonic acid
T39	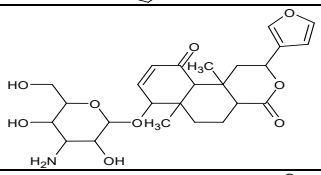	The glucose molecule was replaced with glucosamine.	7-[4-amino-3,5-dihydroxy-6-(hydroxymethyl)oxan-2-yl]oxy-2-(furan-3-yl)-6a,10b-dimethyl-2,4a,5,6,7,10a-hexahydro-1H-benzo[f]isochromene-4,10-dione
T40	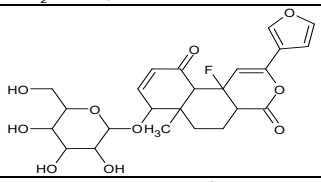	Added fluorine to the junction of the lactone ring and the diterpenoid. Added a double bond to the lactone ring.	10b-fluoro-2-(furan-3-yl)-6a-methyl-7-[3,4,5-trihydroxy-6-(hydroxymethyl)oxan-2-yl]oxy-5,6,7,10a-tetrahydro-4aH-benzo[f]isochromene-4,10-dione
T41	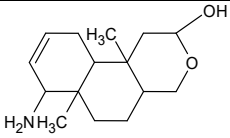	Both the glucose and furan ring was removed. ketone groups were removed and one of them replaced to OH group i.e., in the Lactone ring. Added NH2 group to the diterpenoid ring that was attached to glucose.	7-amino-6a,10b-dimethyl-2,4,4a,5,6,7,10,10a-octahydro-1H-benzo[f]isochromen-2-ol
T42	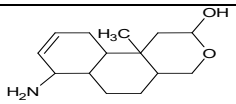	Removed one of the CH3 groups from the above structure.	7-amino-10b-methyl-1,2,4,4a,5,6,6a,7,10,10a-decahydrobenzo[f]isochromen-2-ol
T43	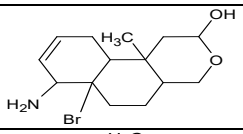	Added the Bromine group near the NH2 in the above structure.	7-amino-6a-bromo-10b-methyl-2,4,4a,5,6,7,10,10a-octahydro-1H-benzo[f]isochromen-2-ol
T44	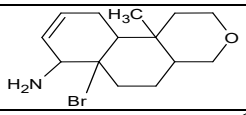	Removed the OH group from the above structure.	6a-bromo-10b-methyl-2,4,4a,5,6,7,10,10a-octahydro-1H-benzo[f]isochromen-7-amine
T45	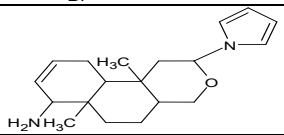	Added the pyrrole ring to the above structure.	6a,10b-dimethyl-2-pyrrol-1-yl-2,4,4a,5,6,7,10,10a-octahydro-1H-benzo[f]isochromen-7-amine
T46	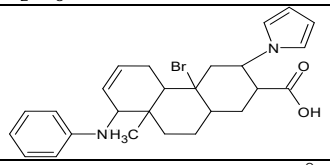	Bromine was introduced by replacing the CH_3 group, and a benzene ring was attached to the NH group in the modified structure.	8-anilino-4a-bromo-8a-methyl-3-pyrrol-1-yl-1,2,3,4,4b,5,8,9,10,10a-decahydrophenanthrene-2-carboxylic acid
T47	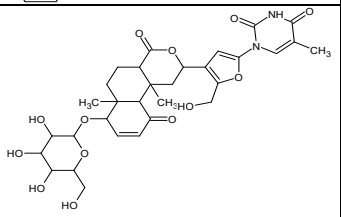	1st and 2nd position of furan was attached with 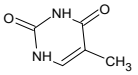 and CH3OH respectively – part of azidothymidine.	1-[4-[6a,10b-dimethyl-4,10-dioxo-7-[3,4,5-trihydroxy-6-(hydroxymethyl)oxan-2-yl]oxy-2,4a,5,6,7,10a-hexahydro-1H-benzo[f]isochromen-2-yl]-5-(hydroxymethyl)furan-2-yl]-5-methylpyrimidine-2,4-dione

T48	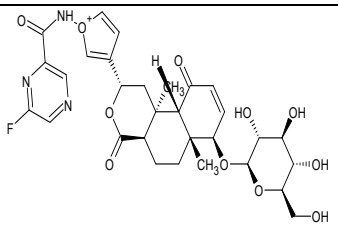	The oxygen ring of furan 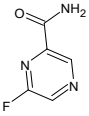 was attached with part of favipiravir.	N-[3-[(2S,4aR,6aR,7R,10aS,10bS)-6a,10b-dimethyl-4,10-dioxo-7-[(2R,3R,4S,5S,6R)-3,4,5-trihydroxy-6-(hydroxymethyl)oxan-2-yl]oxy-2,4a,5,6,7,10a-hexahydro-1H-benzo[f]isochromen-2-yl]furan-1-ium-1-yl]-6-fluoropyrazine-2-carboxamide
T49	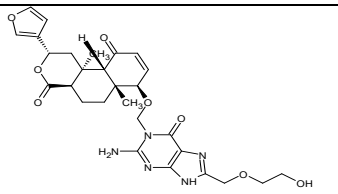	The glucose molecule was replaced with acyclovir (an Antiviral drug).	(2S,4aR,6aR,7R,10aS,10bS)-7-[[2-amino-8-(2-hydroxyethoxymethyl)-6-oxo-9H-purin-1-yl]methoxy]-2-(furan-3-yl)-6a,10b-dimethyl-2,4a,5,6,7,10a-hexahydro-1H-benzo[f]isochromene-4,10-dione
T50	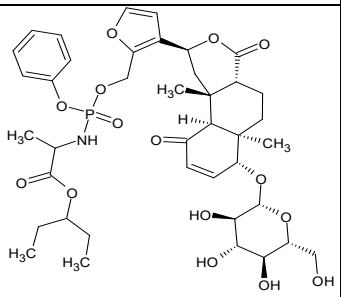	The furan ring was attached to Remdesivir (an Antiviral Drug)	pentan-3-yl 2-[[[3-[(2S,4aR,6aR,7R,10aS,10bS)-6a,10b-dimethyl-4,10-dioxo-7-[(2R,3R,4S,5S,6R)-3,4,5-trihydroxy-6-(hydroxymethyl)oxan-2-yl]oxy-2,4a,5,6,7,10a-hexahydro-1H-benzo[f]isochromen-2-yl]furan-2-yl]methoxy-phenoxyphosphoryl]amino]propanoate
T51	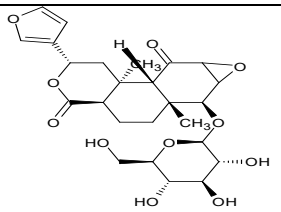	Added epoxide to the ring near glucose.	(1S,2S,4S,7R,10R,11S)-4-(furan-3-yl)-2,10-dimethyl-11-[(2R,3R,4S,5S,6R)-3,4,5-trihydroxy-6-(hydroxymethyl)oxan-2-yl]oxy-5,13-dioxatetracyclo[8.5.0.0^2,7.0^12,14]pentadecane-6,15-dione
T52	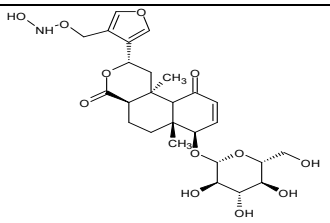	Added CONHOH to the 3rd position of furan.	(2S,4aR,6aR,7R,10bS)-2-[4-[(hydroxyamino)oxymethyl]furan-3-yl]-6a,10b-dimethyl-7-[(2R,3R,4S,5S,6R)-3,4,5-trihydroxy-6-(hydroxymethyl)oxan-2-yl]oxy-2,4a,5,6,7,10a-hexahydro-1H-benzo[f]isochromene-4,10-dione
T53	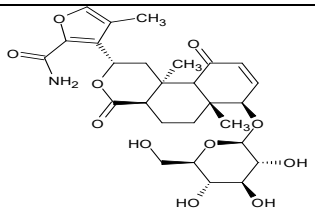	Added CH3 group to the 4th position and CONH2 to the 2nd position of furan.	3-[(2S,4aR,6aR,7R,10bS)-6a,10b-dimethyl-4,10-dioxo-7-[(2R,3R,4S,5S,6R)-3,4,5-trihydroxy-6-(hydroxymethyl)oxan-2-yl]oxy-2,4a,5,6,7,10a-hexahydro-1H-benzo[f]isochromen-2-yl]-4-methylfuran-2-carboxamide

T54	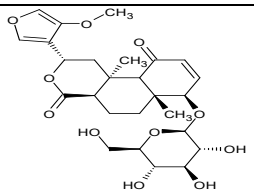	Added OCH3 to the 3rd position of Furan.	(2S,4aR,6aR,7R,10bS)-2-(4-methoxyfuran-3-yl)-6a,10b-dimethyl-7-[(2R,3R,4S,5S,6R)-3,4,5-trihydroxy-6-(hydroxymethyl)oxan-2-yl]oxy-2,4a,5,6,7,10a-hexahydro-1H-benzo[f]isochromene-4,10-dione
T55	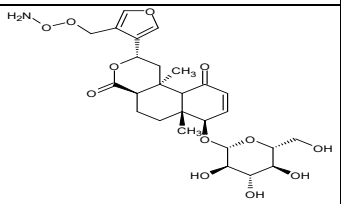	Added COONH2 to the 3rd position of Furan.	(2S,4aR,6aR,7R,10bS)-2-[4-(aminoperoxymethyl)furan-3-yl]-6a,10b-dimethyl-7-[(2R,3R,4S,5S,6R)-3,4,5-trihydroxy-6-(hydroxymethyl)oxan-2-yl]oxy-2,4a,5,6,7,10a-hexahydro-1H-benzo[f]isochromene-4,10-dione
T56	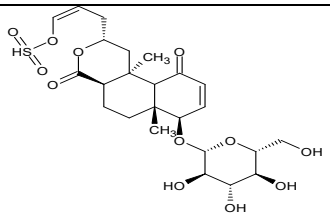	The furan ring was opened, and the SO2 group was added.	[(Z)-3-[(2S,4aR,6aR,7R,10bS)-6a,10b-dimethyl-4,10-dioxo-7-[(2R,3R,4S,5S,6R)-3,4,5-trihydroxy-6-(hydroxymethyl)oxan-2-yl]oxy-2,4a,5,6,7,10a-hexahydro-1H-benzo[f]isochromen-2-yl]prop-1-enyl] sulfamate

4.2.3 Drug Administration Suitability and Lipinski's Rule of Five Analysis

Assessing whether a drug candidate is suitable for oral administration or requires intravenous (IV) delivery is a key step in early drug development. The route of administration directly impacts a compound's absorption, bioavailability, patient compliance, and overall therapeutic success. For COVID-19 treatments in particular, compounds with high GI absorption are preferred for oral delivery, while those with low absorption may require IV administration. Another important factor is BBB permeability. Since COVID-19 primarily targets the respiratory system rather than the central nervous system, BBB penetration is generally unnecessary, and a BBB value of "No" is acceptable unless neurological complications are being addressed. Additionally, PAINS (Pan-Assay Interference Compounds) filters identify molecules likely to interfere with biological assays, often producing misleading results. Compounds that do not trigger PAINS alerts are considered more reliable for further screening.

To further assess oral bioavailability, Lipinski's RO5 was applied as a guideline. This rule evaluated drug-likeness based on molecular weight, lipophilicity (MlogP), hydrogen bond donors, and hydrogen bond acceptors. A compound is typically acceptable if it meets at least

three of the four criteria. Among the fifty-six modified compounds analyzed, ten were found to violate the RO5 and were excluded from further studies. Table 2 presents an overview of the predicted physicochemical properties and drug-likeness generated using the SwissADME tool.

Table 4: Physicochemical properties and drug-likeness predictions.

Compound No.	**Lipinski**	**Molecular weight(g/mol)**	**H-bond acceptors**	**H-bond donors**	**M Log P**	**GI absorption/ BBB permeant**	**PAINS**
T0	Yes	492.52	10	4	-0.71	Low, No	No
T1	Yes	480.55	9	5	-0.70	Low, No	No
T2	Yes	330.37	5	1	1.53	High, Yes	No
T3	Yes	426.46	9	4	-0.57	Low, No	No
T4	Yes	264.32	4	1	1.62	High, Yes	No
T5	Yes	387.40	7	1	1.08	High, No	No
T6	Yes	472.48	10	1	2.25	Low, No	No
T7	Yes	385.46	6	0	2.40	High, No	No
T8	Yes	573.87	12	0	3.24	Low, No	No
T9	Yes	475.54	7	1	2.01	High, No	No
T10	Yes	359.31	8	3	0.33	Low, No	No
T11	Yes	468.49	10	4	-1.04	Low, No	No
T12	Yes	480.50	10	4	-0.92	Low, No	No
T13	Yes	466.48	10	4	-1.13	Low, No	No
T14	Yes	502.52	10	3	1.29	High, No	No
T15	Yes	375.46	6	2	1.25	High, No	No
T16	Yes	510.51	11	4	-0.60	Low, No	Yes
T17	Yes	458.50	10	4	-0.62	Low, No	No
T18	Yes	479.56	9	4	0.23	High, No	No
T19	Yes	494.53	10	5	-1.44	Low, No	No
T20	Yes	494.53	10	4	-0.54	Low, No	No
T21	Yes	494.53	10	4	-0.62	Low, No	No
T22	Yes	457.47	10	4	-0.01	Low, No	No
T23	Yes	510.55	10	4	-0.92	Low, No	No
T24	Yes	494.55	10	5	-0.49	Low, No	No
T25	Yes	482.52	10	4	-0.56	Low, No	No
T26	Yes	496.55	10	4	-0.49	Low, No	No
T27	Yes	571.41	10	4	-0.13	Low, No	No
T28	Yes	511.59	9	4	-0.38	Low, No	No
T29	Yes	344.42	6	2	1.67	High, No	No
T30	Yes	491.53	9	5	-1.11	Low, No	No
T31	Yes	506.54	10	4	-0.50	Low, No	No
T32	Yes	460.52	8	2	0.84	High, No	No
T33	Yes	520.57	10	2	-0.30	High, No	No
T34	Yes	492.52	10	3	-0.30	Low, No	No
T35	Yes	349.42	6	3	1.70	High, No	No
T36	Yes	520.59	9	3	-3.58	High, No	No
T37	Yes	495.52	11	5	-0.89	Low, No	No
T38	Yes	394.36	7	2	1.06	High, No	No
T39	Yes	491.53	10	4	-0.71	Low, No	No
T40	Yes	494.46	11	4	-0.89	Low, No	No

T41	Yes	251.36	3	2	2.27	High, Yes	No
T42	Yes	237.34	3	2	2.01	High, Yes	No
T43	Yes	316.23	3	2	2.39	High, Yes	No
T44	Yes	300.23	2	1	2.87	High, Yes	No
T45	Yes	300.44	2	1	2.98	High, Yes	No
T46	Yes	483.44	2	2	4.28	High, No	No
T47	No	646.64	13	6	-1.36	Low, No	No
T48	No	632.61	14	5	-1.15	Low, No	No
T49	No	569.61	10	3	-0.17	Low, No	No
T50	No	819.83	16	5	-0.07	Low, No	No
T51	No	508.51	11	4	-1.39	Low, No	No
T52	No	553.56	13	6	-1.14	Low, No	No
T53	No	549.57	11	5	-1.23	Low, No	No
T54	No	522.54	11	4	-1.00	Low, No	No
T55	No	553.56	13	5	-1.14	Low, No	No
T56	No	546.58	12	4	-0.85	Low, No	No

4.3 Docking Studies and Binding Affinity Evaluation

A total of forty-six ligands were selected for molecular docking studies. The prepared ligands were grouped with their respective target proteins: one folder containing Protein A along with the selected ligands, and another containing Protein B with the same set of ligands. Docking was performed using AutoDock Vina. The results were evaluated based on binding affinity scores, and the top-ranked poses- those with a root mean square deviation (RMSD) of zero- were selected for analysis. An RMSD value of less than 2 Å is generally considered acceptable for reliable docking, with zero indicating a perfect alignment with the predicted pose. More negative binding affinity values suggest stronger binding interactions, as they indicate a greater release of energy and better fitting within the protein's binding site. The binding affinities of the forty-six compounds, along with the original reference molecule T0, docked with both Protein A and Protein B, are summarized in Table 3.

Table 5: Binding affinity scores of forty-six selected ligands and reference compound T0 with Protein A and Protein B, as determined by AutoDock Vina.

PROTEIN A		**PROTEIN B**	
Compound No.	Binding Affinity (kcal/mol)	Compound No.	Binding Affinity (kcal/mol)
AT0	**-8.5**	**BT0**	**-8.9**
AT1	-8.4	BT1	-9.4
AT2	-7.4	BT2	-7.2
AT3	-9.6	BT3	-7.9
AT4	-6.2	BT4	-6.3
AT5	-7.6	BT5	-7.9
AT6	-7.7	BT6	-7.9
AT7	-7	BT7	-8.7
AT8	-9.3	BT8	-9.4

AT9	-8.5	BT9	-8.6
AT10	-6.8	BT10	-7.6
AT11	-8.5	BT11	-9.2
AT12	-9.3	BT12	-8.9
AT13	-9.1	BT13	-8.5
AT14	-9.4	BT14	-8.6
AT15	-6.6	BT15	-7.6
AT16	-9.5	BT16	-8.7
AT17	-8.2	BT17	-9.0
AT18	-7.8	BT18	-9.0
AT19	-9.0	BT19	-9.8
AT20	-8.2	BT20	-8.4
AT21	-9.2	BT21	-8.7
AT22	-8.0	BT22	-8.1
AT23	-9.3	BT23	-8.9
AT24	-9.3	BT24	-9.0
AT25	-7.3	BT25	-9.2
AT26	-9.6	BT26	-8.7
AT27	-8.7	BT27	-9.3
AT28	-9.1	BT28	-8.8
AT29	-6.9	BT29	-7.5
AT30	-8.5	BT30	-8.8
AT31	-10	BT31	-9.2
AT32	-8.8	BT32	-8.5
AT33	-8.1	BT33	-8.9
AT34	-9.3	BT34	-8.8
AT35	-8.2	BT35	-8.0
AT36	-8.8	BT36	-8.9
AT37	-9.3	BT37	-9.1
AT38	-8.5	BT38	-7.6
AT39	-9.1	BT39	-8.9
AT40	-9.5	BT40	-8.9
AT41	-6.5	BT41	-6.6
AT42	-5.5	BT42	-6.4
AT43	-6.7	BT43	-6.4
AT44	-5.5	BT44	-5.7
AT45	-7.1	BT45	-7.0
AT46	-8.7	BT46	-8.9

The binding affinities of the reference compound T0 with Protein A and Protein B were found to be –8.5 kcal/mol and –8.9 kcal/mol, respectively. These values were used as cut-off thresholds for selecting potential dual-acting ligands. Only those ligands that demonstrated binding affinities equal to or more negative than these cut-off values with both proteins were considered for further analysis, indicating their potential for dual inhibition. A total of thirteen ligands satisfied these criteria, namely: (AT8, BT8), (AT11, BT11), (AT12, BT12), (AT19, BT19), (AT23, BT23), (AT24, BT24), (AT27, BT27), (AT31, BT31), (AT36, BT36), (AT37, BT37), (AT39, BT39), (AT40, BT40), and (AT46, BT46).

4.4 Amino Acid Interaction in Protein-Ligand Docking

This study focused on examining how potential drug molecules, or ligands, interact with critical amino acids in the active sites of the SARS-CoV-2 M^{pro} and PL^{pro}. Molecular docking was performed to assess the types of interactions and to determine if the ligands effectively bound to the active site residues. By visualizing these interactions in 2D and 3D, a more detailed understanding of ligand binding was gained, which helped to guide the identification and optimization of promising antiviral drug candidates.

4.4.1 Protein A Interaction Insights

Thirteen ligands with strong docking scores, along with the reference compound T0, were selected for detailed interaction analysis with Protein A. BIOVIA Discovery Studio was used to generate 2D and 3D visualizations, which helped examine how each ligand was positioned within the binding site and how it interacted with surrounding amino acid residues.

These visualizations provided useful insights, including:

- The specific amino acids involved in ligand binding
- The types of molecular interactions observed.
- The spatial orientation and fit of each ligand within the binding pocket

This analysis played an important role in the next step screening to find out the promising lead compounds by showing how effectively each ligand engaged with the target site. The figures below illustrate these interactions and support the next steps in compound refinement and optimization.

Table 6: 3D and 2D Illustrations of Thirteen Selected Compounds Binding to Protein A, Interacting and Pocket Amino Acids highlighted in Annexure III

Comp. No.	3D visualization	2D visualization
AT0	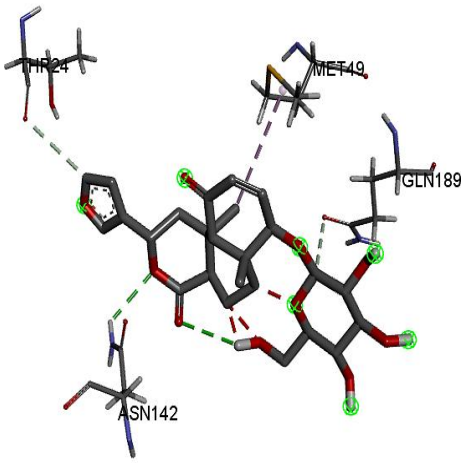	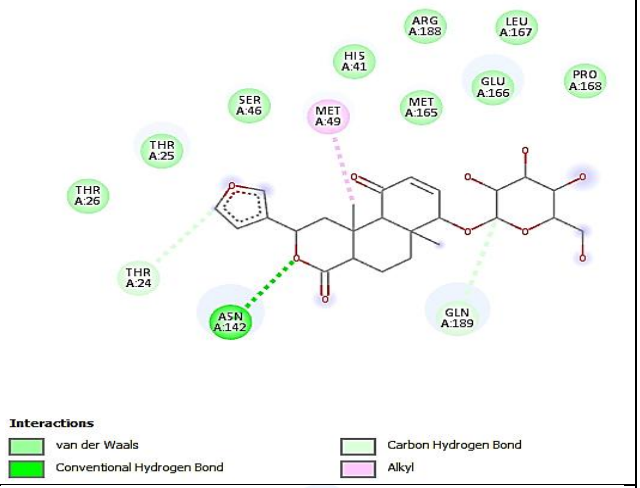
AT8	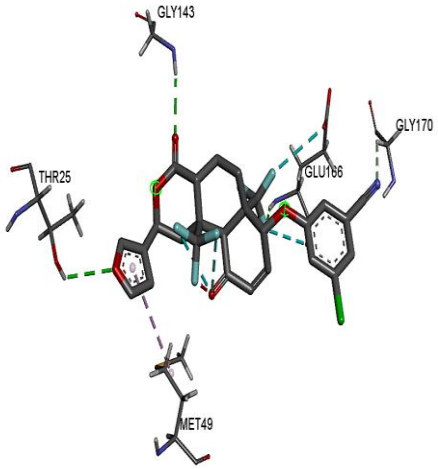	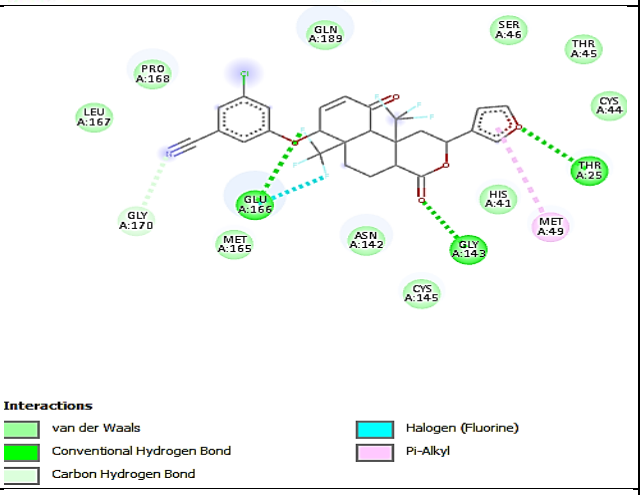
AT11	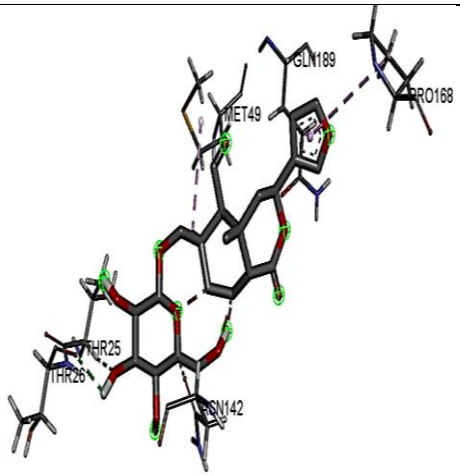	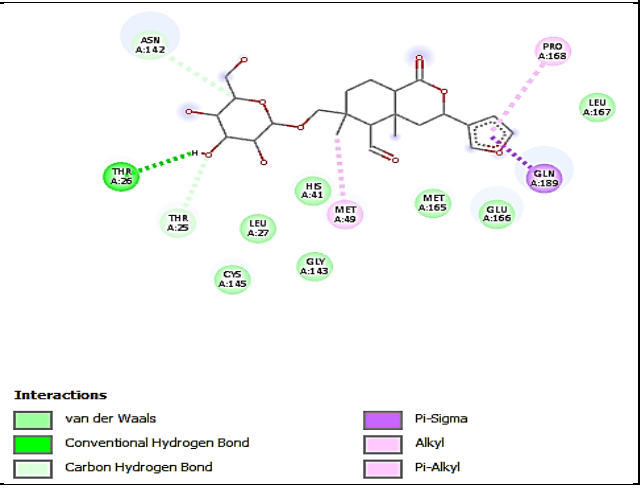

AT12	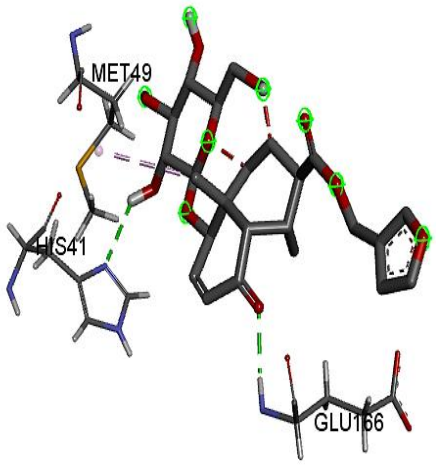	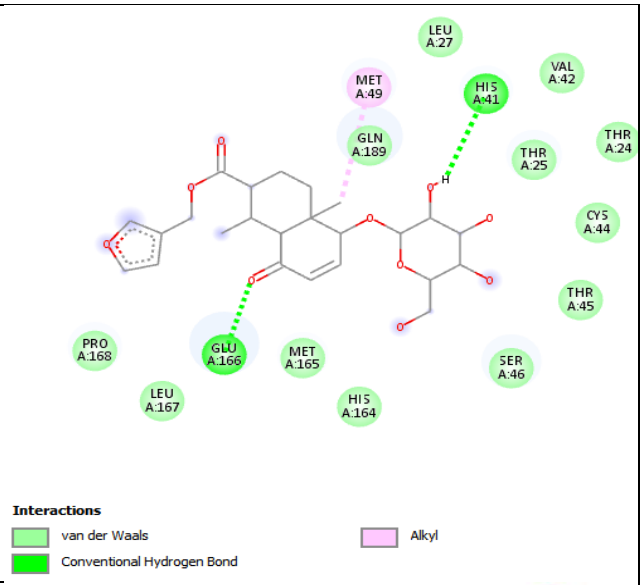
AT19	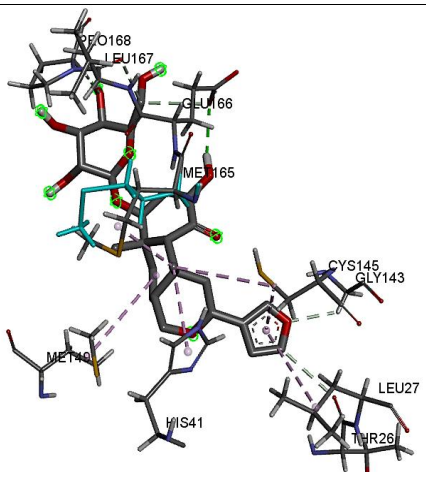	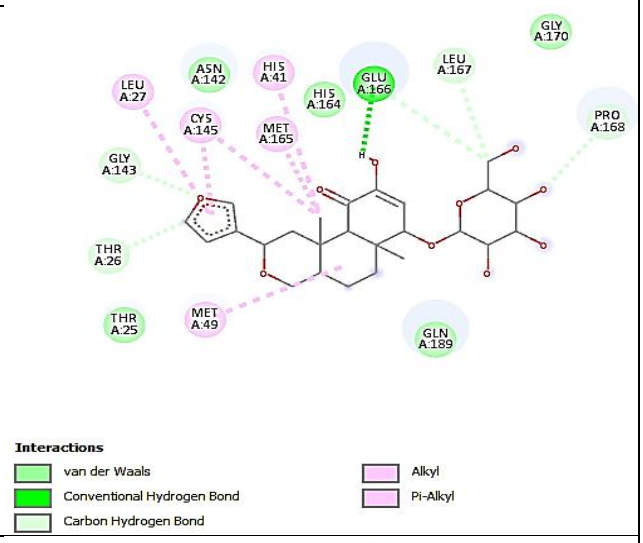
AT23	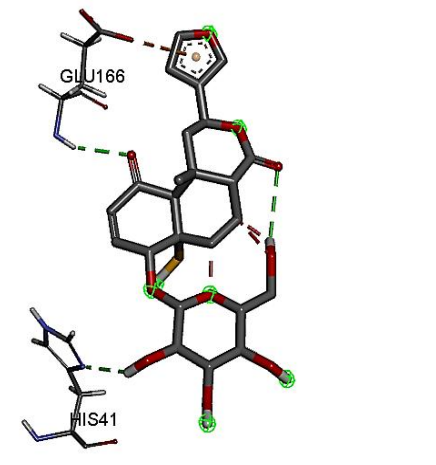	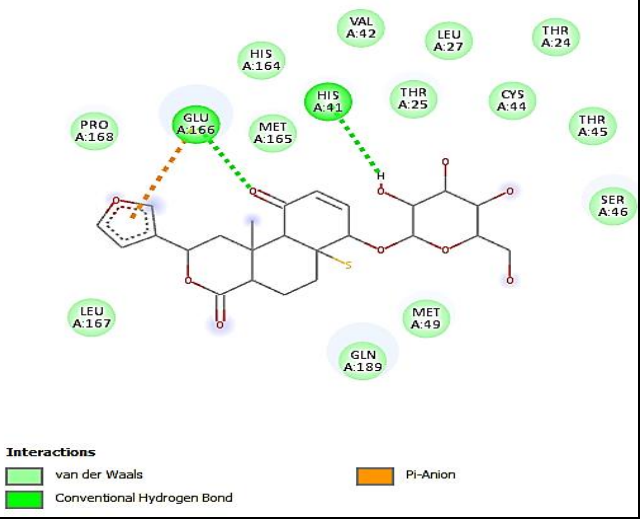

AT24	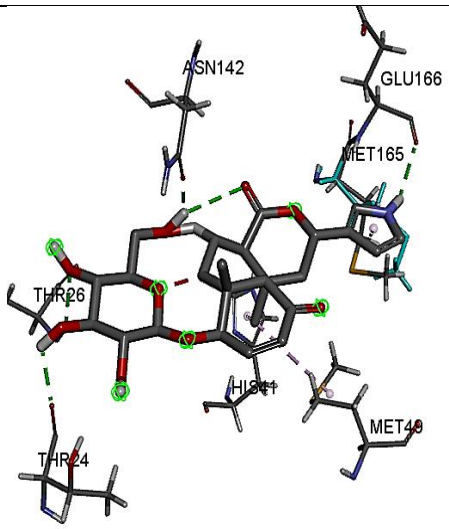	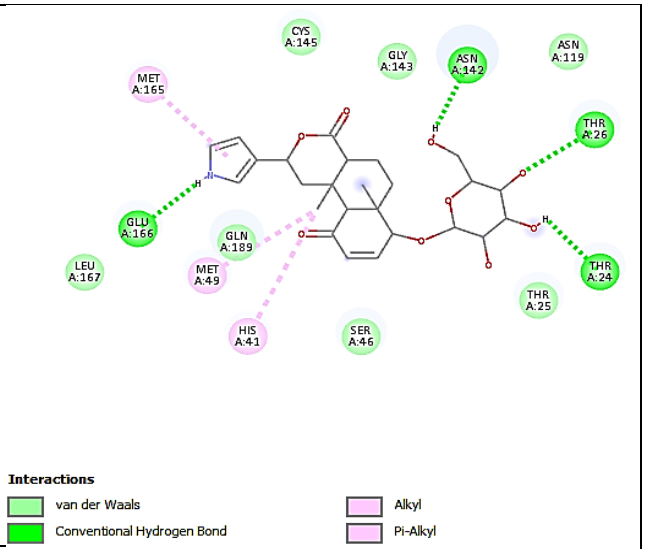
AT27	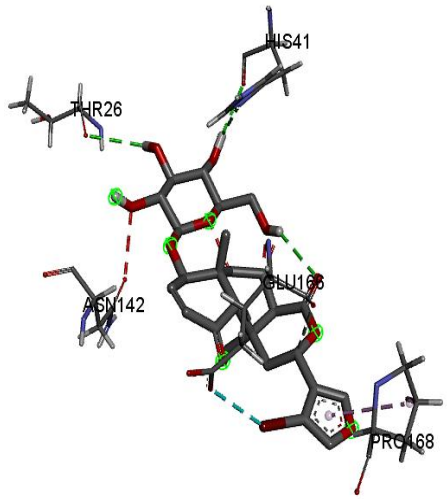	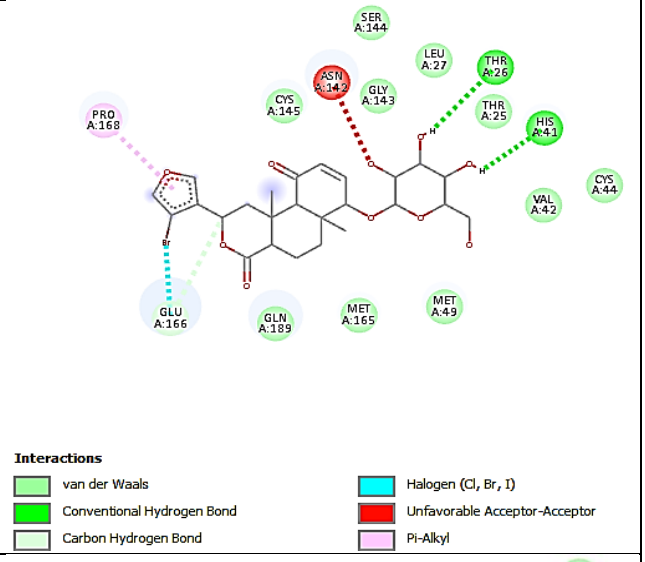
AT31	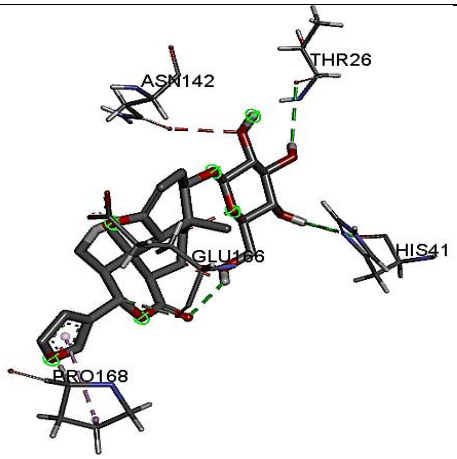	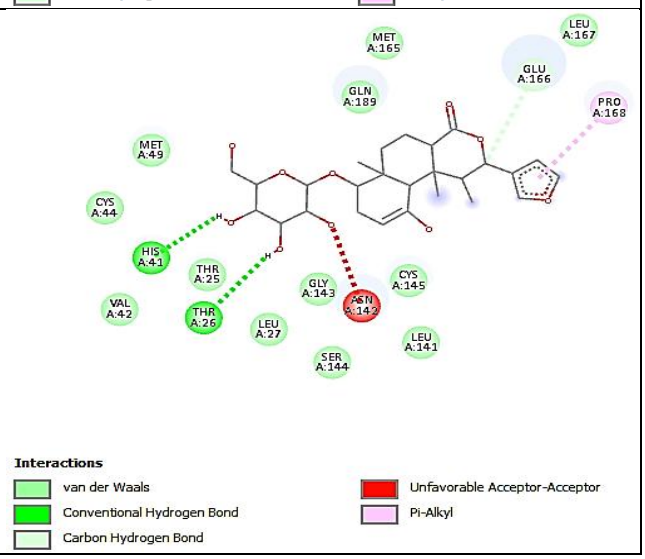

AT36	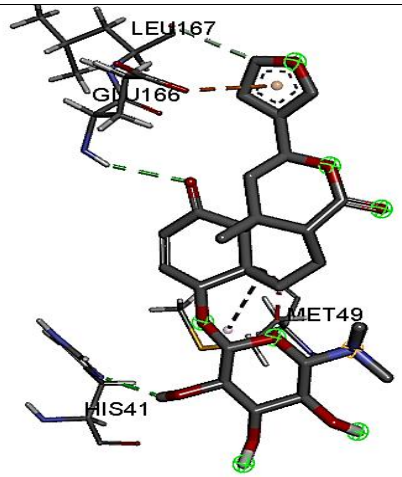	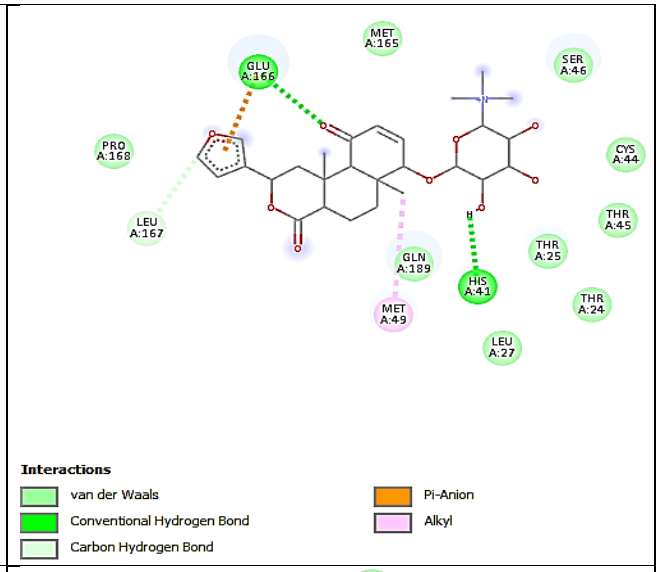
AT37	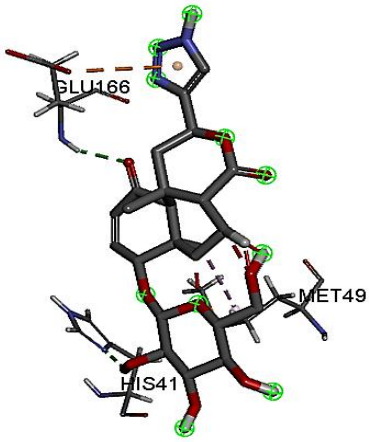	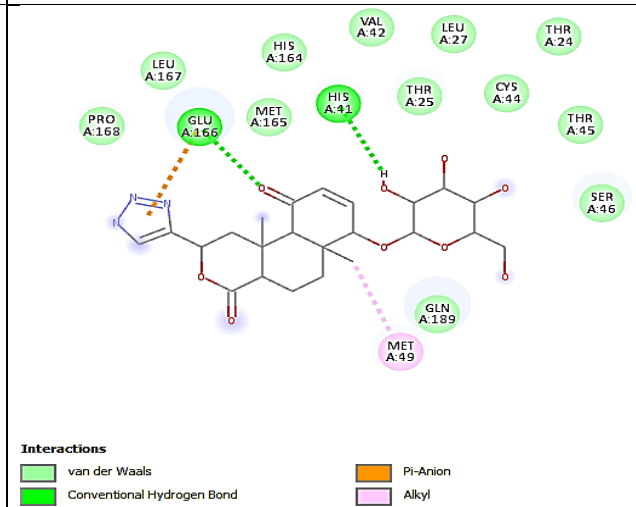
AT39	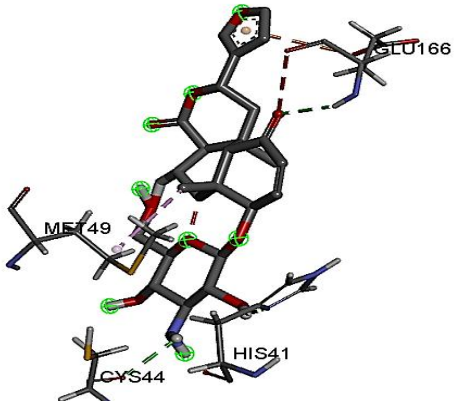	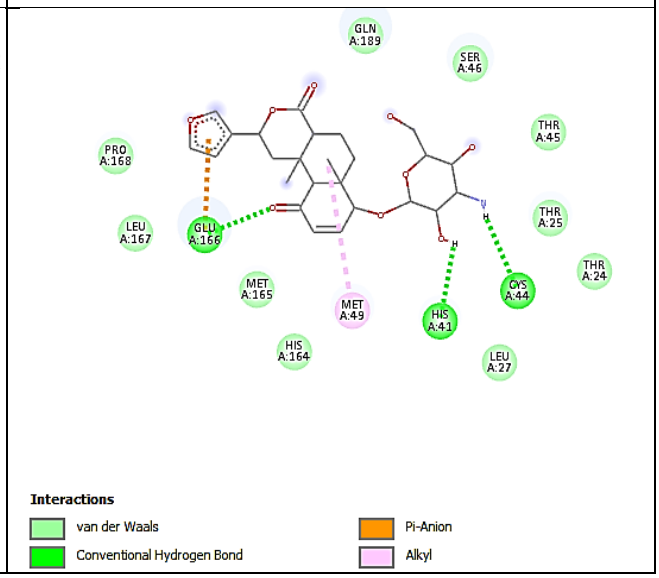

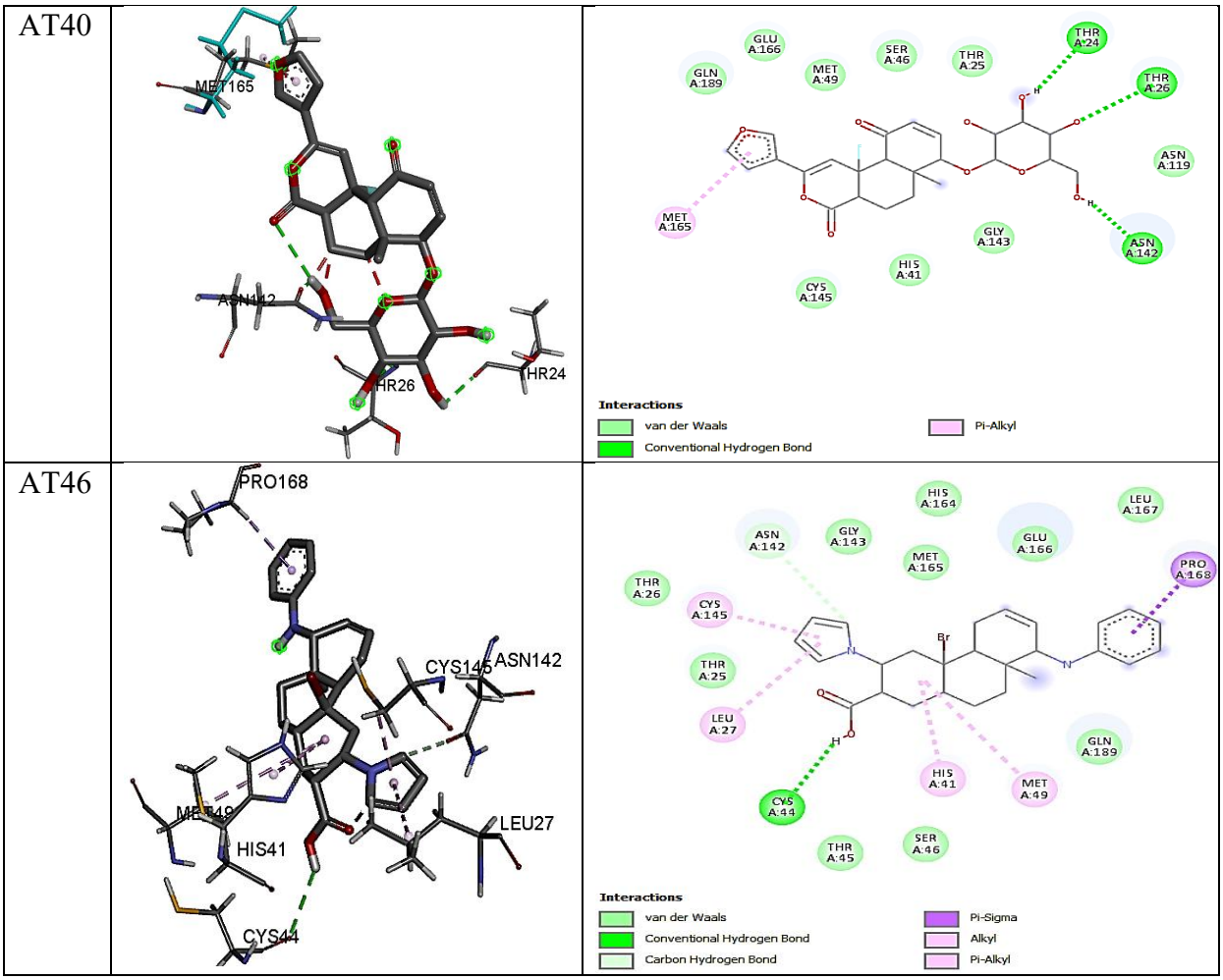

The docking study of T0 and its thirteen modified derivatives, using Protein A (PDB ID: 7ALH) as a model for the SARS-CoV-2 main protease, revealed several crucial amino acid residues that contribute to the stability, specificity, and therapeutic potential of the ligand–protein complex. These interactions were primarily observed within Chain A, which contains the enzyme's active sites.

4.4.1.1 Interactions of Tinosporaside

T0 demonstrated strong binding interactions with several key residues in the protease's active site, including MET A:49, MET A:165, LEU A:167, GLU A:166, GLN A:189, and ARG A:188. These interactions played a critical role in stabilizing the ligand within the binding pocket, primarily through hydrogen bonds, hydrophobic forces, and polar interactions. The collective effect of these forces results in a robust binding affinity between Tinosporaside and the protease, a key factor for its potential as an antiviral compound.

4.4.1.2 Modified Structures and Improved Therapeutic Potential

When compared to T0, the modified derivatives demonstrated not only similar interactions with the same key residues but also enhanced binding, particularly with the catalytic dyad of the protease. Notably, **modified compound T46** exhibited stronger and more stable interactions with the catalytic residues, particularly the CYS A:145-HIS A:41 dyads(Ferreira *et al.*, 2021). This enhanced engagement significantly improves its ability to inhibit the protease's enzymatic activity, making the compound a more potent inhibitor than T0. Moreover, these modifications did not disrupt the important interactions with residues like MET A:49, MET A:165, LEU A:167, GLN A:189, and ARG A:188, ensuring similar stability while adding stronger catalytic dyad engagement.

4.4.1.3 Additional Stabilizing Interactions

These compounds also exhibited additional stabilizing interactions with GLU 166 & HIS A:164, residues that play a key role in stabilizing ligands within the S1 subsite (Shawky *et al.*, 2024). This further supports the idea that **modified compounds** have improved binding affinity and greater stability within the active site of the protease, thereby enhancing its potential as effective antiviral agent.

4.4.1.4 Interaction vs. Pocket Residues

Understanding the difference between interaction residues and pocket residues is vital for interpreting the docking study results. **Interaction residues** directly bind to the ligand, dictating binding strength and specificity. **Pocket residues** form the binding cavity, influencing ligand fit. This distinction is crucial for understanding ligand engagement with the SARS-CoV-2 protease.

4.4.2 Protein B Interaction Insights

Similar to Protein A, thirteen ligands with favorable docking results were selected for further analysis with Protein B. These compounds were examined using BIOVIA Discovery Studio, which provided detailed 2D and 3D visualizations of how each ligand interacted within the binding site of Protein B. This interaction mapping helped assess the binding efficiency and compatibility of the ligands with Protein B’s active site. The visualization tabulated served as a foundation for identifying the most promising candidates for future refinement.

Table 7: 3D and 2D Illustrations of Thirteen Selected Compounds Binding to Protein B, Interacting and Pocket Amino Acids are highlighted in Annexure IV

Comp. No.	3D Visualization	2D Visualization
BT0	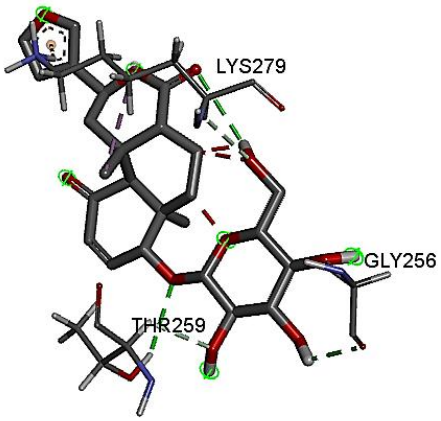	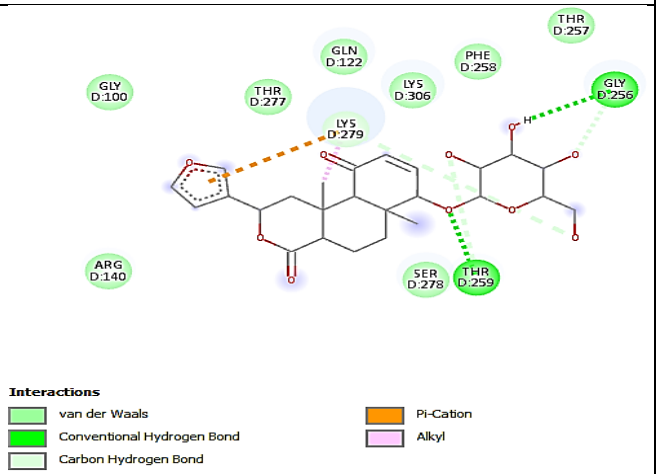
BT8	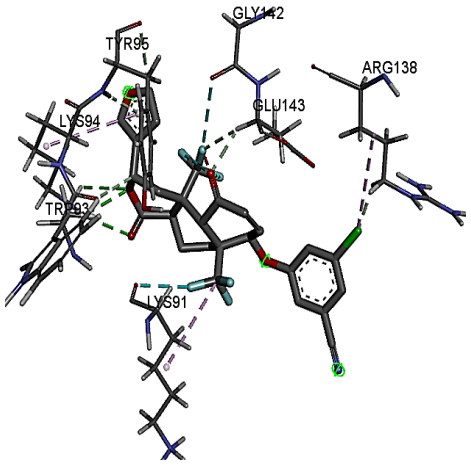	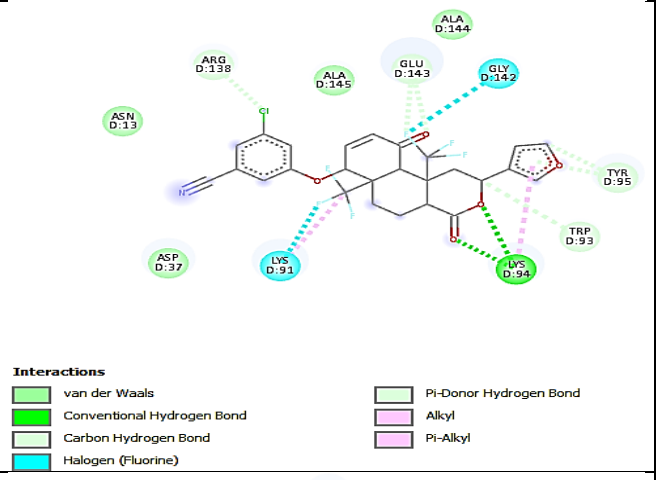
BT11	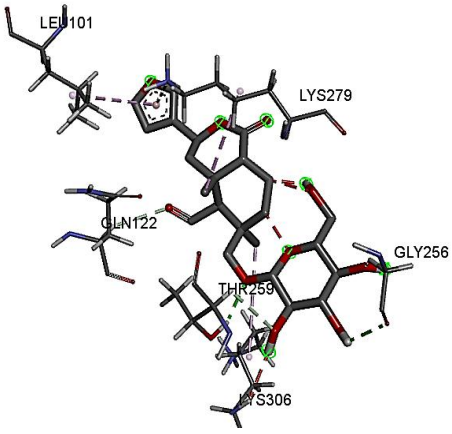	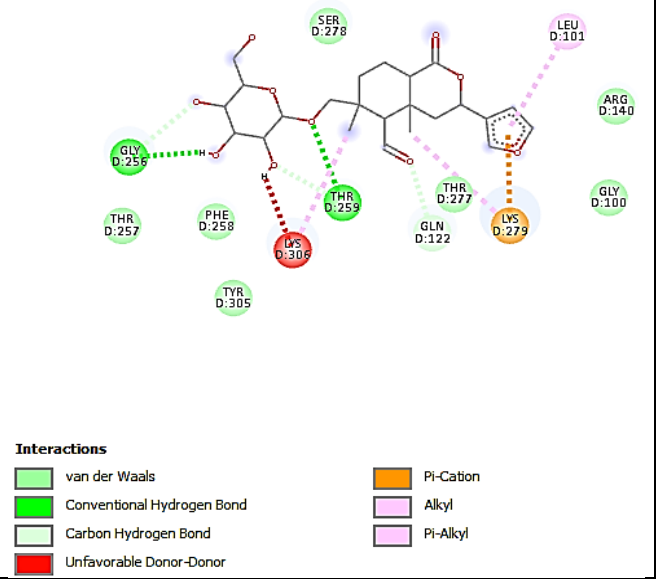

BT12	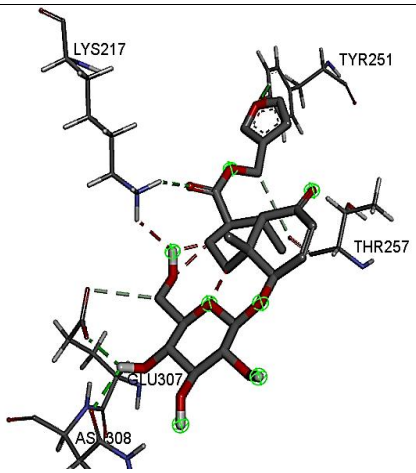	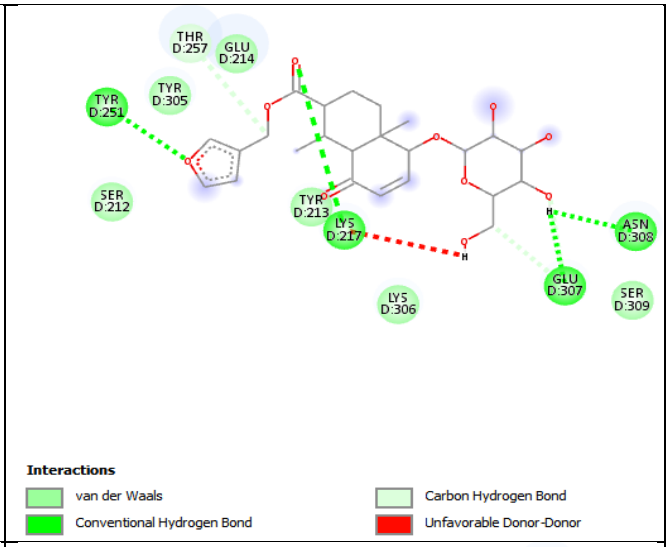
BT19	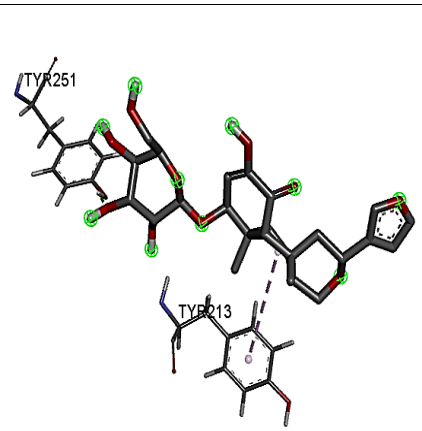	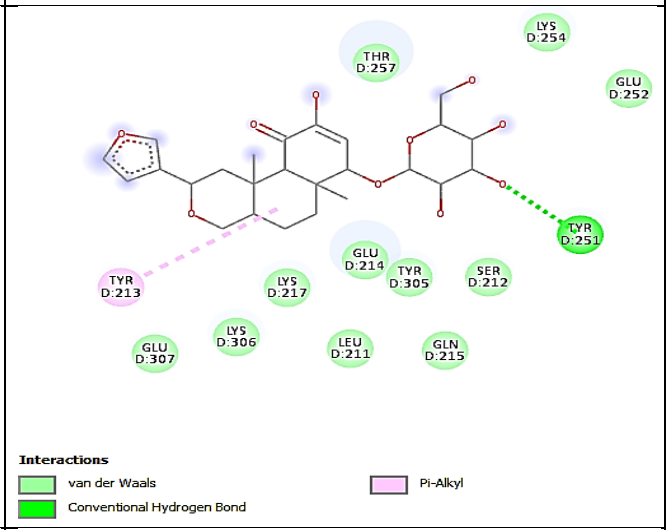
BT23	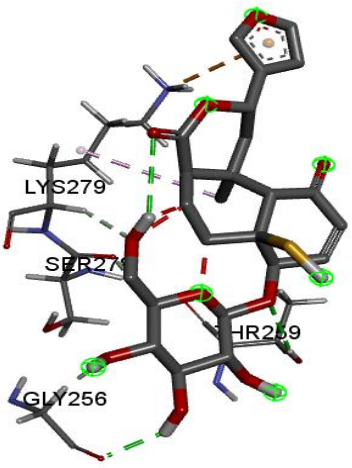	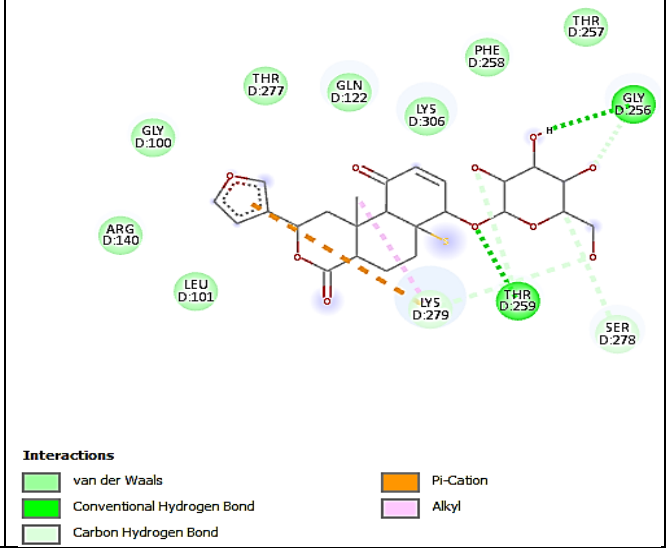

BT24	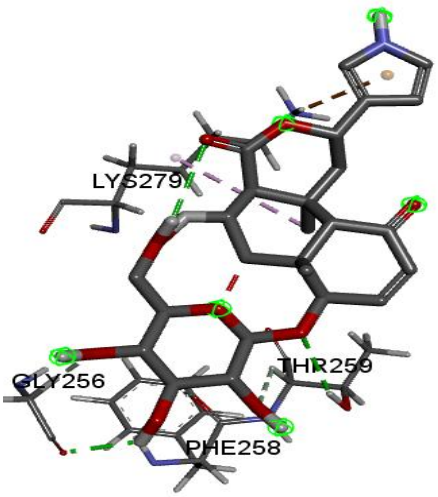	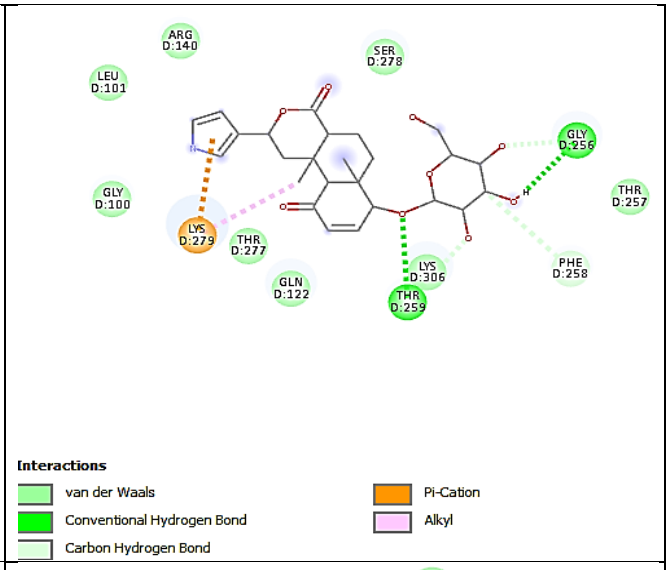
BT27	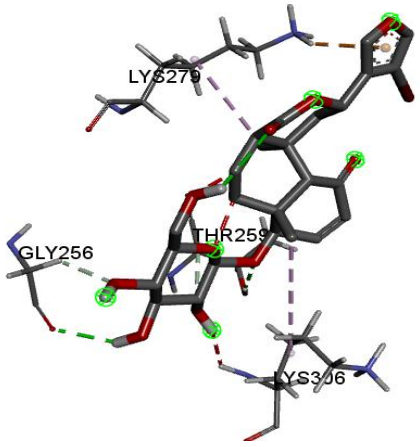	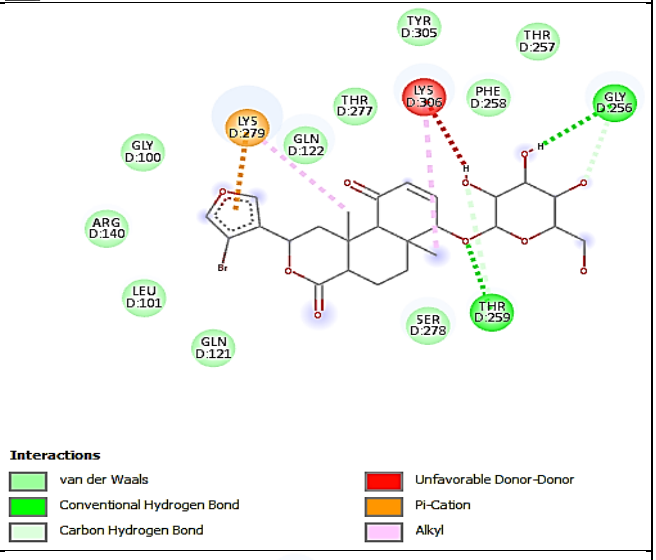
BT31	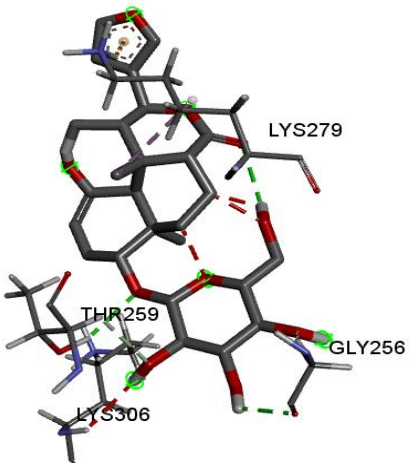	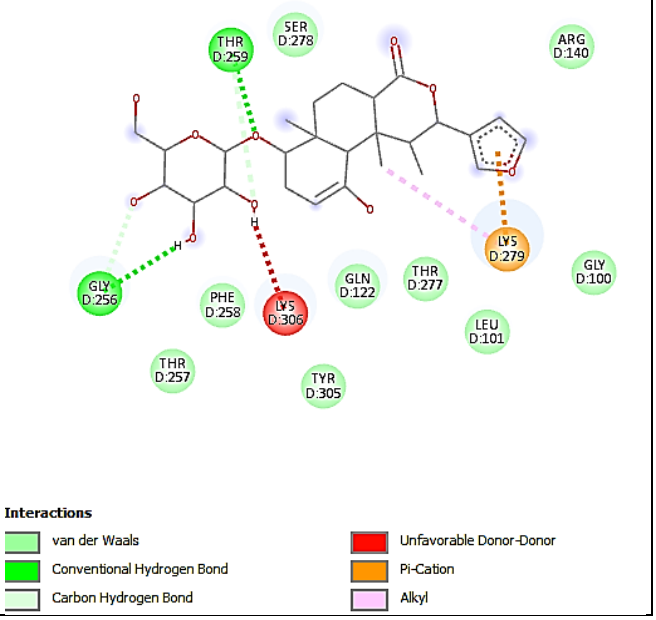

BT36	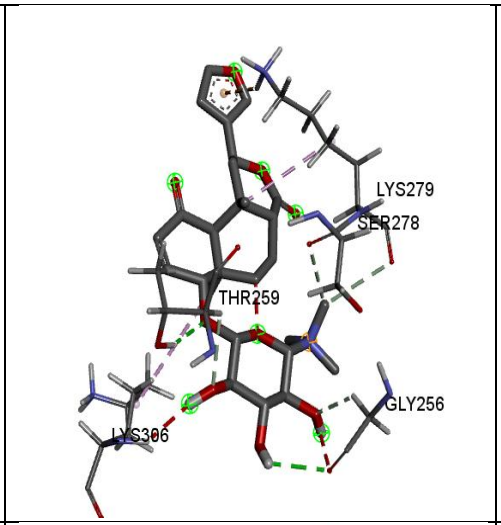	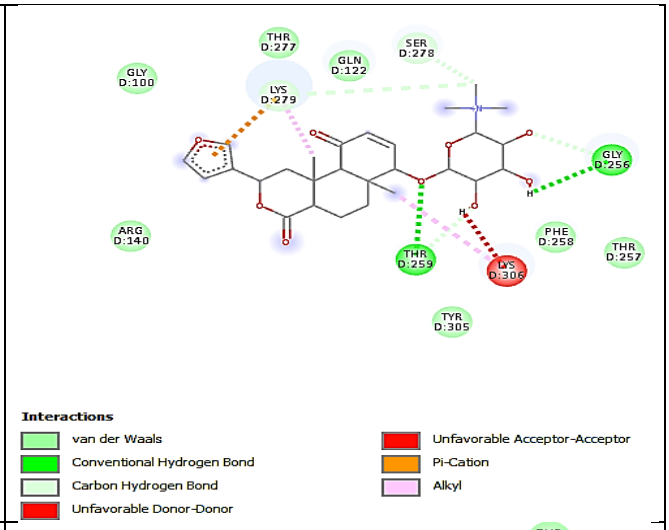
BT37	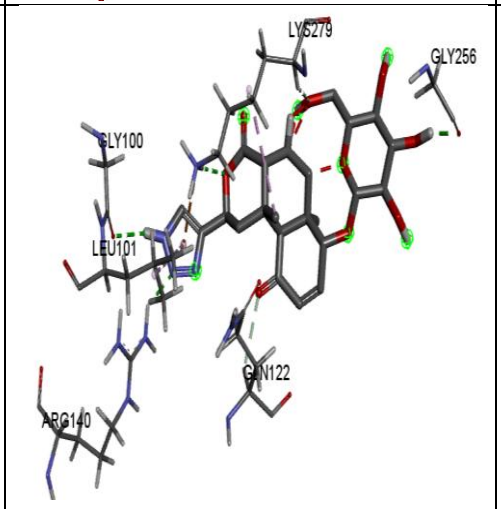	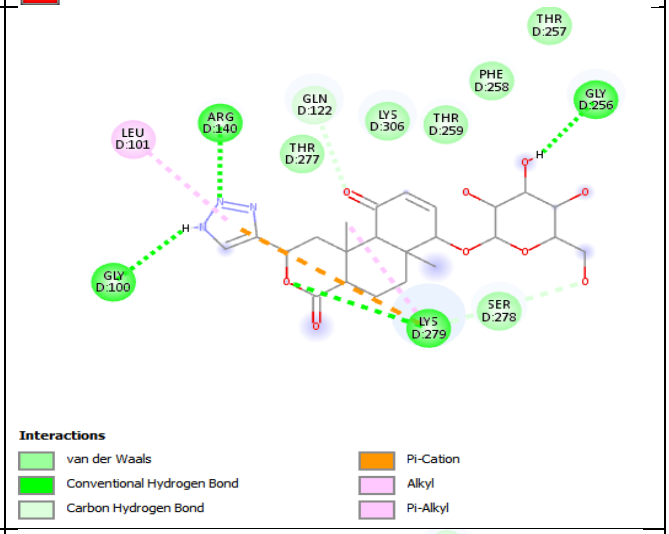
BT39	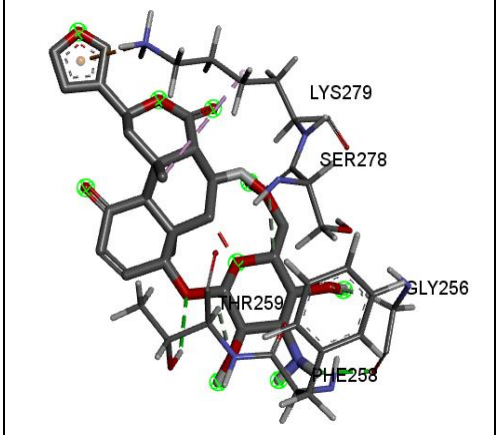	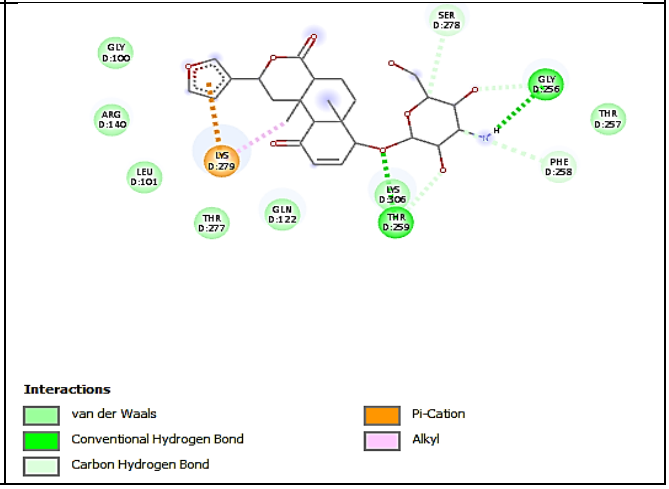

BT40	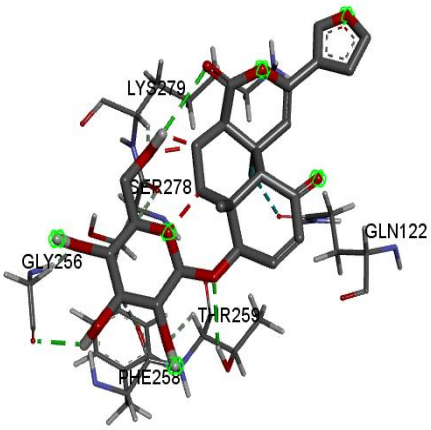	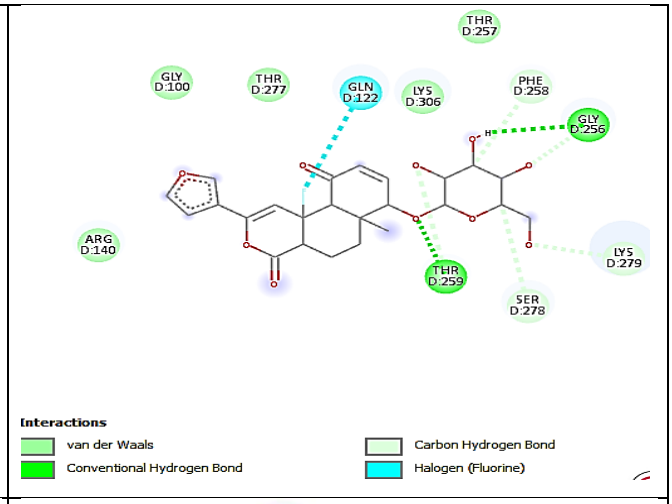
BT46	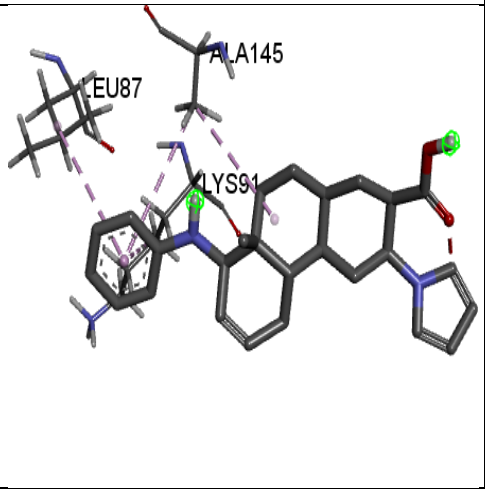	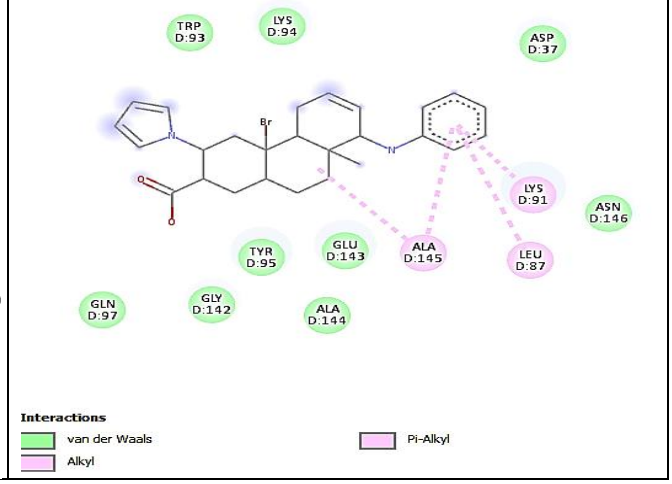

4.4.2.1 Interaction with Protein B

Docking studies revealed that T0 and its modified derivatives did not bind directly to active sites, i.e., the catalytic triad of SARS-CoV-2 PL^{pro} (Cys111, His272, Asp286)(Báez-Santos, St John, *et al.*, 2015). Instead, they formed interactions with residues such as Glu143, Gly142, Ala144, Ala145, Asn146, and Phe258, located near or outside the active sites in chain D. These interactions suggested a potential **allosteric mode of inhibition**, where the ligands influenced protease function by stabilizing non-catalytic regions.

4.4.2.2 Additional Stabilizing Interactions

Additional polar and charged residues- Lys91, Lys94, Glu214, Glu307, and Ser278- contributed to ligand binding through hydrogen bonds and electrostatic contacts. Aromatic

and hydrophobic residues like Trp93, Tyr95, Tyr213, and Phe258 further stabilized the ligands through stacking and hydrophobic effects.

Overall, the findings supported that T0 and its derivatives may inhibit PL^{pro} via **allosteric interactions**, offering a promising alternative to active-site targeting strategies.

4.4.3 Unfavourable Amino Acid Interactions

The ligands T11, T12, T36, T27, and T31 displayed unfavourable interactions with Protein A, Protein B, or both. These included donor–donor or acceptor–acceptor interactions, which could lead to steric clashes or poor hydrogen bonding. These problems can weaken the binding between the ligand and the protein(Luscombe *et al.*, 2001). Due to these issues, these five ligands were excluded from further analysis. Some adjustments in the ligand structure or refinement of their positioning will be needed to enhance their binding.

4.4.4 Benchmarking

The approved inhibitors **Nirmatrelvir** and **PF-07957472** showed similar amino acid interactions with the SARS-CoV-2 proteases (7ALH and 6WX4**,** respectively), as observed with T0 and its modified structures. This suggests that T0 and its modified ligands could also exhibit **inhibitory activity** against COVID-19, similar to the approved inhibitors. The study was designed to determine whether these ligands bind to the same amino acids as the approved inhibitors, focusing on their 2D and 3D interactions. The **interacting and pocket amino acids** for **Nirmatrelvir** and **PF-07957472** are provided in Annexure V along with their interactions, allowing for a direct comparison of their binding patterns with those of Tinosporaside and its modified structures.

4.4.5 Hydrogen and Hydrophobic Interaction Analysis

The remaining eight compounds and T0, after screening out five with unfavourable donor interactions, were further analysed using PLIP to identify key hydrogen bonds and hydrophobic interactions. Table 9 summarizes these interactions.

Table 8: PLIP Analysis of Hydrogen and Hydrophobic Interactions for Selected Compounds

Compound No.	Protein A		Protein B	
	H- Bonds	**Hydrophobic Interactions**	**H- Bonds**	**Hydrophobic Interactions**
T0	Asn A:142	Thr A:25	Gly D:256, Thr D:259, Lys D:279	Thr D:259, Lys D:279
T8	Thr A:25, Gly A:143, Glu A:166, Gly A:170 Halogen Bond: Glu A:166 (2)	0	Asp D:37, Lys D:94, Tyr D:95, Ala D:144	Lys D:91, Tyr D:95
T19	Gly A:143	Glu A:166	Tyr D:213, Glu D:214, Tyr D:251, Tyr D:305	Tyr D:213, Tyr D:305
T23	Thr A:25 (2) , His A:41, Glu A:166	Glu A:166	Gly D:256, Thr D:259, Lys D:279	Lys D:279
T24	Thr A:24 (3), Thr A:26, Asn A:142, Gly A:143, Glu A:166 (2)	Gln A:189	Gly D:100, Gly D:256, Thr D:259(2), Ser D:278, Lys D:279	Thr D:259, Lys D:279
T37	Thr A:25 (2), His A:41, Glu A:166 (2)	0	Gly D:100, Arg D:140(3), Gly D:256, Lys D:279	Thr D:259, Lys D:279
T39	Thr A:25 (2), His A:41, Glu A:166	Glu A:166	Gly D:258, Thr D:259, Lys D:279	Thr D:259, Lys D:279
T40	Thr A:24 (3), Thr A:26, Asn A:142, Gly A:143, Glu A:166	0	Gly D:258, Thr D:259, Ser D:278	Thr D:259, Lys D:279
T46	Cys A:44 Halogen Bond: His A:164	Thr A: 25, Leu A: 27, Glu A:166, Pro A:168	0	Leu D:87, Lys D:91 (2), Tyr D:95, Ala D:145

The table compares how eight compounds and T0 interact with **Protein A** and **Protein B**, focusing on hydrogen bonds and hydrophobic interactions. Most compounds formed hydrogen bonds with **Protein A** at residues like THR A:24–253, GLY A:143, GLU A:166, and ASN A:142, with some (e.g., **T8**, **T46**) also forming halogen bonds. Hydrophobic contacts are frequently involved in GLU A:166. In contrast, with **Protein B**, hydrophobic interactions were more consistent, especially with THR D:259 and LYS D:279, while hydrogen bonds were fewer, mainly involving GLY D:256 and SER D:278. Overall, the compounds showed stronger H-bonding with Protein A and more stable hydrophobic interactions with Protein B, suggesting different binding preferences.

4.5 Toxicity Analysis

The toxicities of the eight selected compounds, along with **T0**, were evaluated using the **pkCSM** and **ProTox-3.0** online tools. Predicted toxicity parameters, including classification levels, are summarized in Table 8**.**

Table 9:Predicted Toxicity Profiles and Classification of Selected Compounds and T0 Using pkCSM and ProTox-3.0 Tools.

Comp. No.	pkCSM software Predictions					ProTox 3 prediction
	CYP Inhibition	AMES Toxicity	Cardiac Toxicity	Hepatotoxicity	Skin Sensitivity	Class Prediction
T0	No	No	Yes	No	No	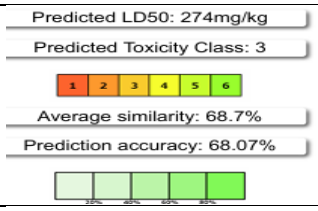
T8	Yes	No	Yes	No	No	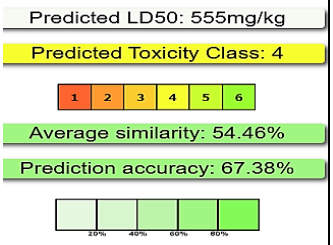
T19	No	No	No	No	No	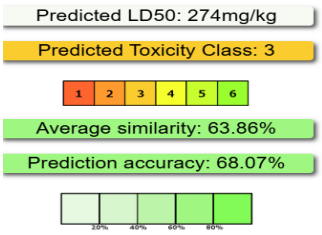
T23	No	No	No	No	No	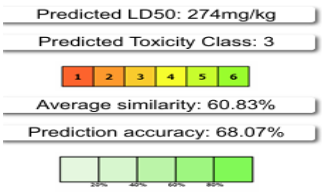
T24	No	No	No	No	No	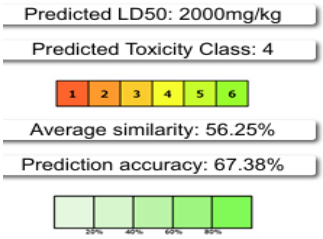
T37	No	No	No	No	No	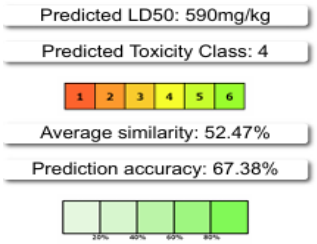

T39	No	No	No	Yes	No	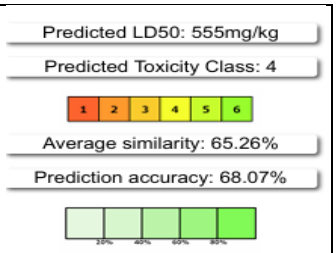
T40	No	No	No	No	No	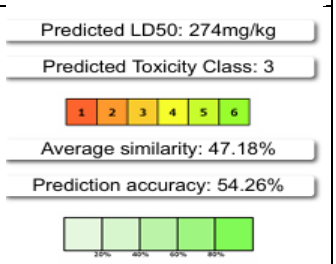
T46	No	No	No	No	No	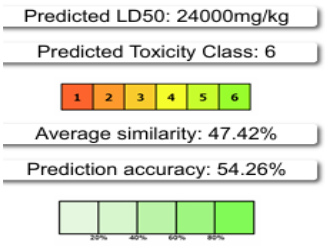

The reference **T0** compound was predicted to be a **Class 3 toxic compound if swallowed**, with potential nephrotoxicity, immunotoxicity, cardiotoxicity, and cytotoxicity, along with low GI absorption. Among the eight modified derivatives, **T8, T24, T37**, and **T39** showed improved safety, shifting to **Class 4**, indicating reduced oral toxicity. **T19, T23**, and **T40** remained in **Class 3**, while **T46** stood out as the only compound predicted to be **non-toxic (Class 6)**. Notably, **T46** also showed improved GI absorption, unlike the other compounds, which continued to exhibit low absorption potential.

Despite these improvements, compounds still showed signs of **mild neurotoxicity, respiratory toxicity, immunotoxicity**, and **clinical toxicity**, suggesting the need for further optimization before advancing toward preclinical studies. These findings suggest that while structural modifications led to improvements in safety for some candidates, further optimization is necessary to fully eliminate toxicity risks and enhance drug-likeness. **T46**, with its favorable toxicity class and absorption profile, represents the most promising lead compound for further development.

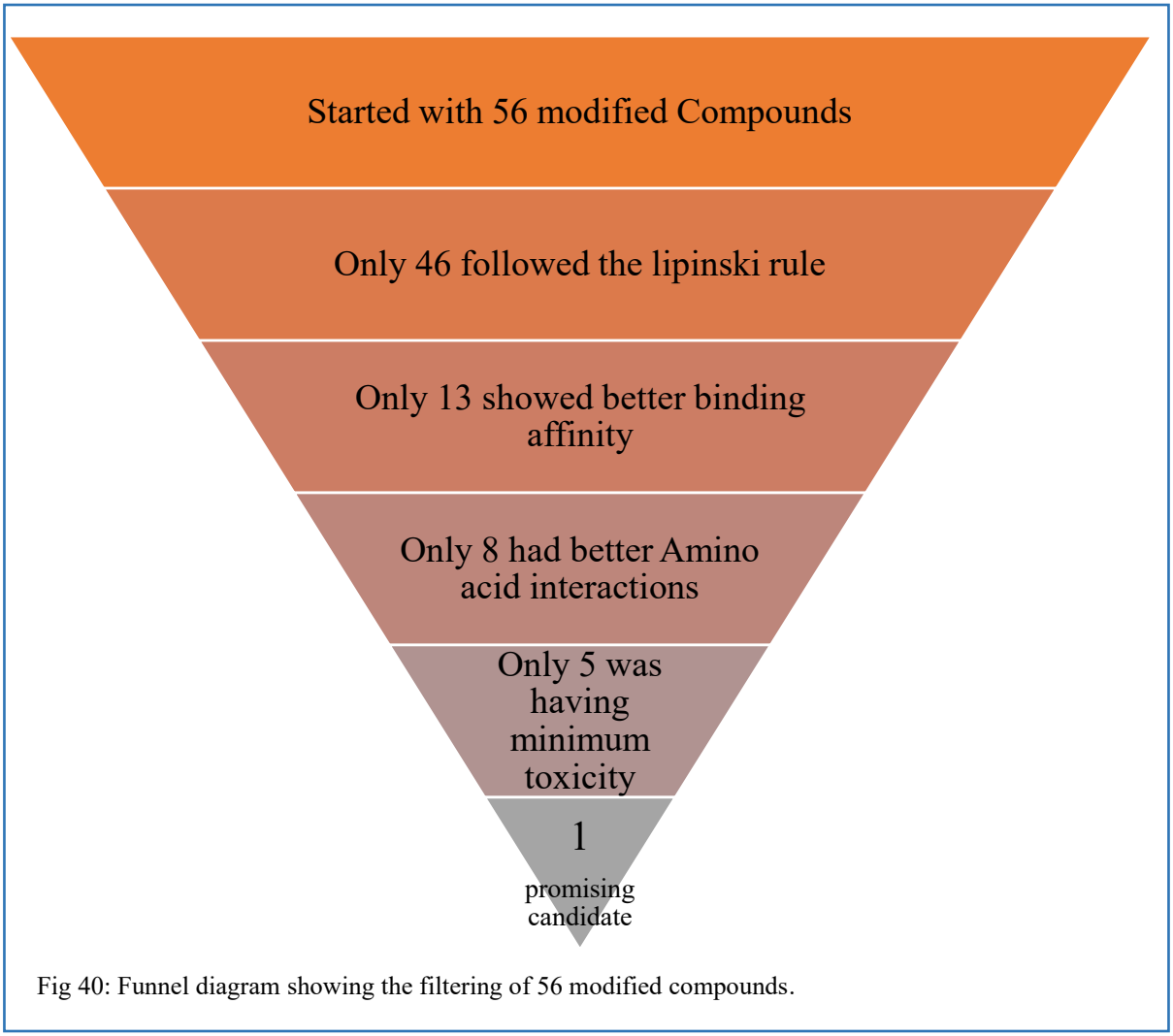

Fig 40: Funnel diagram showing the filtering of 56 modified compounds.

4.6 Pharmacophore Insights and Structural Evaluation

The **diterpenoid core** and **lactone ring** were initially considered key elements of the **pharmacophore**. Despite modifying the **furan** and **glucose side chains**, most derivatives retained this core scaffold and showed persistent **toxicity** and **low GI absorption**. Among the eight selected compounds (**T8, T19, T23, T24, T37, T39, and T40**), this **diterpenoid-lactone structure** remained largely unchanged, contributing to their **low absorption** and **limited drug-likeness**.

In contrast, **T46** displayed a structurally distinct and more favorable profile. It consists of **three fused six-membered rings** attached to a **five-membered pyrrole ring** (together **steroid-like framework**). The molecule includes a **phenyl group** connected via an **NH linker**, a **bromine atom** at the junction of the A/B rings, and a **carboxylic acid (COOH)**

group extending from the pyrrole ring. This configuration suggests a **different pharmacophoric arrangement**, enabling more specific and potentially stronger interactions with the target protein.

4.7 MD Simulation using iMOD

The MD NMA analysis of protein A with its modified ligand T46 reveals significant flexibility, particularly in two regions-atoms 50–100 and 250–300. These flexible zones are evident in the deformability (A) plot, and the match between experimental and calculated B-factors (B) shows that the simulation is accurately capturing the protein's natural movement. The first eigenvalue (C, D) suggests low-energy, large shifts, with most motion concentrated in the first few modes, especially mode 1, which contributes nearly 40%. The covariance map (E) and elastic network (F) also show that these flexible regions move together, likely influenced by the ligand. Overall, it seems that the modified ligand plays a key role in the protein's behaviour.

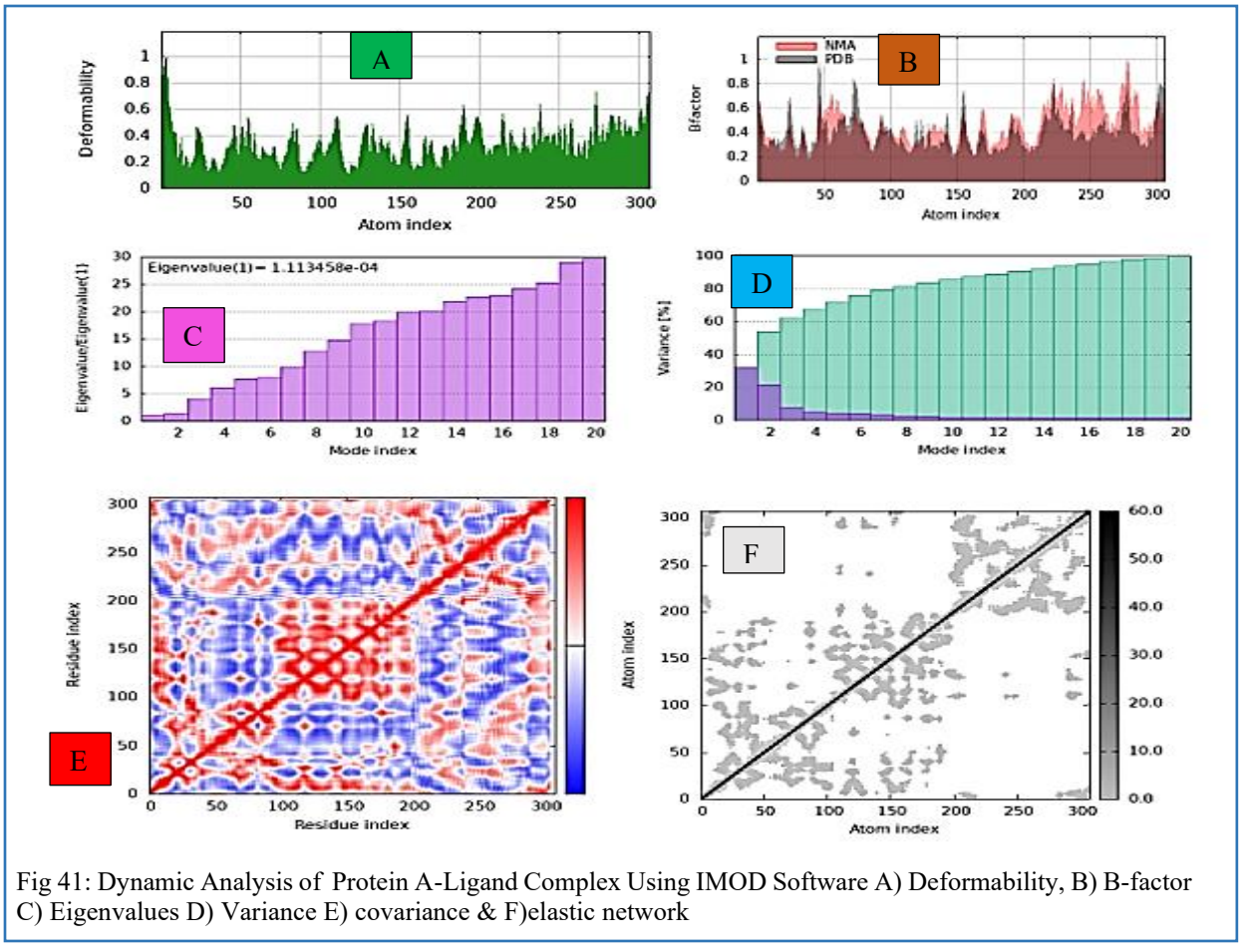

Fig 41: Dynamic Analysis of Protein A-Ligand Complex Using IMOD Software A) Deformability, B) B-factor C) Eigenvalues D) Variance E) covariance & F)elastic network

In a similar analysis of protein B to ligand T46, the flexibility is concentrated in regions around atoms 50–100 and 150–200(A). The calculated B-factor (B) data matches the experimental data, supporting the reliability of the simulation. The first eigenvalue (C, D) is low, indicating the protein is also easy to deform and undergoes low-energy movements. Like 7ALH, most of the motion is concentrated in the first few modes, and the covariance (E) and elastic network (F) models suggest that the ligand binding might trigger allosteric effects, influencing the protein's structure.

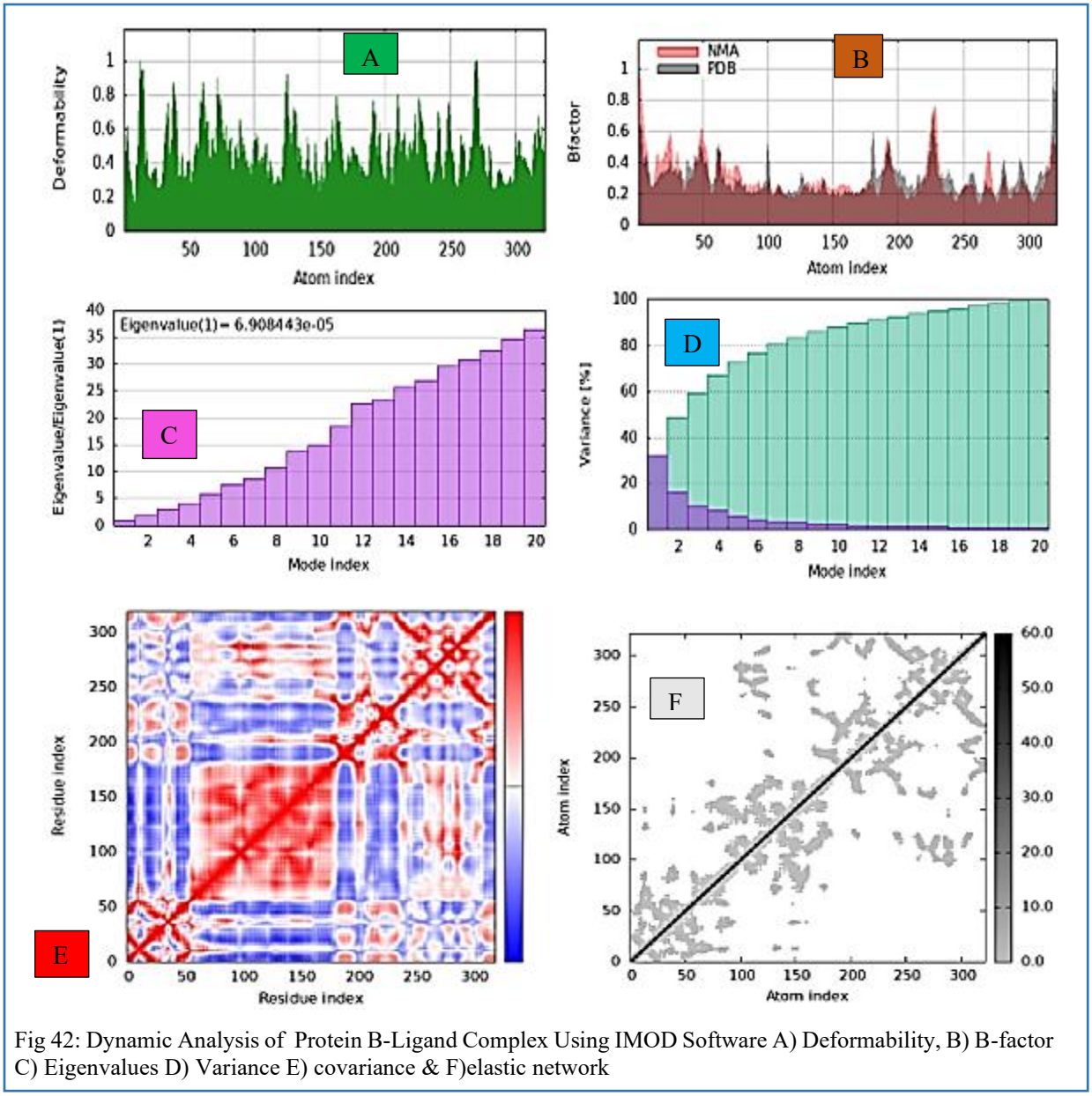

Fig 42: Dynamic Analysis of Protein B-Ligand Complex Using IMOD Software A) Deformability, B) B-factor C) Eigenvalues D) Variance E) covariance & F)elastic network

CHAPTER 5

CONCLUSION

5.1 Key Findings and Research Implications

Advancement of Tinosporaside Derivatives as Dual-Target Inhibitors for SARS-CoV-2: From in-silico Discovery to Preclinical Development

Recent in-silico investigations into T0 and its structurally modified derivatives have revealed promising antiviral potential against SARS-CoV-2, specifically targeting two critical viral proteases: M^{pro} (PDB ID: 7ALH) and PL^{pro} (PDB ID: 6WX4). Computational tools were employed to design and evaluate fifty-six Tinosporaside analogs. Among these, compound T46 emerged as the top-performing derivative, showing strong dual inhibition, enhanced binding affinity, and improved pharmacokinetic properties. These findings position T46 not only as a lead compound but also as a framework for future antiviral drug development.

- **Dual-Target Inhibition Potential: T0** and its derivative **T46** demonstrated effective binding to both SARS-CoV-2 proteases, with T46 significantly improving the original molecule's ability to bind and inhibit M^{pro} and PLpro. This highlights that T46 may have dual-inhibitory potential, a critical feature for reducing viral replication and potentially minimizing resistance mechanisms. The dual-target inhibition was further amplified by T46, showing improved interactions with key active sites, including the **CYS145-HIS41 catalytic dyad** in **M^{pro}** and **allosteric sites** in **PL^{pro}**.
- **Lead Compound Identification:** T46 emerged as the top-performing compound, demonstrating superior **binding energy**, **selectivity**, and **pharmacokinetic profile**. Compared to Tinosporaside and other analogs, T46 showed:

  - **High binding affinity** to both proteases,
  - **No predicted toxicity** (Class 6),
  - **High gastrointestinal absorption**, and
  - No **PAINS** alerts.

These characteristics make T46 a promising lead for further antiviral development and optimization.

- **Critical Structural Features and Modifications:** Key structural modifications played a crucial role in improving T46's performance:

  - **Steroid-like scaffold** and **pyrrole ring** enhanced target engagement and binding affinity,
  - The **COOH functional group** improved solubility and selectivity,
  - **Bromine** enhances binding via halogen bonds, increases lipophilicity, and improves metabolic stability.

These modifications contribute significantly to T46's improved **drug-likeness** and **pharmacological activity**.

- **Pharmacophore Shift and Activity Enhancement:** The shift in the pharmacophore from T0's diterpenoid-lactone core to T46's novel structure enhanced specificity and interaction efficiency with the proteases. This change not only increased binding affinity but also improved bioavailability, making T46 a promising candidate for further development.
- **MD Validation:** MD simulations confirmed that T46 enhances structural flexibility in both proteases, stabilizing key functional regions. Induced correlated motions and conformational shifts suggest T46 may disrupt protease activity, supporting its potential as a dual-site antiviral inhibitor.
- **Lead Compound Progression and Preclinical Development:** Starting with 56 Tinosporaside analogs, the screening process narrowed down to **one compound** (T46), which showed the best results across all computational analyses. T46's superior **binding affinity**, **selectivity**, and **pharmacokinetic properties** justify its progression from in-silico validation to preclinical studies, including ***in vitro & in vivo* studies**. The structural features and binding interactions identified in this research provide a solid foundation for **experimental validation** and **optimization** of T46 and similar derivatives.

The comprehensive in-silico study of T0 and its derivatives, particularly T46, presents strong evidence for their dual-target inhibition against SARS-CoV-2 proteases. This research highlights T46 as a promising lead compound with potential for preclinical and clinical development. Moving forward, experimental validation of T46 and other derivatives in cellular and in vivo models will be crucial to assess their antiviral efficacy and safety profile, paving the way for Tinosporaside-based therapies in the fight against COVID-19.

5.2 Comparison with Prior Research

- **Scarcity of Tinosporaside-Focused Studies**: There is a noticeable gap in the literature regarding Tinosporaside, a phytoconstituent extracted from *T. cordifolia*. While the plant itself is well-documented for its antiviral and immune-enhancing properties, specific investigations into Tinosporaside, particularly about SARS-CoV-2 protease inhibition, are lacking.
- **Evidence from Related Tinospora Species**: Existing studies on *T. cordifolia* and *T. sinensis* underscore their broad-spectrum antiviral activity and immunomodulatory potential. Nonetheless, these investigations typically address whole plant extracts or crude compounds rather than isolating and characterizing the role of Tinosporaside. Its specific interaction with viral proteases, including those of SARS-CoV-2, remains underexplored.
- **Preliminary Docking Insights**: An earlier in silico evaluation (unpublished) of several *Tinospora* compounds highlighted Tinosporaside as exhibiting notably high affinity for the SARS-CoV-2 main protease (PDB ID: 6LU7). Although the study awaits formal peer review, these results suggest that Tinosporaside could serve as a viable molecular scaffold for future antiviral agents.
- **Advancements in the Present Study**: This research expands upon those preliminary findings by exploring both the native and structurally modified forms of Tinosporaside. Computational docking and MD simulations were employed to assess binding behaviour and stability. Enhanced binding affinities observed in modified derivatives support their potential as lead compounds in antiviral therapy development.

5.3 Study Contributions and Limitations

Contributions:

- This study introduces a novel computational evaluation of Tinosporaside and its derivatives' potential as a SARS-CoV-2 protease inhibitor, filling a significant knowledge gap in phytochemical research.
- By combining docking and MD methods, the study provides a more comprehensive understanding of ligand-receptor interactions over time.
- Structure-activity relationship insights gained from modification offer a direction for optimizing pharmacokinetic and safety profiles.
- Open-source software tools were used, promoting cost-effective research and reproducibility for other academic groups.

Limitations:

- The findings are predictive and require experimental validation through *in vitro* and *in vivo* models to confirm bioactivity and therapeutic viability.
- While open-source tools increase accessibility, they may have limitations in precision compared to proprietary platforms.
- Protein conformational flexibility, though partially modelled using simulations, cannot be fully accounted for in-silico, potentially affecting interaction accuracy.
- Only a limited range of chemical modifications was tested. Broader structural analysis and longer simulations would enhance understanding of toxicity and drug-likeness.

5.4 Future Directions

To transition from computational predictions to real-world applications, the following areas need further investigation:

- **Improved Computational Resources**: Future studies should incorporate more advanced and commercially validated platforms for enhanced accuracy in molecular modelling.

- **Experimental Validation**: Laboratory studies are essential to verify antiviral activity, assess pharmacodynamics, and evaluate toxicity in biological systems.
- **Synthetic Optimization**: Efficient synthetic routes for Tinosporaside derivatives must be developed to support potential scale-up and sustainable production.
- **Mechanistic Elucidation**: Further investigation into the molecular mechanism of action, including specificity for viral versus host targets, is critical for drug development.

This study offers a starting point for further exploration of Tinosporaside as an antiviral lead compound. Moving forward, a multidisciplinary approach involving medicinal chemistry, virology, and pharmacology will be key to unlocking its clinical potential.

Final Reflection

This dissertation marks the culmination of a journey that began in our very first semester, when we drafted our initial research proposals. What started as a simple idea evolved into a fully committed project- one that demanded persistence, curiosity, and resilience. The process was far from easy. There were times when my efforts led to inconclusive or even failed results. But I learned, as my professor reminded me, that even negative results have value- they are part of the scientific process. Each setback became a lesson, guiding me to modify my approach and refine my methods. Gradually, those failures turned into insights and eventually into success. The moment I finally achieved a meaningful outcome was one of true satisfaction, a reflection of the growth and learning that this dissertation journey has brought.

REFERENCE

ACD/Labs. (2024) *Free Chemical Drawing Software for Students | ChemSketch*. *ACD/Labs*. Available at: https://www.acdlabs.com/resources/free-chemistry-software-apps/chemsketch-freeware/ (Accessed: 16 February 2025).

Ada, M.K. team. (2025) *COVID-19 Variants: 2024 Dominant Variants and Symptoms*. *Ada*. Available at: https://ada.com/covid/what-strain-of-covid-is-going-around/ (Accessed: 10 April 2025).

Adasme, M.F. *et al.* (2021) 'PLIP 2021: Expanding the Scope of the Protein–Ligand Interaction Profiler to DNA and RNA'. *Nucleic Acids Research*, 49(W1), pp. W530–W534. DOI: 10.1093/nar/gkab294.

Adeosun, W.B. and Loots, D.T. (2024) 'Medicinal Plants against Viral Infections: A Review of Metabolomics Evidence for the Antiviral Properties and Potentials in Plant Sources'. *Viruses*, 16(2), p. 218. DOI: 10.3390/v16020218.

Agu, P.C. *et al.* (2023) 'Molecular Docking as a Tool for the Discovery of Molecular Targets of Nutraceuticals in Diseases Management'. *Scientific Reports*, 13(1), p. 13398. DOI: 10.1038/s41598-023-40160-2.

Anderson, A.C. (2003) 'The Process of Structure-Based Drug Design'. *Chemistry & Biology*, 10(9), pp. 787–797. DOI: 10.1016/j.chembiol.2003.09.002.

Atampugbire, G., Adomako, E.E.A. and Quaye, O. (2024) 'Medicinal Plants as Effective Antiviral Agents and Their Potential Benefits'. *Natural Product Communications*, 19(9), p. 1934578X241282923. DOI: 10.1177/1934578X241282923.

Báez-Santos, Y.M., St. John, S.E. and Mesecar, A.D. (2015) 'The SARS-Coronavirus Papain-like Protease: Structure, Function and Inhibition by Designed Antiviral Compounds'. *Antiviral Research*, 115, pp. 21–38. DOI: 10.1016/j.antiviral.2014.12.015.

Báez-Santos, Y.M., St John, S.E. and Mesecar, A.D. (2015) 'The SARS-Coronavirus Papain-like Protease: Structure, Function and Inhibition by Designed Antiviral Compounds'. *Antiviral Research*, 115, pp. 21–38. DOI: 10.1016/j.antiviral.2014.12.015.

Banerjee, P. *et al.* (2024) 'ProTox 3.0: A Webserver for the Prediction of Toxicity of Chemicals'. *Nucleic Acids Research*, 52(W1), pp. W513–W520. DOI: 10.1093/nar/gkae303.

Bastikar, V., Bastikar, A. and Gupta, P. (2022) 'Quantitative Structure–Activity Relationship-Based Computational Approaches'. *Computational Approaches for Novel Therapeutic and Diagnostic Designing to Mitigate SARS-CoV-2 Infection*, pp. 191–205. DOI: 10.1016/B978-0-323-91172-6.00001-7.

Burley, S.K. *et al.* (2022) 'Protein Data Bank: A Comprehensive Review of 3D Structure Holdings and Worldwide Utilization by Researchers, Educators, and Students'. *Biomolecules*, 12(10), p. 1425. DOI: 10.3390/biom12101425.

Carvajal, J.J. *et al.* (2024) 'New Insights into the Pathogenesis of SARS-CoV-2 during and after the COVID-19 Pandemic'. *Frontiers in Immunology*, 15. DOI: 10.3389/fimmu.2024.1363572.

Cascella, M. *et al.* (2025) 'Features, Evaluation, and Treatment of Coronavirus (COVID-19)'. In *StatPearls*. Treasure Island (FL): StatPearls Publishing. Available at: http://www.ncbi.nlm.nih.gov/books/NBK554776/ (Accessed: 10 April 2025).

Chaudhary, A. *et al.* (2024) 'Indian Herb Tinospora Cordifolia and Tinospora Species: Phytochemical and Therapeutic Application'. *Heliyon*, 10(10), p. e31229. DOI: 10.1016/j.heliyon.2024.e31229.

Cheriyedath, S. (2017) *Protein Folding*. *News-Medical*. Available at: https://www.news-medical.net/life-sciences/Protein-Folding.aspx (Accessed: 9 April 2025).

Chowdhury, P. (2020) 'In Silico Investigation of Phytoconstituents from Indian Medicinal Herb "Tinospora Cordifolia (Giloy)" against SARS-CoV-2 (COVID-19) by Molecular Dynamics Approach'. *Journal of Biomolecular Structure & Dynamics*, pp. 1–18. DOI: 10.1080/07391102.2020.1803968.

Combet, C. *et al.* (2000) 'NPS@: Network Protein Sequence Analysis'. *Trends in Biochemical Sciences*, 25(3), pp. 147–150. DOI: 10.1016/S0968-0004(99)01540-6.

Costanzi, E. *et al.* (2021) (21) 'Structural and Biochemical Analysis of the Dual Inhibition of MG-132 against SARS-CoV-2 Main Protease (Mpro/3CLpro) and Human Cathepsin-L'. *International Journal of Molecular Sciences*, 22(21), p. 11779. DOI: 10.3390/ijms222111779.

Daina, A., Michielin, O. and Zoete, V. (2017) 'SwissADME: A Free Web Tool to Evaluate Pharmacokinetics, Drug-Likeness and Medicinal Chemistry Friendliness of Small Molecules'. *Scientific Reports*, 7, p. 42717. DOI: 10.1038/srep42717.

Dassault Systèmes. (2025) *BIOVIA Discovery Studio | Dassault Systèmes*. Available at: https://www.3ds.com/products/biovia/discovery-studio (Accessed: 16 February 2025).

Davis, A.M. (2017) '3.15 - Quantitative Structure–Activity Relationships'. In Chackalamannil, S.Rotella, D.and Ward, S.E. (eds.) *Comprehensive Medicinal Chemistry III*. Oxford: Elsevier, pp. 379–392. DOI: 10.1016/B978-0-12-409547-2.12348-0.

Eberhardt, J. *et al.* (2021) 'AutoDock Vina 1.2.0: New Docking Methods, Expanded Force Field, and Python Bindings'. *Journal of Chemical Information and Modeling*, 61(8), pp. 3891–3898. DOI: 10.1021/acs.jcim.1c00203.

ECDC. (2025) *SARS-CoV-2 Variants of Concern as of 28 February 2025*. Available at: https://www.ecdc.europa.eu/en/covid-19/variants-concern (Accessed: 11 March 2025).

El Sayed, K.A. (2000) 'Natural Products as Antiviral Agents'. *Studies in Natural Products Chemistry*, 24, pp. 473–572. DOI: 10.1016/S1572-5995(00)80051-4.

Expasy. (2024) *Expasy - ProtParam Documentation*. Available at: https://web.expasy.org/protparam/protparam-doc.html (Accessed: 16 February 2025).

Fan, J., Fu, A. and Zhang, L. (2019) 'Progress in Molecular Docking'. *Quantitative Biology*, 7(2), pp. 83–89. DOI: 10.1007/s40484-019-0172-y.

Ferreira, J.C. *et al.* (2021) 'Catalytic Dyad Residues His41 and Cys145 Impact the Catalytic Activity and Overall Conformational Fold of the Main SARS-CoV-2 Protease 3-Chymotrypsin-Like Protease'. *Frontiers in Chemistry*, 9, p. 692168. DOI: 10.3389/fchem.2021.692168.

Focosi, D., Sullivan, D.J. and Franchini, M. (2025) 'Development of Antiviral Drugs for COVID-19 in 2025: Unmet Needs and Future Challenges'. *Expert Review of Anti-Infective Therapy*. Available at: https://www.tandfonline.com/doi/abs/10.1080/14787210.2025.2473044 (Accessed: 10 March 2025).

Forli, S. *et al.* (2016) 'Computational Protein-Ligand Docking and Virtual Drug Screening with the AutoDock Suite'. *Nature Protocols*, 11(5), pp. 905–919. DOI: 10.1038/nprot.2016.051.

Garnsey, M.R. *et al.* (2024) 'Discovery of SARS-CoV-2 Papain-like Protease (PLpro) Inhibitors with Efficacy in a Murine Infection Model'. *Science Advances*, 10(35), p. eado4288. DOI: 10.1126/sciadv.ado4288.

Geourjon, C. and Deléage, G. (1995) 'SOPMA: Significant Improvements in Protein Secondary Structure Prediction by Consensus Prediction from Multiple Alignments'. *Computer Applications in the Biosciences: CABIOS*, 11(6), pp. 681–684. DOI: 10.1093/bioinformatics/11.6.681.

Grum-Tokars, V. *et al.* (2008) 'Evaluating the 3C-like Protease Activity of SARS-Coronavirus: Recommendations for Standardized Assays for Drug Discovery'. *Virus Research*, 133(1), pp. 63–73. DOI: 10.1016/j.virusres.2007.02.015.

Hu, Q. *et al.* (2022) 'The SARS-CoV-2 Main Protease (Mpro): Structure, Function, and Emerging Therapies for COVID-19'. *MedComm*, 3(3), p. e151. DOI: 10.1002/mco2.151.

iStock. (2020) *Virus inside to Respiratory System*. *iStock*. Available at: https://www.istockphoto.com/photo/corona-virus-or-covid-19-gm1218710372-356207840 (Accessed: 11 March 2025).

Jain, H. (2020) *Figure 1: Tinospora Cordifolia (Giloy) Plant (Leaves, Stems and Root)*. *ResearchGate*. Available at: https://www.researchgate.net/figure/Tinospora-cordifolia-Giloy-plant-Leaves-stems-and-root_fig1_351816448 (Accessed: 12 March 2025).

Jiang, X. *et al.* (2023) (6) 'Molecular Dynamics Simulation of the Effect of Low Temperature on the Properties of Lignocellulosic Amorphous Region'. *Forests*, 14(6), p. 1208. DOI: 10.3390/f14061208.

Jiménez, J. *et al.* (2017) 'DeepSite: Protein-Binding Site Predictor Using 3D-Convolutional Neural Networks'. *Bioinformatics*, 33(19), pp. 3036–3042. DOI: 10.1093/bioinformatics/btx350.

Jogalekar, A. (Ash). (2021) *The Human Problems with Molecular Modeling*. *Wavefunction*. Available at: http://wavefunction.fieldofscience.com/2021/04/the-human-problems-with-molecular.html (Accessed: 13 March 2025).

Joshi, A. and Kaushik, V. (2021) (1) 'Insights of Molecular Docking in Autodock-Vina: A Practical Approach'. *Journal of Pharmacology and Clinical Toxicology*, 9(1), pp. 1–6. DOI: 10.47739/1055.

Khan, M.A., Gray, A.I. and Waterman, P.G. (1989) 'Tinosporaside, an 18-Norclerodane Glucoside from *Tinospora Cordifolia*'. *Phytochemistry*, 28(1), pp. 273–275. DOI: 10.1016/0031-9422(89)85057-5.

khanacedamy. (2025) *Protein Structure: Primary, Secondary, Tertiary & Quatrenary (Article)*. *Khan Academy*. Available at: https://www.khanacademy.org/science/biology/macromolecules/proteins-and-amino-acids/a/orders-of-protein-structure (Accessed: 9 April 2025).

Lipinski, C.A. *et al.* (2001) 'Experimental and Computational Approaches to Estimate Solubility and Permeability in Drug Discovery and Development Settings1'. *Advanced Drug Delivery Reviews*, 46(1), pp. 3–26. DOI: 10.1016/S0169-409X(00)00129-0.

Liu, Y. *et al.* (2020) 'The Development of Coronavirus 3C-Like Protease (3CLpro) Inhibitors from 2010 to 2020'. *European Journal of Medicinal Chemistry*, 206, p. 112711. DOI: 10.1016/j.ejmech.2020.112711.

Lopéz-Blanco, J.R., Garzón, J.I. and Chacón, P. (2011) 'iMod: Multipurpose Normal Mode Analysis in Internal Coordinates'. *Bioinformatics*, 27(20), pp. 2843–2850. DOI: 10.1093/bioinformatics/btr497.

Luscombe, N.M., Laskowski, R.A. and Thornton, J.M. (2001) 'Amino Acid–Base Interactions: A Three-Dimensional Analysis of Protein–DNA Interactions at an Atomic Level'. *Nucleic Acids Research*, 29(13), pp. 2860–2874.

mgl-admin (2018) *Manual-AutoDock Vina Manual*. *AutoDock Vina*. Available at: https://vina.scripps.edu/manual/ (Accessed: 30 January 2025).

Mishra, A. *et al.* (2023) 'Tinosporaside from Tinospora Cordifolia Encourages Skeletal Muscle Glucose Transport through Both PI-3-Kinase- and AMPK-Dependent Mechanisms'. *Molecules (Basel, Switzerland)*, 28(2), p. 483. DOI: 10.3390/molecules28020483.

Mukherjee, R. and Dikic, I. (2023) 'Proteases of SARS Coronaviruses'. *Encyclopedia of Cell Biology*, pp. 930–941. DOI: 10.1016/B978-0-12-821618-7.00111-5.

Nadendla, R. and Yemineni, G. (2024) '(PDF) "Molecular Modification: A Strategy in Drug Discovery and Drug Design"'. *ResearchGate*, 52(2). DOI: 10.26717/BJSTR.2023.52.008220.

Najmi, A. *et al.* (2020) *(PDF) Review of Antiviral Activities Present in Some Indian Medicinal Plants -Can They Be Used against SARS- CoV-2?*. *ResearchGate*. DOI: 10.21276/iabcr.2020.6.4.1.

NCCIH. (2022) *COVID-19 and 'Alternative' Treatments: What You Need To Know*. *NCCIH*. Available at: https://www.nccih.nih.gov/health/covid-19-and-alternative-treatments-what-you-need-to-know (Accessed: 12 March 2025).

Ogino, M.H. and Tadi, P. (2025) 'Cyclophosphamide'. In *StatPearls*. Treasure Island (FL): StatPearls Publishing. Available at: http://www.ncbi.nlm.nih.gov/books/NBK553087/ (Accessed: 16 February 2025).

Osipiuk, J. *et al.* (2021) 'Structure of Papain-like Protease from SARS-CoV-2 and Its Complexes with Non-Covalent Inhibitors'. *Nature Communications*, 12(1), p. 743. DOI: 10.1038/s41467-021-21060-3.

PDB, R.P.D. (2020a) *RCSB PDB - 6WX4: Crystal Structure of the SARS CoV-2 Papain-like Protease in Complex with Peptide Inhibitor VIR251*. Available at: https://www.rcsb.org/structure/6wx4 (Accessed: 12 March 2025).

PDB, R.P.D. (2020b) *RCSB PDB - 7ALH: Crystal Structure of the Main Protease (3CLpro/Mpro) of SARS-CoV-2 at 1.65A Resolution (Spacegroup C2).* Available at: https://www.rcsb.org/structure/7ALH (Accessed: 11 March 2025).

PDB, R.P.D. (2025) *RCSB PDB: Homepage*. Available at: https://www.rcsb.org/ (Accessed: 13 March 2025).

Pillai, Parvathy, K.S.& S. (2024) *GHS Classification of Drugs Based on LD50 - More Cons than Prose*. Available at: https://www.pharmabiz.com/NewsDetails.aspx?aid=166058&sid=9 (Accessed: 10 April 2025).

Pires, D.E.V., Blundell, T.L. and Ascher, D.B. (2015) 'pkCSM: Predicting Small-Molecule Pharmacokinetic and Toxicity Properties Using Graph-Based Signatures'. *Journal of Medicinal Chemistry*, 58(9), pp. 4066–4072. DOI: 10.1021/acs.jmedchem.5b00104.

PkCSM. (2025) *pkCSM*. Available at: https://biosig.lab.uq.edu.au/pkcsm/prediction (Accessed: 13 March 2025).

Plummer, R. (2024) *Share Covid Data, World Health Organization Tells China*. *BBC*. Available at: https://www.bbc.com/news/articles/c1d3y5zvxzeo (Accessed: 11 March 2025).

PubChem. (2007) *Tinosporaside*. Available at: https://pubchem.ncbi.nlm.nih.gov/compound/14194109 (Accessed: 12 March 2025).

Sadybekov, A.V. and Katritch, V. (2023) 'Computational Approaches Streamlining Drug Discovery'. *Nature*, 616(7958), pp. 673–685. DOI: 10.1038/s41586-023-05905-z.

Salentin, S. *et al.* (2015) 'PLIP: Fully Automated Protein-Ligand Interaction Profiler'. *Nucleic Acids Research*, 43(W1), pp. W443-447. DOI: 10.1093/nar/gkv315.

Seuring, S., Stella, T. and Stella, M. (2024) '(PDF) Developing and Publishing Strong Empirical Research in Sustainability Management—Addressing the Intersection of Theory, Method, and Empirical Field'. *ResearchGate*. DOI: 10.3389/frsus.2020.617870.

Shawky, A.M. *et al.* (2024) 'Covalent Small-Molecule Inhibitors of SARS-CoV-2 Mpro: Insights into Their Design, Classification, Biological Activity, and Binding Interactions'. *European Journal of Medicinal Chemistry*, 277, p. 116704. DOI: 10.1016/j.ejmech.2024.116704.

Singh, B., Nathawat, S. and Sharma, R.A. (2021) 'Ethnopharmacological and Phytochemical Attributes of Indian *Tinospora* Species: A Comprehensive Review'. *Arabian Journal of Chemistry*, 14(10), p. 103381. DOI: 10.1016/j.arabjc.2021.103381.

Snapse. (2025) *What Is LD50?*. Available at: https://synapse.patsnap.com/blog/what-is-ld50 (Accessed: 30 April 2025).

Syntelly. (2024) *Syntelly*. Available at: https://syntelly.com (Accessed: 8 May 2025).

Tenorio, Y. (2013) *Figure 1. Elements in Molecular Docking. ResearchGate*. Available at: https://www.researchgate.net/figure/Elements-in-molecular-docking_fig1_237012127 (Accessed: 12 March 2025).

Trott, O. and Olson, A.J. (2010) 'AutoDock Vina: Improving the Speed and Accuracy of Docking with a New Scoring Function, Efficient Optimization, and Multithreading'. *Journal of Computational Chemistry*, 31(2), pp. 455–461. DOI: 10.1002/jcc.21334.

Tumskiy, R.S. *et al.* (2023) 'SARS-CoV-2 Proteases Mpro and PLpro: Design of Inhibitors with Predicted High Potency and Low Mammalian Toxicity Using Artificial Neural Networks, Ligand-Protein Docking, Molecular Dynamics Simulations, and ADMET Calculations'. *Computers in Biology and Medicine*, 153, p. 106449. DOI: 10.1016/j.compbiomed.2022.106449.

V'kovski, P. *et al.* (2021) 'Coronavirus Biology and Replication: Implications for SARS-CoV-2'. *Nature Reviews. Microbiology*, 19(3), pp. 155–170. DOI: 10.1038/s41579-020-00468-6.

Wang, Y. *et al.* (2009) 'PubChem: A Public Information System for Analyzing Bioactivities of Small Molecules'. *Nucleic Acids Research*, 37(Web Server issue), pp. W623–W633. DOI: 10.1093/nar/gkp456.

Ward et al, D.P. (2020) *COVID-19/SARS-CoV-2 Pandemic*. *FPM*. Available at: https://www.fpm.org.uk/blog/covid-19-sars-cov-2-pandemic/ (Accessed: 11 March 2025).

WHO. (2020) *Naming the Coronavirus Disease (COVID-19) and the Virus That Causes It*. Available at: https://www.who.int/emergencies/diseases/novel-coronavirus-2019/technical-guidance/naming-the-coronavirus-disease-(covid-2019)-and-the-virus-that-causes-it (Accessed: 7 February 2025).

WHO. (2023) *Traditional Medicine Has a Long History of Contributing to Conventional Medicine and Continues to Hold Promise*. *World Health Organisation*. Available at: https://www.who.int/news-room/feature-stories/detail/traditional-medicine-has-a-long-history-of-contributing-to-conventional-medicine-and-continues-to-hold-promise (Accessed: 10 March 2025).

Xu, Z. *et al.* (2022) (23) 'Lead/Drug Discovery from Natural Resources'. *Molecules*, 27(23), p. 8280. DOI: 10.3390/molecules27238280.

Yevsieieva, L.V. *et al.* (2023) 'Main and Papain-like Proteases as Prospective Targets for Pharmacological Treatment of Coronavirus SARS-CoV-2'. *RSC Advances*, 13(50), pp. 35500–35524. DOI: 10.1039/D3RA06479D.

Ying, Y. *et al.* (2008) 'Total Synthesis and Molecular Target of Largazole, a Histone Deacetylase Inhibitor'. *Journal of the American Chemical Society*, 130(26), pp. 8455–8459. DOI: 10.1021/ja8013727.

yuan, shuguang., chan, H.C. stephen. and Hu, Z. (2024) '(PDF) Using PyMOL as a Platform for Computational Drug Design'. *ResearchGate*. DOI: 10.1002/wcms.1298.

Zhang, B. *et al.* (2022) 'Molecular Docking-Based Computational Platform for High-Throughput Virtual Screening'. *Ccf Transactions on High Performance Computing*, 4(1), pp. 63–74. DOI: 10.1007/s42514-021-00086-5.

Zhang, Q. *et al.* (2021) 'Molecular Mechanism of Interaction between SARS-CoV-2 and Host Cells and Interventional Therapy'. *Signal Transduction and Targeted Therapy*, 6(1), pp. 1–19. DOI: 10.1038/s41392-021-00653-w

ANNEXURE

ANNEXURE I: Amino Acid Sequences of SARS-CoV-2 Proteases

COVID Protease	PDB ID	Amino Acid Sequence	No. of A.A
Main Protease	7ALH (Protein A)	SGFRKMAFPSGKVEGCMVQVTCGTTTLNGLWLDDVVYCPRHVICTSEDMLNPNYEDLLI RKSNHNFLVQAGNVQLRVIGHSMQNCVLKLKVDTANPKTPKYKFVRIQPGQTFSVLACYN GSPSGVYQCAMRPNFTIKGSFLNGSCGSVGFNIDYDCVSFCYMHHMELPTGVHAGTDLEGN FYGPFVDRQTAQAAGTDTTITVNVLAWLYAAVINGDRWFLNRFTTTLNDFNLVAMKYNYE PLTQDHVDILGPLSAQTGIAVLDMCASLKELLQNGMNGRTILGSALLEDEFTPFDVVRQCSGV TFQ	306
Papain-like Protease	6WX4 (Protein B)	MREVRTIKVFTTVDNINLHTQVVDMSMTYGQQFGPTYLDGADVTKIKPHNSHEGKTFYVLP NDDTLRVEAFEYYHTTDPSFLGRYMSALNHTKKWKYPQVNGLTSIKWADNNCYLATALLT LQQIELKFNPPALQDAYYRARAGEAANFCALILAYCNKTVGELGDVRETMSYLFQHANLDS CKRVLNVVCKTCGQQQTTLKGVEAVMYMGTLSYEQFKKGVQIPCTCGKQATKYLVQQESP FVMMSAPPAQYELKHGTFTCASEYTGNYQCGHYKHITSKETLYCIDGALLTKSSEYKGPITDV FYKENSYTTTIKPLEHHHHHH	326

ANNEXURE II: SMILES Notations and Molecular Formulas of Tinosporaside (T0) and fifty-six Related Compounds Generated Using ChemSketch.

Compound No.	SMILES Notations	Molecular Formula
T0	O=C1OC(CC2(C)C3C(=O)C=CC(OC4OC(CO)C(O)C(O)C4O)C3(C)CCC12)c1ccoc 1	$C_{25}H_{32}O_{10}$
T1	OC1C(OC2C=CC(=O)C3C4CC(OCC4CCC32C)N2C=CCNC2)OC(CO)C(O)C1O	$C_{24}H_{36}N_2O_8$
T2	O=C1OC(CC2(C)C3C(=O)C=CC(O)C3(C)CCC12)c1ccoc1	$C_{19}H_{22}O_5$
T3	O=C1OCCC2(C)C3C(=O)C=CC(OC4OC(CO)C(O)C(O)C4O)C3(C)CCC12	$C_{21}H_{30}O_9$
T4	CC12CCC3C(=O)OCCC3(C)C1C(=O)C=CC2O	$C_{15}H_{20}O_4$
T5	O=C1OC(CC2(C)C3C(=O)C=CCC3(C)CCC12)c1ncc(nc1F)C(=O)N	$C_{20}H_{22}FN_3O_4$

T6	O=[S@@](=O)(NC1OC(=O)C2CCC3(C)CC=CC(=O)C3C2(C)C1)c1ccc(cn1)C(F)(F)F	$C_{21}H_{23}F_3N_2O_5S$
T7	O=C1OC(CC2(C)C3C(=O)C=CCC3(C)CCC12)C1CC(OC1)n1ncnc1	$C_{21}H_{27}N_3O_4$
T8	O=C1OC(CC2(C3C(=O)C=CC(Oc4cc(Cl)cc(c4)C#N)C3(CCC12)C(F)(F)F)C(F)(F)F)c1ccoc1	$C_{26}H_{18}ClF_6NO_5$
T9	O=C1OC(CC2(C)C3C(=O)C=CCC3(C)CCC12)C1COC(C#N)(C1)c1ccc2[n@]1ncnc2N	$C_{26}H_{29}N_5O_4$
T10	O[P@](=O)(N)OC1CC2(C)C(CCC3(C)C2C(=O)C=CC3O)C(=O)O1	$C_{15}H_{22}NO_7P$
T11	O=C1OC(CC2(C)C(C=O)C(C)(CCC12)COC1OC(CO)C(O)C(O)C1O)c1ccoc1	$C_{23}H_{32}O_{10}$
T12	O=C(OCc1ccoc1)C1CCC2(C)C(C(=O)C=CC2OC2OC(CO)C(O)C(O)C2O)C1C	$C_{24}H_{32}O_{10}$
T13	OC1C(OC(CO)C(O)C1O)OC1C=CC(=O)C(C1C)C1(C)CC(=O)OC(C1)c1ccoc1	$C_{23}H_{30}O_{10}$
T14	OC1C(OC2C=CC(F)C3C4(C)CC(OC(F)C4CCC32C)c2ccoc2)OC(CF)C(O)C1O	$C_{25}H_{33}F_3O_7$
T15	CC12CC(OC(CON)C2CCC2(C)C1C(=O)C(C)=CC2O)c1ccoc1	$C_{21}H_{29}NO_5$
T16	O=C1OC(CC2(C)C3C(=O)C(F)=CC(OC4OC(CO)C(O)C(O)C4O)C3(C)CCC12)c1ccoc1	$C_{25}H_{31}FO_{10}$
T17	COOC1OCCC2(C)C3C(=O)C=CC(OC4OC(CO)C(O)C(O)C4O)C3(C)CCC12	$C_{22}H_{34}O_{10}$
T18	OC1C(OC2C=CC(CON)C3C2CCC2COC(CC32C)c2ccoc2)OC(C)C(O)C1O	$C_{25}H_{37}NO_8$
T19	OC1C(OC2C=C(O)C(=O)C3C4(C)CC(OCC4CCC32C)c2ccoc2)OC(CO)C(O)C1O	$C_{25}H_{34}O_{10}$
T20	O=C1OC(CC2(C)C3CC4OC4C(OC4OC(CO)C(O)C(O)C4O)C3(C)CCC12)c1ccoc1	$C_{25}H_{34}O_{10}$
T21	O=C1OC(CC2(C)C3C(=O)CCC(OC4OC(CO)C(O)C(O)C4O)C3(C)CCC12)c1ccoc1	$C_{25}H_{34}O_{10}$
T22	[O-][N+](=O)C1C=CC(OC2OC(CO)C(O)C(O)C2O)C2(C)CCC3C(=O)OCCC3(C)C12	$C_{21}H_{31}NO_{10}$
T23	SC12CCC3C(=O)OC(CC3(C)C1C(=O)C=CC2OC1OC(CO)C(O)C(O)C1O)c1ccoc1	$C_{24}H_{30}O_{10}S$
T24	O=C1OC(CC2(C)C3C(=O)C=CC(OC4OC(CO)C(O)C(O)C4O)C3(C)CCC12)c1cc[NH]c1	$C_{25}H_{33}NO_9$
T25	COc1cocc1C1CC2CC(C)(CCC2C(=O)O1)C(C=C)OC1OC(CO)C(O)C(O)C1O	$C_{24}H_{34}O_{10}$
T26	O=C1OC(CC2(C)C3C(=O)C=CC(OC4OC(CO)C(O)C(O)C4O)C3(C)CCC12)C1CCOC1	$C_{25}H_{36}O_{10}$
T27	O=C1OC(CC2(C)C3C(=O)C=CC(OC4OC(CO)C(O)C(O)C4O)C3(C)CCC12)c1cocc1Br	$C_{25}H_{31}BrO_{10}$
T28	O=C1OC(CC2(C)C3C(=O)C=CC(OC4OC(CO)C(O)C(O)C4O)C3(C)CCC12)N1C=CSC1	$C_{24}H_{33}NO_9S$

T29	CC1(CO)CCC2C(=O)OC(CC2C1C[S@@](=O)(=O)O)C(=C)C=C	$C_{16}H_{24}O_6S$
T30	O=C1NC(CC2(C)C3C(=O)C=CC(OC4OC(CO)C(O)C(O)C4O)C3(C)CCC12)c1ccoc1	$C_{25}H_{33}NO_9$
T31	O=C1OC(c2ccoc2)C(C)C2(C)C3C(=O)C=CC(OC4OC(CO)C(O)C(O)C4O)C3(C)CCC12	$C_{26}H_{34}O_{10}$
T32	O=C1OC(CC2(C)C3C(=O)C=CC(OC4OC(CC(O)C4)CO)C3(C)CCC12)c1ccoc1	$C_{25}H_{32}O_8$
T33	COC1C(O)C(OC2C=CC(=O)C3C4(C)CC(OC(=O)C4CCC32C)c2ccoc2)OC(COC)C1O	$C_{27}H_{36}O_{10}$
T34	O=C1OC(CC2(C)C3C(=O)C=CC(OC4OC(OC)C(O)C(O)C4O)C3(C)CCC12)c1ccoc1	$C_{25}H_{32}O_{10}$
T35	ONOCC12CC(OCC2CCC2(C)CC=CC(O)C12)c1ccoc1	$C_{19}H_{27}NO_5$
T36	C[N+](C)(C)C1OC(OC2C=CC(=O)C3C4(C)CC(OC(=O)C4CCC32C)c2ccoc2)C(O)C(O)C1O	$C_{27}H_{38}NO_9^+$
T37	O=C1OC(CC2(C)C3C(=O)C=CC(OC4OC(CO)C(O)C(O)C4O)C3(C)CCC12)c1c[NH]nn1	$C_{23}H_{31}N_3O_9$
T38	O=[P@](O)(O)C12C(=O)C=CCC2(C)CCC2C(=O)OC(CC21C)c1ccoc1	$C_{19}H_{23}O_7P$
T39	O=C1OC(CC2(C)C3C(=O)C=CC(OC4OC(CO)C(O)C(N)C4O)C3(C)CCC12)c1ccoc1	$C_{25}H_{33}NO_9$
T40	O=C1OC(=CC2(F)C3C(=O)C=CC(OC4OC(CO)C(O)C(O)C4O)C3(C)CCC12)c1ccoc1	$C_{24}H_{27}FO_{10}$
T41	CC12CC(O)OCC2CCC2(C)C(N)C=CCC12	$C_{15}H_{25}NO_2$
T42	OC1CC2(C)C(CO1)CCC1C(N)C=CCC12	$C_{14}H_{23}NO_2$
T43	OC1CC2(C)C(CO1)CCC1(Br)C(N)C=CCC12	$C_{14}H_{22}BrNO_2$
T44	NC1C=CCC2C1(Br)CCC1COCCC21C	$C_{14}H_{22}BrNO$
T45	NC1C=CCC2C3(C)CC(OCC3CCC12C)n1cccc1	$C_{19}H_{28}N_2O$
T46	OC(=O)C1CC2CCC3(C)C(Nc4ccccc4)C=CCC3C2(Br)CC1n1cccc1	$C_{26}H_{31}BrN_2O_2$
T47	O=C1NC(=O)C(C)=CN1c1cc(c(o1)CO)C1CC2(C)C3C(=O)C=CC(OC4OC(CO)C(O)C(O)C4O)C3(C)CCC2C(=O)O1	$C_{31}H_{38}N_2O_{13}$
T48	O=C1O[C@@H](C[C@@]2(C)[C@@H]3C(=O)C=C[C@@H](O[C@@H]4O[C@H](CO)[C@@H](O)[C@H](O)[C@H]4O)[C@]3(C)CC[C@@H]12)c1cc[o+](NC(=O)c2nc(F)cnc2)c1	$C_{30}H_{35}FN_3O_{11}^+$

T49	O=C1O[C@@H](C[C@@]2(C)[C@@H]3C(=O)C=C[C@@H](OCN4C(N)=Nc5[NH]c(nc5C4=O)COCCO)[C@]3(C)CC[C@@H]12)c1ccoc1	$C_{28}H_{33}N_5O_8$
T50	C[C@]12C[C@H](OC(=O)[C@@H]2CC[C@]2(C)[C@H]1C(=O)C=C[C@H]2O[C@@H]1O[C@H](CO)[C@@H](O)[C@H](O)[C@H]1O)c1ccoc1COP(=O)(Oc1ccccc1)NC(C)C(=O)OC(CC)CC	$C_{40}H_{54}NO_{15}P$
T51	O=C1O[C@@H](C[C@@]2(C)[C@@H]3C(=O)C4OC4[C@@H](O[C@@H]4O[C@H](CO)[C@@H](O)[C@H](O)[C@H]4O)[C@]3(C)CC[C@@H]12)c1cocc1	$C_{25}H_{32}O_{11}$
T52	ONOCc1cocc1[C@@H]1C[C@@]2(C)C3C(=O)C=C[C@@H](O[C@@H]4O[C@H](CO)[C@@H](O)[C@H](O)[C@H]4O)[C@]3(C)CC[C@H]2C(=O)O1	$C_{26}H_{35}NO_{12}$
T53	O=C1O[C@@H](C[C@@]2(C)C3C(=O)C=C[C@@H](O[C@@H]4O[C@H](CO)[C@@H](O)[C@H](O)[C@H]4O)[C@]3(C)CC[C@@H]12)c1c(occ1C)C(=O)N	$C_{27}H_{35}NO_{11}$
T54	O=C1O[C@@H](C[C@@]2(C)C3C(=O)C=C[C@@H](O[C@@H]4O[C@H](CO)[C@@H](O)[C@H](O)[C@H]4O)[C@]3(C)CC[C@@H]12)c1cocc1OC	$C_{26}H_{34}O_{11}$
T55	O=C1O[C@@H](C[C@@]2(C)C3C(=O)C=C[C@@H](O[C@@H]4O[C@H](CO)[C@@H](O)[C@H](O)[C@H]4O)[C@]3(C)CC[C@@H]12)c1cocc1COON	$C_{26}H_{35}NO_{12}$
T56	O=S(=O)O\C=C/C[C@H]1OC(=O)[C@@H]2CC[C@]3(C)C(C(=O)C=C[C@H]3O[C@@H]3O[C@H](CO)[C@@H](O)[C@H](O)[C@H]3O)[C@]2(C)C1	$C_{24}H_{34}O_{12}S$

ANNEXURE III: Interacting and Pocket amino acids of Protein A and Ligands

Amino Acid Interactions of Protein A	
Interacting A.A	**Pocket A.A**
Met A:49, Gln A:189, Asna:142, Thr A:24	Thr A:26, Thr A:25, Ser A:46, His A:41, Arg A:188, Leu A:167, Met A:165, Glu A:166, Pro A:168
Gly A:143, Thr A:25, Met A:49, Gly A:170, Glu A:166,	Leu A:167, Pro A:168, Gln A:189, Ser A:46, Thr A:45, Cys A:44, His A:41, Cys A:145, Asn A:142, Met A:165
Asn A:142, Thr A:26, Thr A:25, Met A:49, Gln A:189, Pro A:168	Cys A:145, Leu A:27, Gly A:143, His A:41, Met A:165, Glu A:166, Leu A:167
Met A:49, Glu A:166, His A:41	Gln A:189, Leu A:27, Val A:42, Thr A:25, Thr A:24, Cys A:44, Thr A:45, Ser A:46, His A:164, Met A:165, Leu A:167, Pro A:168
Thr A:26, Gly A:143, Leu A:27, Cys A:145, Met A:165, His A:41, Glu A:166, Leu A:167, Pro A:168, Met A:49	Asn A:142, His A:164, Gly A:170, Gln A:189, Thr A:25
Glu A:166, His A:41	Pro A:168, His A:164, Met A:165, Val A:42, Thr A:25, Leu A:27, Cys A:44, Thr A:24, Thr A:45, Ser A:46, Met A:49, Gln A:189, Leu A: 167
Met A:165, Glu A:166, Met A:49, His A:41, Asn A:142, Thr A:26, Thr A:24	Cys A:145, Gly A:143, Asn A:119, Thr A:25, Ser A:46, Gln A:189, Leu A:167
Pro A:168, Glu A:166, Thr A:26, His A:41 Unfavourable Acceptor-Acceptor: Asn A:142	Cys A:145, Gly A:143, Leu A:27, Ser A:144, Leu A:27, Thr A:25, Val A:42, Cys A:44, Gln A:189, Met A:165, Met A:49
His A:41, Thr A:26, Glu A:166, Pro A: 168 Unfavorable Acceptor-Acceptor: Asn A:142	Met A:49, Cys A:44, Gln A:189, Met A:165, Leu A:167, Cys A:145, Leu A:141, Gly A:143, Ser A:144, Leu A:27, Thr A:25, Val A:42

Glu A:166, Met A:49, Leu A:167, His A:41	Pro A:168, Met A:165, Ser A:46, Cys A:44, Thr A:45, Thr A:25, Thr A:24, Leu A:27, Gln A:189
Glu A:166, His A:41, Met A:49	Pro A:168, Leu A:167, His A:164, Met A:165, Val A:42, Thr A:25, Leu A:27, Cys A:44, Thr A:45, Thr A:24, Ser A:46, Gln A:189
Glu A:166, Met A:49, His A:41, Cys A:44	Pro A:168, Leu A:167, Gln A:189, Ser A:46, Thr A:45, Thr A:25, Thr A:24, Leu A:27, His A:164, Met A:165
Met A:165, Asn A:142, Thr A:26, Thr A:24	Gln A:189, Glu A:166, Met A:49, Ser A:46, Thr A:25, Asn A:119, Gly A:143, His A:41, Cys A:145
Cys A:145, Leu A:27, Cys A:44, His A:41, Met A:49, Pro A:168, Asn A:142	Thr A:26, Thr A:25, Gly A:143, Met A:165, His A:164, Glu A:166, Leu A:167, Gln A:189, Ser A:46, Thr A:45

ANNEXURE IV: Interacting and Pocket amino acids of Protein B and Ligands

Amino Acid Interactions of Protein B	
Interacting A.A	**Pocket A.A**
Lys D:279, Gly D:256, Thr D:259	Gly D:100, Thr D:277, Gln D:122, Lys D:306, Phe D:258, Thr D:257, Ser D:278, Arg D:140
Gly D:142, Arg D:138, Glu D:143, Tyr D:95, Trp D:93, Lys D: 94, Lys D:91	Asn D:13, Ala D: 145, Ala D: 144, Asp D:37
Gly D:256, Leu D:101, Lys D:279, Gln D:122, Thr D:259, Lys D:306 Unfavorable Donor-Donor: Lys D:306	Ser D:278, Arg D:140, Gly D:100, Thr D:277, Phe D:258, Tyr D:305, Thr D:257
Tyr D:251, Lys D:217, Glu D:307, Asn D:308, Thr D:257 Unfavorable Donor-Donor: Lys D:217	Tyr D:305, Glu D:214, Tyr D:213, Lys D:306, Ser D:309, Ser D:212
Tyr D:213, Tyr D:251	Thr D:257, Lys D:254, Glu D:252, Ser D:212, Tyr D:305, Glu D:214, Leu D:211, Lys D:217, Lys D:306, Glu D:307
Lys D:279, Thr D:259, Lys D:279, Ser D:278	Gly D:100, Thr D:277, Gln D:122, Lys D:306, Phe D:258, Thr D:257, Leu D:101, Arg D:140
Lys D:279, Gly D:256, Phe D:258, Lys D:306, Thr D:259	Leu D:101, Arg D:140, Ser D:278, Thr D:257, Gln D:122, Gly D:100, Thr D:277
Lys D:279, Lys D:306, Gly D:256, Thr D:259 Unfavorable Donor-Donor: Lys D:306	Gly D:122, Thr D:277, Tyr D:305, Thr D:257, Phe D:258, Ser D:278, Gln D:121, Leu D:101, Arg D:140, Gly D:100
Gly D:256, Thr D:259, Lys D:279, Lys D:306 Unfavorable Donor-Donor: Lys D:306	Ser D:278, Arg D:140, Gly D:100, Leu D:101, Thr D:277, Gln D:122, Tyr D:305, Phe D:258, Thr D:257
Lys D:279, Ser D:278, Gly D:256, Lys D:306, Thr D:259 Unfavorable Acceptor-Acceptor: Lys D:279, Unfavorable Donor-Donor: Lys D:306	Gly D:100, Thr D:277, Gln D:122, Phe D:258, Thr D:257, Tyr D:305, Arg D:140
Leu D:101, Arg D:140, Gln D:122, Lys D:279, Gly D:256, Gly D:100	Thr D:277, Lys D:306, Thr D:259, Phe D:258, Thr D:257, Ser D:278
Ser D:278, Gly D:256, Phe D:258, Lys D:279, Thr D:259	Lys D:306, Gly D:100, Arg D:140, Thr D:257, Gln D:122, Thr D:277, Leu D:101
Gln D:122, Phe D:258, Gly D:256, Thr D:259, Lys D:279, Ser D:278	Gly D:100, Thr D:277, Arg D:140, Lys D:306, Thr D:257

Ala D:145, Lys D:91, Leu D:87	Trp D:93, Lys D:94, Asp D:37, Asn D:146, Glu D:143, Tyr D:95, Ala D:144, Gln D:97, Gly D:142

ANNEXURE V: 3D and 2D Illustrations of inhibitors to Protein A and B, Highlighting Interacting and Pocket Amino Acids

Approved Inhibitors	**3D Visualization**	**2D Visualization**	**Amino Acid Interactions**	
Target: Protein A (7ALH)			**Interacting A.A**	**Pocket A.A**
Nirmatrelvir (M^{pro} Inhibitor)	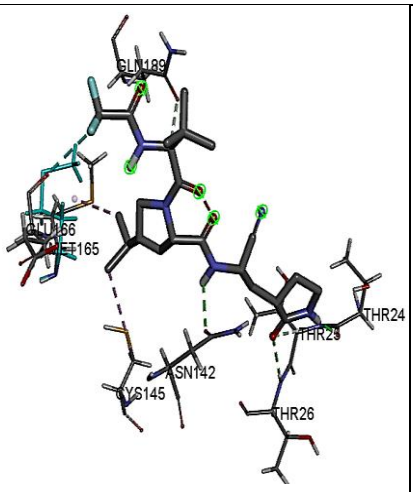	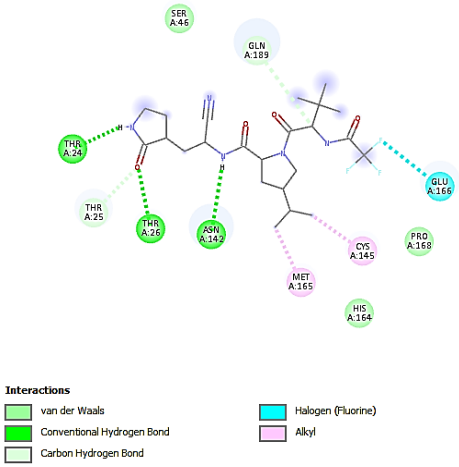	GLN A:189, GLU A:166, CYS A:145, MET A:165, ASN A:142, THR A:26, THR A:25, THR A:24	SER A:46, PRO A:168, HIS A:164
Target: Protein B (6WX4)				
PF-07957472 (PL^{pro} Inhibitor)	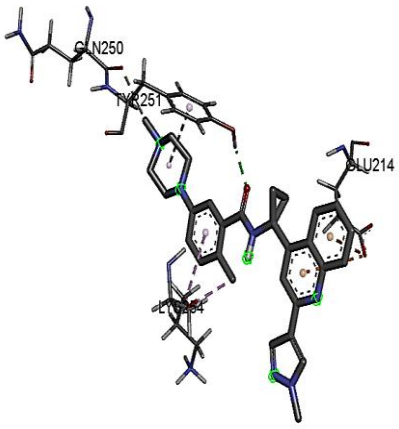	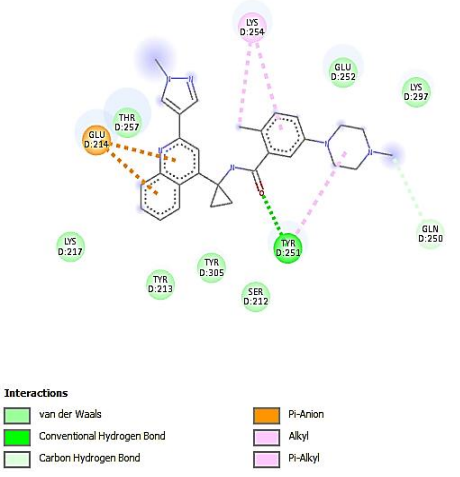	LYS D:254, GLU D:214, TYR D:251, GLN D:250	THR D:257, GLU D:252, LYS D:297, SER D:212, TYR D:213, LYS D:217

ANNEXURE VI: Concise Glossary

Words	Meanings
B-factor	Measure of atomic displacement or flexibility in a crystal structure; higher values indicate greater motion or disorder.
Binding Site	Region on a molecule where specific substances chemically bind.
Covariance	Shows how residue pairs move-together, independently, or oppositely
Eigenvalues	Indicates stiffness of motion; lower values mean easier deformation.
Elastic Network	Atoms linked by springs; darker dots = stiffer connections.
Exhaustiveness	Number of random trials in ligand docking search.
In-silico	Performed using computer simulations.
Pan assay interfering compounds	Compounds causing false positives in assays.

ANNEXURE VII: Amino acid full forms

Abbreviation	Full Forms
Arg	Arginine
Asn	Asparagine
Ala	Alanine
Asp	Aspartic acid
Cys	Cysteine
Glu	Glutamic acid
Gln	Glutamine
His	Histidine
Met	Methionine
Leu	Leucine
lys	lysine
Phe	Phenylalanine
Pro	Proline
Ser	Serine
Thr	Threonine
Tyr	Tyrosine
Val	Valine

ANNEXURE VIII: Ethics Application and Declaration form

Innopharma education

GRIFFITH COLLEGE

Ethics Application & Declaration Form

DISSERTATION TITLE: **Blending Nature and Technology: Optimizing Tinosporaside, a Natural Lead, for Advanced COVID-19 Therapy**

RESEARCHER'S NAME: **Christy Saji**

PROGRAMME OF STUDY: **Master's in Pharmaceutical Business and technology**

SUPERVISOR'S NAME: **Dr.Victor David Vendrell**

DECLARATION:
The information in this application form is accurate to the best of my knowledge. I undertake to abide by the principles outlined by Innopharma/Griffith College ethics policy in my research dissertation. I confirm that I have completed a full ethics assessment for my research dissertation as per the college guidelines. I will not begin my primary research until such approval from my supervisor and/or ethics Committee has been obtained.
I pledge to carry out my research according to the Innopharma/Griffith College academic integrity standards. Any results presented in my dissertation will be from my own, original research, I will reference and/or acknowledge any material or sources used in its preparation and I will not plagiarise the work of anyone else.

For Student:

STUDENT SIGNATURE: 

DATE: 21/03/2025

The research contained within this research dissertation proposal has been approved.

For Supervisor:

Ethics Committee Approval Required: Yes ☐ No ☐

SUPERVISOR SIGNATURE: 

DATE: 21/03/2025

For Ethics Committee (if required):

Ethics Committee Approval Given: Yes ☐ No ☑

ETHICS COMMITTEE MEMBER SIGNATURE:

DATE:

NOTE: Supervisors are responsible for ensuring their students fill in this form correctly and that all ethical areas have been considered.

SECTION 1: DESCRIPTION OF RESEARCH STUDY

1.1 Purpose and objectives of research [*300 words maximum/ use literature review findings to guide]*

This study explores the potential of Tinosporaside, a natural compound found in Tinospora species, as an antiviral agent against SARS-CoV-2. Specifically, the research investigates whether Tinosporaside can effectively bind to and inhibit key viral proteases—main protease (Mpro, 7ALH) and papain-like protease (Plpro, 6WX4)—which play crucial roles in viral replication. By analyzing these interactions through computational methods such as molecular docking and MD simulations, the study seeks to determine Tinosporaside's potential as a therapeutic candidate for COVID-19.

The primary objective is to assess Tinosporaside's binding affinity and stability with SARS-CoV-2 proteases, evaluating its potential as a dual-acting inhibitor. Additionally, the study explores whether structural modifications can enhance its antiviral efficacy. Understanding the essential structural features that contribute to its binding efficiency will help refine its molecular properties for improved drug-like characteristics, such as bioavailability and safety.

This research aligns with the urgent need for novel antiviral treatments due to the limitations of existing therapies, especially for immunocompromised individuals and emerging variants. By leveraging Computer-Aided Drug Design (CADD), the study provides a cost-effective and environmentally sustainable approach to drug discovery. It also highlights the growing importance of plant-based compounds in modern medicine, integrating traditional knowledge with advanced computational techniques to accelerate drug development. Ultimately, this study aims to contribute valuable insights into the development of plant-derived antiviral treatments, potentially paving the way for future clinical applications. The findings could lay the foundation for further in vitro and in vivo testing, bringing Tinosporaside closer to becoming a viable antiviral therapy for COVID-19 and other viral diseases.

1.2 Research methodology: [*300 words maximum/ detail how you will acquire your primary data (focus groups/interviews/online surveys etc). Proposed questions for questionnaires and/or interviews **must be included** in the appendix].*

This study does not involve any surveys or interviews, as it focuses entirely on computational approaches to assess the antiviral potential of Tinosporoside against SARS-CoV-2 proteases.

The methodology integrates molecular docking, structural modifications, MD simulations, and ADMET predictions to assess the compound's efficacy and drug-like properties.

1. Molecular Docking

AutoDock Vina will dock Tinosporoside with SARS-CoV-2 Mpro (PDB ID: 7ALH) and PLpro (PDB ID: 6WX4) to estimate binding affinities and interaction profiles. Hydrogen bonding & hydrophobic interactions will be analyzed to evaluate binding efficiency. The docking scores will determine the molecule's inhibitory potential against viral proteases.

2. Structural Modifications

Chemical modifications will be performed using ChemSketch to improve potency, bioavailability, and drug-like properties. Functional groups will be added or altered, and Lipinski's rule of five will validate drug-likeness. Re-docking of modified structures will assess their enhanced binding affinities compared to the native compound.

3. MD Simulations

imod software will MD simulations to study the structural stability of the protein-ligand complexes. Stability will be assessed through Normal mode analysis.

4. ADMET Predictions

Pharmacokinetic properties will be predicted using pkCSM, evaluating absorption, distribution, metabolism, excretion, and toxicity. The drug-likeness and safety profiles of both unmodified and modified compounds will be analyzed.

5. Comparative Efficacy Analysis

Binding affinities, stability metrics, and ADMET properties will be compared to determine if structural modifications enhance Tinosporaside's therapeutic potential.

Data will be presented through tables, graphs, and visual diagrams to offer comprehensive insights into Tinosporaside's antiviral activity, supporting its role as a promising lead molecule for antiviral drug development.

SECTION 2: POSSIBLE ETHICAL ISSUES

Answer 'yes' or 'no' to the following questions.

SUBJECT MATTER

Does the research proposal involve:	
Research into specific company activities that would be deemed sensitive or confidential	No
Research into politically and/or racially/ethnically and/or commercially sensitive areas	No
Sensitive, personal, professional or corporate issues	No

RESEARCH PROCEDURES

Does the research proposal involve:	
Research that might damage the reputation of companies or participants	No
Research that may negatively affect the reputation of Griffith College/Innopharma	No
Use of personal records without consent	No
Use of company data without consent	No
The offer of any inducements to participate	No
Audio or visual recording without consent	No
Using a language other than English	No

PARTICIPANTS

Does the research proposal involve:	
People who are not competent and/or fluent in English	No
Does your research group include any of the following vulnerable groups *(Adults with psychological impairments; Adults with learning difficulties; Adults under the protection/control /influence of others (e.g. in care/prison); Relatives of ill people (e.g. parents of sick children); Hospital or GP participants recruited in a medical facility; persons under the age of 18)*	No

If you have answered NO to ALL questions, please go straight to Section 4.

If you have answered YES to ANY question in SECTION 2, you must fill in SECTION 3

SECTION 3: STEPS TAKEN TO AVOID ETHICAL ISSUES

[Only fill in this section if you answered YES to ANY of the questions in Section 3. For example, if you answered yes to including participants who are not fluent in English, you might put forward a plan that offers your survey in two languages to take this into account. Another example could be a study where the researcher wants to include information about the care received by children with a long-term condition but it would not be ethical to approach the children directly but it might be acceptable to instead ask parents questions about their child's care. If these plans are acceptable to your supervisor, you may not need to apply for ethical approval from the Ethics Committee].

3.1. If your ethics relates to ***Subject Matter***, outline your action plan to work around any sensitive issues.
3.2. If your ethics relates to ***Research Procedures***, outline your action plan to deal with possible ethical issues in your research procedures.
3.3. If your ethics relates to ***Participants***, outline how you will protect vulnerable persons or those that do not have English as their first language.

SECTION 4: ABOUT YOUR PARTICIPANTS

4.1. Outline your participant profile and why you have chosen them for this study *[Do not provide names except where it is deemed impossible to conceal identity].*

4.2 How do you plan to gain access to/contact/approach your participant(s).

SECTION 5: INFORMATION, CONSENT AND CONFIDENTIALITY

5.1 Participant Information Letter (PIL) for participants

[You must submit an information letter for participants with this application, as part of your appendices document. For online surveys, it is sufficient to include a paragraph summarising and explaining the purpose of the research at the beginning of the survey. In all other research e.g. interviews, phonecalls, a PIL should be provided to each participant before they are asked for their consent to take part. A template PIL is available in Moodle].

Please confirm below that your information letter covers:

Description of the research topic and method	N/A	
Details of what participation will involve	N/A	
Rights to anonymity	N/A	
Confidentiality	N/A	
Rights to withdraw from the research		N/A
The contact details of the researcher and supervisor (if necessary)	N/A	

5.2 Informed Consent Form (ICF) for participants

[Informed consent is required for most research. For online surveys, it is sufficient to get the participant to tick two boxes at the beginning of the survey – one to state they understand the research and one to give consent. In all other research e.g. interviews, phonecalls, a signed consent form is required. If the data is gathered online e.g. zoom, a signed consent form can be scanned and sent to the researcher. A template ICF is available in Moodle. The signed ICFs, along with the surveys, audio files or interview notes etc. must be stored in the primary data folder on moodle

and can be accessed by Innopharma staff for the purposes of verifying the authenticity of the research carried out and the data collected].

Please indicate below if your research requires a signed consent form by selecting the relevant option only:

No: My research study does not include an online survey, nor does it require signed consent.

SECTION 6: STORAGE OF DATA

[Please ensure that you are abiding by GDPR and the national Data protection laws https://www.hrb.ie/funding/gdpr-guidance-for-researchers/gdpr-and-health-research/).

*The student is responsible for storage of data and this will be handed over to the college in an electronic format as part of the thesis submission i.e. primary data and completed ICFs where applicable will be added to the primary data folder on moodle. The rationale is to keep data **as long as it is still useful** and there is an intention to use it further **for research** so if this is not the case then this can be stipulated here and a shorter retention period given.]*

6.1. How will you store the research data and for how long? How will you manage data protection issues?

Data will be stored on my computer as long as it remains relevant, as my research utilizes free, open-source online software tools. Since no sensitive or personal data is involved, there are no data protection concerns.

SECTION 7: NON-DISCLOSURE AGREEMENT & STUDENT CONSENT

7.1 **Non-Disclosure Agreement (NDA)**

Will the final dissertation contain any information pertaining to any source what would warrant the use of a Non-Disclosure Agreement (NDA) e.g. industry-based research?

No

7.2 **Student consent**

If a Non-Disclosure Agreement (NDA) is not required, does the Student consent to allow their completed dissertation to be held/published by Innopharma/Griffith College?

Yes

SECTION 8: RECORDING AND RETENTION OF DISSERTATION VIVA

8.1 **Viva Recording**

The Dissertation viva will be recorded. This recording may be used to facilitate assessment by Innopharma staff, a third reader if necessary and/or if requested by the external examiner for the Programme. The recording will be held in line with current GDPR guidelines and will not be made publicly available.

SECTION 9: DOCUMENT CHECKLIST

NOTE: Applicants must attach the following documents in electronic format to the appendix.

Which documents are added to the appendix? Please tick N/A if not applicable:

9.1 Participant Information Letter (PIL) for participant	N/A
9.2 Informed Consent Form (ICF) for participant	N/A
9.3 Questions/survey for interviewees/focus groups etc *(can be in draft form)*	N/A
9.4 Any other documents e.g. Non-Disclosure Agreement	N/A

I confirm that this application is complete and all required documents are included in the appendix.

For Student:

STUDENT SIGNATURE: 

DATE: 21/03/2025

SECTION 10: APPENDIX

It is novel and if it fulfils the criteria below then it is valid and can proceed.

- **My supervisor has a strong background in molecular biology, with expertise in genetics, viral vectors, and computational tools. Given his knowledge and experience in these areas, he is well-equipped to confidently supervise this project.**
- **As a pharmacy student and researcher, I have studied and worked extensively with all the computational tools and software used in this research during my undergraduate research work. My academic background and hands-on experience with AutoDock Vina, AutoDock Tools, iMod, ChemSketch, and pkCSM equip me with the necessary skills to independently conduct this study. The research will be carried out entirely by myself.**
- **Additionally, there are no conflicts with any of the software, as they are freely available and open-source tools.**